Missouri University of Science and Technology
Scholars' Mine

Physics Faculty Research & Creative Works | Physics

01 Jan 1985

Charge Transfer Of Hydrogen Ions And Atoms In Metal Vapors

T. J. Morgan

Ronald E. Olson
Missouri University of Science and Technology, olson@mst.edu

A. S. Schlachter

J. W. Gallagher

Follow this and additional works at: https://scholarsmine.mst.edu/phys_facwork

 Part of the Physics Commons

Recommended Citation

T. J. Morgan et al., "Charge Transfer Of Hydrogen Ions And Atoms In Metal Vapors," *Journal of Physical and Chemical Reference Data*, vol. 14, no. 4, pp. 971 - 1040, American Institute of Physics, Jan 1985.
The definitive version is available at https://doi.org/10.1063/1.555752

This Article - Journal is brought to you for free and open access by Scholars' Mine. It has been accepted for inclusion in Physics Faculty Research & Creative Works by an authorized administrator of Scholars' Mine. This work is protected by U. S. Copyright Law. Unauthorized use including reproduction for redistribution requires the permission of the copyright holder. For more information, please contact scholarsmine@mst.edu.

Journal of Physical and Chemical Reference Data

RESEARCH ARTICLE | OCTOBER 01 1985

Charge Transfer of Hydrogen Ions and Atoms in Metal Vapors

T. J. Morgan; R. E. Olson; A. S. Schlachter; J. W. Gallagher

Check for updates

Journal of Physical and Chemical Reference Data 14, 971–1040 (1985)
https://doi.org/10.1063/1.555752

View Online
Export Citation
CrossMark

17 July 2023 14:50:05

AIP Publishing


The Journal of Chemical Physics
Special Topic: Adhesion and Friction
Submit Today!
AIP Publishing

Charge Transfer of Hydrogen Ions and Atoms in Metal Vapors

T. J. Morgan

Wesleyan University, Middletown, Connecticut 06457

R. E. Olson

University of Missouri—Rolla, Rolla, Missouri 65401

A. S. Schlachter

Lawrence Berkeley Laboratory, University of California, Berkeley, California 94720

and

J. W. Gallagher

Joint Institute for Laboratory Astrophysics, University of Colorado and National Bureau of Standards, Boulder, Colorado 80309

Cross sections and equilibrium fractions for energetic H^+, H^-, and H^0 in collisions with metal-vapor targets have been compiled and evaluated. Both experimental and theoretical results are reported. Sources of errors are discussed, and recommended values for the data are presented.

Key words: atomic hydrogen; charge transfer; cross sections; equilibrium fractions; hydrogen ions; metal vapors; recommended values.

Contents

List of Tables

© 1985 by the U.S. Secretary of Commerce on behalf of the United States. This copyright is assigned to the American Institute of Physics and the American Chemical Society.
Reprints available from ACS; see Reprints List at back of issue.

17 July 2023 14:50:05

1. Introduction

Charge transfer of hydrogen ions and atoms has been reviewed[1,2] several times in the past 25 years, primarily for gas targets. Much of the research on charge transfer in metal-vapor targets has been done in recent years, and has only been reviewed in conference proceedings.[3–6] A recent unpublished report has compiled experimental cross sections, but provided no evaluation.[7] Charge transfer in metal-vapor targets is a topic of particular interest: electron-capture cross sections can be very large, and very high yields of metastable hydrogen atoms and of negative hydrogen ions can be produced.

Data on charge-transfer collisions of hydrogen ions in metal vapors are important for a variety of applications in atomic and nuclear physics. Negative hydrogen ions are often used in accelerators: they are required for tandem electrostatic accelerators, and extraction from circular accelerators is easily accomplished by conversion to positive ions in a foil. Also, circular accelerators can be loaded with positive ions formed by stripping fast negative ions. Charge-transfer collisions are used in some polarized ion sources[8]: Lamb-shift sources require a large yield of metastable hydrogen atoms; atomic beam sources require conversion of polarized positive ions into negative ions; colliding-beam sources use electron attachment to form H^-; and optically pumped sources use electron capture of polarized electrons to form polarized H atoms. Polarized H atoms can be converted to H^- for subsequent acceleration by charge transfer in metal-vapor targets. A new technique, collisional pumping,[9] also uses charge transfer in a polarized alkali-vapor target. Another area of application of negative hydrogen-ion production is neutral-beam heating of magnetically confined plasmas of fusion interest. In this case, H^- ions are accelerated to high energies, where conversion to fast atoms can be efficiently accomplished by collisional- or photodetachment.

In many cases, data for metal-vapor targets exhibit larger discrepancies than gaseous-target data. Consequently, an informed, evaluated compilation of available data is important and, because of many present-day applications, especially timely.

The purpose of this report is to compile, evaluate, and present experimental and theoretical results for charge-changing collisions of hydrogen ions and atoms (H^+, H^0, and H^-) in metal-vapor targets including the alkalis (Li, Na, K, Rb, Cs), the alkaline-earths (Mg, Ca, Sr, Ba), and the group IIB metals (Zn, Cd, Pb). Data are reported in two forms: total cross sections and charge-state equilibrium fractions. Experimental data are presented over the energy range 200 eV/u to 400 keV/u; theoretical results are presented over the range 10 eV/u to 300 keV/u. Definitions of the data are given in Sec. 2. On the basis of considerations discussed in Secs. 3 (experimental approach) and 4 (theoretical methods), the accuracy of all data have been assessed (see Sec. 5). The cross sections and equilibrium fractions are presented in Sec. 6, and recommended values are given.

2. Systematics of Charge Transfer

The behavior of charge-changing collisions between hydrogen ion or atom beams and a target can be described by a set of coupled linear first-order differential equations,

$$[dF_i(\pi)]/d\pi = \sum_j F_j(\pi)\sigma_{ji} - \sum_j F_i(\pi)\sigma_{ij} , \quad (1)$$

where π is the target thickness (atoms cm^{-2}), $F_i(\pi)$ is the fraction of the hydrogen beam in the ith charge state at target thickness π, and σ_{ij} represents the cross section for the charge-changing processes $H^i \rightarrow H^j$, where $i,j = +,0,-$.

Two limiting cases exist. First, if the target is tenuous enough, the probability of a second collision becomes negligible. Under these circumstances, denoting i as the incident component, we have from Eq. (1),

$$[dF_i(\pi)]/d\pi = -\sum_j F_i(\pi)\sigma_{ij}$$

and

$$[dF_j(\pi)]/d\pi = F_i(\pi)\sigma_{ij} . \quad (2)$$

Since $F_i \approx 1$ for this case, the charge-changing cross sections can be obtained directly from the slope of the measured linear relationship between the charge-state fractions and π. Second, if the target is very thick, the charge-state composition of the beam after passage through the target will remain constant as π is increased further. In this case $[dF_i(\pi)]/d\pi = 0$, and the constant value of F_i is designated the equilibrium yield F_i^∞, i.e.,

$$\lim_{\pi\to\infty} F_i(\pi) = F_i^\infty ;$$

F_i^∞ is independent of the charge-state distribution of the incident hydrogen beam. By definition

$$\sum_i F_i(\pi) = \sum_i F_i^\infty = 1.$$

Under these conditions, Eq. (1) becomes

$$F_i^\infty = \left(\sum_j F_j^\infty \sigma_{ji}\right) \Big/ \left(\sum_j \sigma_{ij}\right). \quad (3)$$

Under certain conditions, equilibrium fractions can be expressed quite simply in terms of relevant cross sections. For example, below about 10 keV/u, the H^+ fraction is often quite small in a thick metal-vapor target and may be neglected. Under these circumstances, Eq. (3) combined with the conditions $F_- + F_0 = 1$ yields the relations

$$F_-^\infty = \sigma_{0-}/(\sigma_{0-} + \sigma_{-0})$$

and

$$F_0^\infty = \sigma_{-0}/(\sigma_{0-} + \sigma_{-0}) . \quad (4)$$

These simple relations may be used to check consistency between cross-section and equilibrium-yield measurements, and to estimate the magnitude of an unmeasured cross section or equilibrium fraction.

For values of π between the two limiting cases discussed

17 July 2023 14:50:05

above, multiple collisions occur and the charge-state distribution varies nonlinearly with π. $F_i(\pi)$ is often monotonic with π, but there are systems in which this is not the case. An example is the fraction F_0 for fast H^- incident on a target; F_0 reaches a maximum for some value of π, then decreases with increasing target thickness, eventually reaching a (lower) equilibrium value. Another example is when atomic excited-state fractions in the beam are non-negligible. Low-energy collisions between hydrogen beams and metal vapors produce non-negligible fractional yields of metastable H(2s) atoms, F_{2s}, which are created by electron capture but are easily de-excited in subsequent collisions.

In some cases a quantity called the optimum conversion efficiency is measured. Unlike equilibrium fractions, it is an apparatus-geometry-dependent quantity defined as the fraction of the beam in a charge state leaving the target relative to the incident beam. It is equivalent to F^∞ only if all of the scattered beam is collected. It can be shown that optimum conversion efficiencies are lower bounds to equilibrium fractions.[5]

3. Experimental Approach

3.1. Apparatus

The purpose of this section is to acquaint the reader with the experimental techniques used to measure the data presented in this report. A schematic of a typical apparatus for measurement of charge transfer in a metal-vapor target is shown in Fig. 1. A momentum-analyzed beam of H^+ or H^0 is incident on the target. For H^0 measurements, the ion beam is neutralized in the gas cell before reaching the target. The beam after the collision is charge-state analyzed in a magnetic or transverse electric field, and the charge-state components detected.

Various targets are used for charge-transfer measurements in metal vapors: heated ovens,[10] thermal beams,[11] jets, and heat pipes.[12] Target density is usually inferred from the temperature by use of vapor-pressure data[13]; absolute calibration is possible, however, by optical absorption[14,15] or by ionization of (alkali) atoms by surface ionization.[16,17]

Ion-beam intensities are usually measured using Faraday cups with secondary-electron suppression; single-particle detectors can also be used. The flux of neutral atoms can be measured by several methods, the most common being secondary-electron emission[18] and bolometric detection,[19,20] e.g., pyroelectric. Single-particle detection can also be used.

Apparatus for measuring thick-target yields in a metal vapor is generally similar to that used for measuring cross sections. Target and detector design are, however, quite different for the two kinds of measurements. For equilibrium-yield measurements, nearly all particles have undergone several scattering and charge-changing collisions, which result in equal angular distributions for all particles in the beam. In this case it is not necessary to collect all of the scattered beam from the target, but rather to collect the ions and atoms with equal efficiency. This is accomplished by collimating the beam after the target to an angular spread at the detector that is smaller than the detector acceptance. In this case the equilibrium fraction can be thought of as the fraction of the beam in a specific charge state leaving the target relative to the total beam leaving the target.

For cross-section measurements, where only a small fraction of the incident particles undergo even one charge-changing collision, it is essential that negligibly few scattering collisions take place which result in particles not reaching the detectors. Scattering collisions include both elastic and inelastic processes. This requirement generally necessitates collimation of the beam before the target. Limited detector angular acceptance sets a low-energy limit for cross-section measurements for a given geometry. For collisions in the low keV energy range, angular acceptances of greater than $\pm$ 1° are often needed.

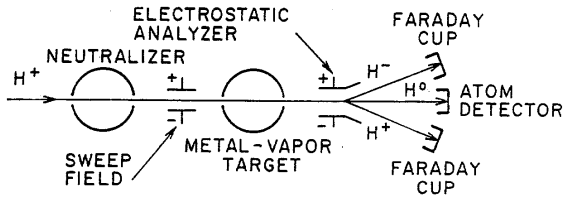

FIG. 1. Apparatus for measurement of charge transfer in metal-vapor targets.

3.2. Sources of Error

a. Cross Sections

Cross-section measurements require determination of incident and scattered particle intensities as well as the effective target thickness through which the beam passes. Sources of error usually are

(1) inaccurate neutral atom intensity determination,

(2) insufficient collection of scattered beams (the angular acceptance of the detectors is too small),

(3) inaccurate knowledge of target thickness,

(4) inadequate accounting of the contribution of multiple collisions to the scattered intensity, and

(5) excited-state contamination of an incident neutral beam.

A few examples will illustrate some of these difficulties. If secondary-electron emission is used to detect neutral atoms, calibration of the detector must frequently be monitored during data collection, since the number of secondary electrons emitted per incident particle depends on surface conditions. Coverage of the emitting surface with metal atoms effusing from the target, as well as changes in the spatial distribution of the beam on the surface of the detector as the target thickness is varied, can introduce non-negligible changes in the secondary-emission properties.

There are several difficulties associated with an accurate knowledge of target thickness. One complication specific to metal-vapor targets is the development of oxide films on the metal which inhibit evaporation. Another is alkali impurities in alkaline-earth metals. The dominant impurities present in the heavier alkaline-earths are alkali metals which have a much higher vapor pressure at a given temperature.

17 July 2023 14:50:05

Thus care must be taken to ensure that all target metals used are of high purity. Other experimental concerns regarding target thickness are the determination of the effective target interaction length and accurate determination of the temperature inside the cell responsible for the target pressure.

Measurements of two-electron-transfer cross sections require careful consideration of competing two-step scattering processes. Consider H^+ collisions with alkali atoms at a few keV. Cross sections for two-electron capture in a single collision, σ_{+-}, are of order 10^{-17} cm^2. However, the two-step collision process $H^+ \rightarrow H^0 \rightarrow H^-$ has cross sections $\sigma_{+0} \sim 10^{-14}$ cm^2 and $\sigma_{0-} \sim 10^{-15}$ cm^2. In this case very tenuous target thicknesses, of order 10^{12} cm^{-2} or less, are required to obtain accurate results for σ_{+-}. Measurements in the range of 10^{13} cm^{-2}, a reasonable and typical value for a large portion of the data presented, lead to serious overestimates of the cross section in this case.

Production of energetic H^0 atoms by a charge-changing collision of H^+ or H^- in a gas or vapor generally leads to an unknown admixture of excited states in the H^0 beam. Electron-loss cross sections measured with H^0 projectiles produced by this method can be affected, because the cross section for electron detachment from excited H^0 can be considerably larger than that for the ground-state atoms. Electron-capture cross sections are generally not affected by a small excited-state H^0 admixture. A beam of primarily ground-state H^0 atoms can be produced by photodetachment of H^-.[18]

b. Equilibrium Fractions

Several of the difficulties discussed in the previous section on cross-section measurements also apply to equilibrium-fraction measurements. In principle, measurement of equilibrium fractions is simpler than that of cross sections, since an absolute knowledge of target thickness is not needed. What is required, however, is to ensure that the measured fractions are independent of changes in target thickness over a sufficiently wide range, to guarantee that the equilibrium has been attained.

c. Excited States

The measurement of absolute cross sections and yields for excited states of hydrogen atoms presents additional difficulties associated with the detection and collection efficiency and the excited-state detector. In this report, data on the formation of H(2*s*) and H(2*p*) in electron-capture collisions of H^+ are presented. Measurements of H(2*p*) usually require a crossed-beam apparatus. H(2*s*) measurements require an electric-field region to induce 2*s*–2*p* mixing in order to detect the metastable H(2*s*) atoms. The additional complexity of these excited-state measurements plus the added uncertainty in the absolute value of the measurements make these data less accurate than simple charge-changing data.

Authors' statements regarding consideration of the sources of error discussed above were used in our assessment of the accuracy of the reported data.

4. Theoretical Methods

For energies $E \lesssim 10$ keV/u, collision processes are best described in a molecular framework. At higher energies the atomic-orbital method is appropriate. The scattering wave function is expanded in terms of molecular orbitals (atomic orbitals) of the collision partners to obtain a set of coupled equations which determine the scattering dynamics. The accuracy of calculated cross sections is thus a reflection of the basis set used to describe the dynamics of the collision.

Several procedures have been developed to calculate cross sections. The most widely used method is the perturbed-stationary-state (PSS) coupled channel approach,[21] which employs adiabatic potentials and coupling matrix elements. The projected-valence-bond (PVB) method[22] is similar to the PSS approach except that the calculations are made within the adiabatic state formalism. A commonly employed approximate method is the multichannel Landau–Zener (LZ) procedure,[23–25] which, if carefully applied, can yield qualitative results.

4.1. Perturbed-Stationary-State (PSS) Method

In the PSS method, the coupled equations are obtained from an expansion of the total wave function in terms of the adiabatic molecular wave functions of the collision partners.[21] The heavy particles are assumed to move classically, while the electronic motion is treated quantum mechanically. The first-order coupled equations involve the numerical solution of the time-dependent Schroedinger equation. Input to the coupled equations are the potential energy differences and the radial $(\partial/\partial R)$ and rotational (L_y) coupling matrix elements between the various states. To obtain meaningful results, the potential energies and wave functions for the various channels must be of high accuracy.

For electron-transfer reactions, an additional complication is the fact that the transferred electron resides on different nuclei before and after the collision. The inclusion of electron translation factors (ETF's) remedies this problem.[26] However, the proper form of the ETF's has not been defined. The inclusion of ETF's is required for relative collision velocities that approach the orbital velocity of the active electron (electrons) on the target atom. At low relative velocities, the ETF's can also be very important for highly nonresonant reactions that are not mediated by a sharp curve-crossing interaction.

The estimates of the accuracy of the various theoretical calculations are based upon: (a) the quality of the molecular interaction potentials and coupling matrix elements, (b) the inclusion of the proper number of states to define the collision reaction, and (c) the incorporation of ETF's for the highly nonresonant collision processes.

4.2. Landau–Zener (LZ) Method

The LZ method is applicable to processes that are induced by a curve crossing between reactant and product states. The basic formula was presented almost simultaneously by Landau,[23] Zener,[24] and Stueckelberg[25] in the early 1930's. In order to apply the formula, one needs to know the potential energy differences and slopes in the curve-

17 July 2023 14:50:05

crossing region between the interacting adiabatic potential curves.

Deficiencies in the LZ model are several. The first problem is that the model poorly describes large-impact-parameter collisions that barely succeed in penetrating into the curve-crossing region. In many cases, these large-impact-parameter collisions make a major contribution to the cross section. A second difficulty is the lack of an adequate procedure to incorporate rotational coupling into the LZ formula. Rotational coupling is velocity dependent and can be very important, especially for systems with low reduced masses (i.e., one species being hydrogen or its isotope), since even a moderate energy results in a large relative velocity. As with any other theoretical method, the LZ procedure requires an accurate knowledge of the interaction potentials. In many cases this information is not present and must be gleaned from approximate semiempirical models.[27] The overall accuracy of a LZ calculation will generally be in the factor of 2–3 range.

4.3. Quantum-Mechanical (QM) Method

Quantum-mechanical methods involve the numerical solution of the time-independent Schroedinger equation, and in general use the same input as the PSS method. In most cases, the adiabatic potentials and coupling matrix elements are transformed to a diabatic basis for ease of calculation and the use of existing standard computer codes. The QM method is efficient at low velocities since the step size for the numerical integration is inversely proportional to the wave number, $k = \mu v/\hbar$, of the collision. At high velocities it is prohibitively expensive to use. Another application of the QM method arises at threshold energies when the cross section is sensitive to the trajectory followed by the collision partners. The PSS method may also be used in this region but there is no unique way of characterizing a single trajectory for a multichannel scattering event. The accuracy of the QM method is determined by the same criteria as that of the PSS method.

4.4. Atomic-Orbital (AO) Method

For higher energy collisions, atomic-orbital methods are appropriate. This method consists of decomposing the time-dependent electronic wave function into a set of traveling atomic orbitals. These functions are used as the basis set for the solution of the coupled differential equations representing the Schroedinger equation. A merit of the AO method is that there is no ambiguity in the choice of the form of the ETF's.[28] As with the molecular-orbital method, the accuracy of the cross sections depends on the basis set employed in the calculations.

5. Accuracy Assessments

In order to assign accuracy ratings and to select recommended values, the original papers were reviewed to determine whether the data presented were subject to the errors discussed in Secs. 3 and 4. In several cases, personal contact and correspondence with authors was necessary in order to clarify some points made in the original papers. In one case, an author informed us that the original data were incorrect and thus we have not included these results in the report. In many cases, the results reported for a particular cross section or equilibrium fraction differ substantially between investigators. Our assessments of the accuracy of individual measurements and calculations are based on careful considerations of the available information, but it should be emphasized that these assessments are estimates.

In the following tables and figures, data have been categorized into four groups according to their estimated accuracies. These are:

Category	Accuracy
(a)	less than $\pm 20\%$
(b)	$\pm 20\%$–$\pm 50\%$
(c)	$\pm 50\%$–$\pm 100\%$
(d)	greater than 100%

Selection of the recommended data was based on these accuracy ratings.

6. Data Presentation and Recommended Values

The data included in this report were identified mainly through a computer survey of the literature carried out at the Joint Institute for Laboratory Astrophysics Data Center. Data presented at conferences and published only as part of the conference proceedings have not been included, since in almost all cases these data appeared in final form in a subsequently published paper in a recognized journal. Table 1 summarizes sources of cross sections and equilibrium fractions for each target, giving the quantities reported, the energy range, and the assessed accuracy of the data. The information is current up to the middle of 1984.

Results for hydrogen and deuterium projectiles are intermixed here. Hydrogen and deuterium projectiles at the same velocity have the same total cross sections and yields over the energy range considered; therefore results for deuterium projectiles are presented in this report as if the experiment had been performed using hydrogen at one-half the energy.

The original data are given as points in Figs. 2–82. The legend or caption of each figure identifies the reference from which the data were taken and the estimated accuracy. The recommended values are shown by solid lines in the figures. Figures 83–108 give composite presentations of the recommended data, and Tables 2–11 give listings of these values.

A few cases arose where it was difficult to select a recommended value because of conflicting results between what appeared to be equally reliable experiments or calculations. In these irreconcilable cases we have chosen recommended values between the results as our best estimate, or have made no recommendation.

Several cases exist for which there are no measurements of equilibrium yields, e.g., H^- formation below 30 keV/u in potassium or lithium vapors (Table 1). When results for equi-

17 July 2023 14:50:05

librium yields are not available, but information on optimum conversion efficiencies exist, we present the latter as dotted lines in the figures (see Sec. 2). Under these circumstances, the data are of value since they indicate trends and should provide a lower bound to the equilibrium yield.

Also, in Fig. 66 we present no original data, but do show dashed lines indicating recommended values for the cross sections, because these results were inferred rather than measured. At low energies these values are inferred from Eq. (4); above 15 keV, a high-energy approximation of σ_{-0} was used.[2]

7. Conclusion

Over the last ten years, many experiments and calculations on charge-changing processes between hydrogen beams and metal-vapor targets have been done, and the data are reasonably comprehensive. However, experimental data below 1 keV are rare, and cross sections for H^- collisions with alkaline-earth targets are needed at all energies.

Qualitative agreement between theory and experiment is generally good and in several cases quantitative agreement exists.

17 July 2023 14:50:05

Table 1. Sources of charge transfer cross sections and equilibrium fractions for hydrogen atoms and ions with metal vapors

Reference	Authors	Year	Exp./Theo.	Projectile	Quantity Reported	Energy Range (keV/u)	Method[a]	Comments	Accuracy
					LITHIUM				
55	Il'in et al.	1967	E	H^+	σ_{+o}	10-180			c
43	Dyachkov	1969	E	H^+	σ_{+o}	8-400			c
				H^o	σ_{o+}	10-425			c
50	Gruebler et al.	1970	E	D^+	σ_{+o}	0.4-8			d
				H^+	σ_{+o}	1-25			d
				D^+	σ_{+-}	0.4-8			d
				H^+	σ_{+-}	1-25			d
58	Janev and Radulovic	1978	T	H^o	σ_{o-}	10^{-3}-2	LZ	Semiempirical matrix elements	d
30	Anderson et al.	1980	E	H^o	σ_{o-}	30-200			b
				H^o	σ_{o+}	30-200			b
				H^-	σ_{-o}	30-200			b
				H^-	σ_{-+}	30-200			b
					F_o^∞	30-100			a
					F_-^∞	30-200			b
79	Olson	1982	T	H^+	σ_{+o}	45-300		Classical method	c
85	Sato and Kimura	1983	T	H^+	σ_{+o}	0.5-10	MO		b
47	Fritsch and Lin	1983	T	H^+	σ_{+o}	0.5-20	AO		b
91	Varghese et al.	1984	E	H^+	σ_{+o}	0.26-4.0			b
					SODIUM				
55	Il'in et al.	1967	E	H^+	σ_{+o}	10-180			c
					F_o^∞	20			b
84	Oparin et al.	1967	E		F_o^∞	13-120			b
50	Gruebler et al.	1970	E	D^+	σ_{+o}	0.4-7			d
				H^+	σ_{+o}	1-20			d
				D^+	σ_{+-}	0.5-8			d
				H^+	σ_{+-}	1-20			d
77	O'Hare et al.	1975	E	H^+	σ_{+o}	20-200			c
58	Janev and Radulovic	1978	T	H^o	σ_{o-}	10^{-3}-2	LZ	Semiempirical matrix elements	d
31	Anderson et al.	1979	E	H^+	σ_{+o}	1-25			b
				H^+	σ_{+-}	1-10			d
					F_+^∞	1-25			b
					F_o^∞	1-25			b
					F_-^∞	1-25			b
30	Anderson et al	1980	E	H^o	σ_{o-}	30-200			b
				H^o	σ_{o+}	30-200			c
				H^-	σ_{-o}	30-200			b
				H^-	σ_{-+}	30-200			c
					F_o^∞	30-200			a
					F_-^∞	30-200			b

17 July 2023 14:50:05

Table 1. Sources of charge transfer cross sections and equilibrium fractions for hydrogen atoms and ions with metal vapors --Continued

Reference	Authors	Year	Exp./Theo.	Projectile	Quantity Reported	Energy Range (keV/u)	Method[a]	Comments	Accuracy
81	Olson and Liu	1980	T	H^-	σ_{-o}	0.02-0.3	PSS		c
74	Nagata	1980	E	H^+	σ_{+o}	0.4-5		Data replaced by later work by request of author	
					σ_{+2s}	0.4-5			
					σ_{o-}	0.6-4			
12	Schlachter et al.	1980	E		F_+^∞	0.3-4			b
					F_o^∞	0.15-4			a
					F_-^∞	0.15-4			b
53	Howald et al.	1981	E	H^-	σ_{-o}	1-25			b
					σ_{-+}	7.5-25			c
61	Kubach and Sidis	1981	T	H^+	σ_{+o}	0.2-5	PVB	7 state	d
75	Nagata	1982	E	H^+	σ_{+o}	0.4-5			b
60	Kimura et al.	1982	T	H^+	σ_{+o}	0.01-10	PSS-ETF	8 state	c
				H^+	$\sigma_{+,2s}$	0.01-10	PSS-ETF	8 state	c
59	Kimura et al.	1982	T	H^+	σ_{+o}	0.1-10	PSS-ETF	8 state	c
				H^+	$\sigma_{+,2s}$	0.1-10	PSS-ETF	8 state	c
45	Ebel	1983	E	H^+	σ_{+o}	1-5			b
				H^+	σ_{+-}	1-5			c
				H^o	σ_{o+}	0.6-5			c
				H^0	σ_{o-}	0.3-5			b
38	Berkowitz and Zorn	1984	E	H^+	$\sigma_{+,2s}$	0.75-2.5			c
42	DuBois	1984	E	H^+	σ_{+o}	2-100			b
46	Fritsch	1984	T	H^+	σ_{+o}	0.2-20	AO		b
					$\sigma_{+,2s}$	0.2-20	AO		b
54	Howald et al.	1984	E	H^o	σ_{o+}	7.5-25			c
				H^o	σ_{o-}	1-25			b
76	Nagata	1984	E	H^+	$\sigma_{+,2s}$	0.4-5			c
				POTASSIUM					
55	Il'in et al.	1967	E	H^+	σ_{+o}	10-180			c
					F_o^∞	20			b
87	Sellin and Granoff	1967	E	H^+	$\sigma_{+,2s}$	10-30		Absolute value of cross section doubtful due to normalization	
50	Gruebler et al.	1970	E	D^+	σ_{+o}	0.5-8.5			d
				H^+	σ_{+o}	1.2-17			d
				D^+	σ_{+o}	0.6-8.5			d
				H^+	σ_{+o}	1.4-17			d
57	Inoue	1972	E	H^+	σ_{+o}	0.15-8.3			d
77	O'Hare et al.	1975	E	H^+	σ_{+o}	20-100			c
58	Janev and Radulovic	1978	T	H^o	σ_{o-}	10^{-3}-2	LZ	Semiempirical elements	d
74	Nagata	1980	E	H^+	σ_{+o}	0.4-5			c
				H^+	$\sigma_{+,2s}$	0.4-5			c
				H^o	σ_{o-}	0.5-5			c

17 July 2023 14:50:05

Table 1. Sources of charge transfer cross sections and equilibrium fractions for hydrogen atoms and ions with metal vapors --Continued

Reference	Authors	Year	Exp./Theo.	Projectile	Quantity Reported	Energy Range (keV/u)	Method[a]	Comments	Accuracy
30	Anderson et al.	1980	E	H^0	σ_{0+}	30-200			c
			E	H^0	σ_{0-}	30-200			b
			E	H^-	σ_{-0}	30-200			b
			E	H^-	σ_{-+}	30-200			c
					F_0^∞	30-200			a
					F_-^∞	30-150			b
81	Olson and Liu	1980	T	H^-	σ_{-0}	0.04-0.3	PSS		c
61	Kubach and Sidis	1981	T	H^+	σ_{+0}	0.2-5	PVB	7-state	b
60	Kimura et al.	1982	T	H^+	σ_{+0}	0.01-10	PSS	8-state	b
				H^+	$\sigma_{+,2s}$	0.01-10	PSS	8-state	b
75	Nagata	1982	E	H^+	σ_{+0}	0.3-5			b
45	Ebel	1983	E	H^+	σ_{+0}	0.3-5			b
				H^+	σ_{+-}	0.4-5			c
				H^0	σ_{0+}	0.7-5			c
				H^0	σ_{0-}	0.2-5			b
38	Berkowitz and Zorn	1984	E	H^+	$\sigma_{+,2s}$	0.5-2.5			c
46	Fritsch	1984	T	H^+	σ_{+0}	0.2-20	AO		b
					$\sigma_{+,2s}$	0.2-20	AO		b
				RUBIDIUM					
87	Sellin and Granoff	1967	E	H^+	$\sigma_{+,2s}$	5-30		Normalization doubtful	
49	Girnius et al.	1977	E	D^+	σ_{+0}	0.5-10			b
				H^+	σ_{+0}	10-20			b
					F_-^∞	0.55-14			a
					F_-^∞	20			a
58	Janev and Radulovic	1978	T	H^0	σ_{0-}	10^{-3}-2	LZ	Semiempirical matrix elements	d
30	Anderson et al.	1980	E	H^0	σ_{0+}	30-200			c
				H^0	σ_{0-}	30-100			b
				H^-	σ_{-0}	30-100			b
				H^-	σ_{-+}	30-100			c
					F_0^∞	30-200			a
					F_-^∞	30-150			b
74	Nagata	1980	E	H^+	σ_{+0}	0.4-5			c
			E	H^+	$\sigma_{+,2s}$	0.4-5			c
				H^0	σ_{0-}	0.5-5			c
81	Olson and Liu	1980	T	H^-	σ_{-0}	0.06-0.3	PSS		c
12	Schlachter et al.	1980	E		F_+^∞	0.75-3.75			b
					F_0^∞	0.15-3.75			a
					F_-^∞	0.15-3.75			a
61	Kubach and Sidis	1981	T	H^+	σ_{+0}	0.2-5	PVD	7-state	b
60	Kimura et al.	1982	T	H^+	σ_{+0}	0.1-10	PSS-ETF	8-state	b
				H^+	$\sigma_{+,2s}$	0.1-10	PSS-ETF	8-state	b

17 July 2023 14:50:05

Table 1. Sources of charge transfer cross sections and equilibrium fractions for hydrogen atoms and ions with metal vapors --Continued

Reference	Authors	Year	Exp./Theo.	Projectile	Quantity Reported	Energy Range (keV/u)	Method[a]	Comments	Accuracy
75	Nagata	1982	E	H^+	σ_{+o}	0.3-5			b
45	Ebel	1983	E	H^+	σ_{+o}	0.2-5			b
				H^+	σ_{+-}	0.4-5			c
				H^o	σ_{o+}	0.5-5			c
				H^o	σ_{o-}	0.2-5			b
				CESIUM					
41	Donnally et al.	1964	E	H^+	$\sigma_{+,2s}$	0.16-3			d
55	Il'in et al.	1967	E	H^+	σ_{+o}	10-18			c
					F_o^∞	12.5			b
87	Sellin and Granoff	1967	E	H^+	$\sigma_{+,2s}$	2-30		Normalization uncertain	
17	Schlachter et al.	1969	E	D^+	σ_{+o}	0.5-1			c
				H^+	σ_{+o}	2-15			c
				H^+	σ_{+-}	2-15			d
				H^o	σ_{o+}	1-5			c
				H^o	σ_{o+}	2-15			d
				D^o	σ_{o-}	1-5			c
				H^o	σ_{o-}	2-15			c
					F_+^∞	0.5-1.5			d
					F_+^∞	1.5-20			d
					F_o^∞	0.5-1.5			b
					F_o^∞	1.5-20			b
					F_-^∞	0.5-1.5			b
					F_-^∞	1.5-20			b
90	Spiess et al.	1970	E	H^o	σ_{o-}	2.5			c
50	Gruebler et al.	1970	E	H^+	σ_{+o}	1.3-20			d
				H^+	σ_{+-}	1-20			d
62	Leslie et al.	1971	E	H^-	σ_{-o}	2-30		Data multiplied by a factor of 2	c
				H^-	σ_{-+}	2-30			c
89	Spiess et al.	1972	E	H^+	σ_{+o}	0.5-2.5			c
				H^+	$\sigma_{+,2s}$	2.4			c
15	Pradel et al.	1974	E	D^+	$\sigma_{+,2s}$	0.1-0.75			b
				H^+	$\sigma_{+,2s}$	1.3-3			b
11	Tuan et al.	1974	E	H^+	$\sigma_{+,2s}$	0.4-3			c
68	Meyer and Anderson	1975	E		F_-^∞	0.75-5.75			b
69	Meyer and Anderson	1975	E	H^+,D^+	σ_{+o}	0.8-30			c
40	Cisneros et al.	1976	E	D^+	σ_{+-}	0.26-1.3			d
83	Olson et al.	1976	T	H^+	σ_{+o}	0.1-3	PSS	4-state	b
				H^+	$\sigma_{+,2s}$	0.1-3	PSS	4-state	c
				H^o	σ_{o-}	0.1-3	PSS	4-state	d
				H^-	σ_{-o}	0.1-3	PSS	4-state	b
67	Meyer et al.	1977	E	H^+	σ_{+o}	40-120			c
49	Girnius et al.	1977	E		F_-^∞	0.5-3			b

17 July 2023 14:50:05

Table 1. Sources of charge transfer cross sections and equilibrium fractions for hydrogen atoms and ions with metal vapors --Continued

Reference	Authors	Year	Exp./Theo.	Projectile	Quantity Reported	Energy Range (keV/u)	Method[a]	Comments	Accuracy
48	Girnius et al.	1977	E	H^0	σ_{0+}	30-200			c
				H^0	σ_{0-}	30-200			c
				H^-	σ_{-0}	30-200			b
				H^-	σ_{-+}	30-200			c
					F_0^∞	30-200			a
52	Hooper and Willmann	1977	T	D^0	σ_{0-}	0.5-2.5		Analysis of equilibrium yields	d
58	Janev and Radulovic	1978	T	H^0	σ_{0-}	10^{-3}-2	LZ	Semiempirical matrix elements	d
88	Sidis and Kubach	1978	T	H^+	σ_{+0}	0.05-4	PVB	6-state	b
				H^+	$\sigma_{+,2s}$	0.05-4	PVB	6-state	c
51	Hiskes et al.	1978	T	H^0	σ_{0-}	0.1-2.5	PSS	4-state	d
30	Anderson et al.	1980	E		F_0^∞	30-200			a
74	Nagata	1980	E	H^+	σ_{+0}	0.4-5			c
				H^+	$\sigma_{+,2s}$	0.4-5			c
				H^0	σ_{0-}	0.5-5			c
66	Meyer	1980	E	H^+	σ_{+0}	0.1-2			b
				H^0	σ_{0-}	0.1-2			c
				H^-	σ_{-0}	0.1-2			b
					F_-^∞	0.1-1			b
78	Olson	1980	T	H^0	σ_{0-}	0.02-1	QM	2-state	b
81	Olson and Liu	1980	T	H^-	σ_{-0}	0.08-0.3	PSS		c
12	Schlachter et al.	1980	E	D^0	σ_{0-}	1.3-5			c
				D^-	σ_{-0}	1.3-5			b
					F_+^∞	1.25-3.75			b
					F_0^∞	0.15-3.75			a
					F_-^∞	0.15-3.75			b
60	Kimura et al.	1982	T	H^+	σ_{+0}	0.01-10	PSS-ETF		b
				H^+	$\sigma_{+,2s}$	0.01-10	PSS-ETF		b
75	Nagata	1982	E	H^+	σ_{+0}	0.3-5			c
70	Miethe et al.	1982	E	D^0	σ_{0-}	0.08-1.3			b
				H^0	σ_{0-}	0.1-5			b
80	Olson et al.	1984	T	H^0	σ_{0-}	0.1-10	MO		b
32	Bae et al.	1985	E	H^+	σ_{+0}	0.05-4			b
				MAGNESIUM					
56	Il'in et al.	1965	E	H^+	σ_{+0}	10-80			c
84	Oparin et al.	1967	E		F_0^∞	12-120			b
35	Berkner et al.	1969	E	H^+	σ_{+0}	5-70			b
				H^0	σ_{0+}	5-70			b
				H^0	σ_{0-}	5-70			b
				H^-	σ_{-0}	5-70			c

17 July 2023 14:50:05

Table 1. Sources of charge transfer cross sections and equilibrium fractions for hydrogen atoms and ions with metal vapors --Continued

Reference	Authors	Year	Exp./Theo.	Projectile	Quantity Reported	Energy Range (keV/u)	Method[a]	Comments	Accuracy
34	Baragiola et al.	1973	E		F_+^∞	4-40			a
					F_o^∞	4-30			a
					F_-^∞	4-40			b
36	Berkner et al.	1977	E		F_+^∞	1.5-19			b
					F_o^∞	1.5-19			a
					F_-^∞	1.5-19			a
72	Morgan and Eriksen	1978	E	H^+	σ_{+-}	1-80			b
73	Morgan et al.	1979	E		F_-^∞	1.2-50			b
71	Morgan and Eriksen	1979	E	H^+	$\sigma_{+,2s}$	3-80			b
10	Morgan and Eriksen	1979	E	D^+	σ_{+o}	1.1-8			b
				H^+	σ_{+o}	3.4-80			b
				H^+,D^+	σ_{+-}	1-80			b
10	Morgan and Eriksen	1979	T	H^+	σ_{+o}	1-100	CBE		d
82	Olson and Liu	1979	T	H^+	σ_{+o}	0.05-10	PSS	3-state	c
63	Mayo	1982	E		F_+^∞	5-50			a
					F_o^∞	1-50			a
65	McFarland et al.	1982	E		F_+^∞	0.75-1.5			b
					F_o^∞	0.15-1.5			a
					F_-^∞	0.15-1.5			a
29	Alvarez et al.	1984	E	H^+	σ_{+-}	0.5-5			b
42	DuBois	1984	E	H^+	σ_{+o}	2-100			b
				CALCIUM					
73	Morgan et al.	1979	E		F_-^∞	1-50			d
63	Mayo	1982	E		F_+^∞	5-50			c
					F_o^∞	1-50			a
65	McFarland et al.	1982	E		F_+^∞	0.75-1.5			c
					F_o^∞	0.15-1.5			a
					F_-^∞	0.15-1.5			a
64	Mayo et al.	1983	E	H^+,D^+	σ_{+o}	1-30			b
				H^o,D^o	σ_{o-}	1-30			b
				H^o,D^o	σ_{o+}	1-30			b
					σ_{-o}	1-30		Inferred	c
				H^+,D^+	σ_{+-}	1-30			b
64	Mayo et al.	1983	T	H^+	σ_{+o}	1-50	CBE		d
				STRONTIUM					
37	Berkner et al.	1977	E		F_+^∞	1.3-15			b
					F_o^∞	1.3-10.5			a
					F_-^∞	1.3-15			a
73	Morgan et al.	1979	E		F_-^∞	0.9-50			a
63	Mayo	1982	E		F_+^∞	5-50			b
					F_o^∞	1-50			a

17 July 2023 14:50:05

Table 1. Sources of charge transfer cross sections and equilibrium fractions for hydrogen atoms and ions with metal vapors --Continued

Reference	Authors	Year	Exp./Theo.	Projectile	Quantity Reported	Energy Range (keV/u)	Method[a]	Comments	Accuracy
65	McFarland et al.	1982	E		F_+^∞	0.4-1.5			b
					F_o^∞	0.15-1.5			a
					F_-^∞	0.15-1.5			a
64	Mayo et al.	1983	E	H^+,D^+	σ_{+o}	1-30			b
				H^+,D^+	σ_{+-}	1-30			b
				H^o,D^o	σ_{o-}	1-30			b
				H^o,D^o	σ_{o+}	1-30			b
					σ_{-o}	1-30		Inferred	c
64	Mayo et al.	1983	T	H^+	σ_{+o}	1-100	CBE		d
				BARIUM					
10	Morgan and Eriksen	1979	E	D^+	σ_{+o}	2-9			b
				H^+	σ_{+o}	4-90			b
				D^+	σ_{+-}	1.5-9			b
				H^+	σ_{+-}	4-93			b
10	Morgan and Eriksen	1979	T	H^+	σ_{+o}	1-100	CBE		d
71	Morgan and Eriksen	1979	E	H^+	$\sigma_{+,2s}$	3-80			b
73	Morgan et al.	1979	E		F_-^∞	0.6-50			b
65	McFarland et al.	1982	E		F_+^∞	0.15-1.5			b
					F_o^∞	0.15-1.5			a
					F_-^∞	0.15-1.5			a
				CADMIUM					
84	Oparin et al.	1967	E		F_-^∞	15-70			b
				LEAD					
33	Baragiola and Salvatelli	1973	E	H^+	σ_{+o}	6-40			b
				H^+	σ_{+-}	7-40			b
				H^o	σ_{o+}	10-40			b
				H^o	σ_{o-}	10-40			b

[a]Definition of method abbreviations:

LZ	Landau Zener approximation
MO	Molecular orbital calculation
AO	Atomic orbital calculation
PSS	Perturbed stationary state approximation
PSS-ETF	Perturbed stationary state approximation with electron translation factors
PVB	Projected valence bond method
QM	Quantum mechanical method
CBE	Classical binary encounter approximation

17 July 2023 14:50:05

Table 2. Recommended values of σ_{+0}, the cross section for electron capture (into all states of the hydrogen atom) in collisions of protons with metal vapor atoms. Cross sections are in 10^{-16} cm^2.

E (keV/u)	Li	Na	K	Rb	Cs	Mg	Ca	Sr	Ba	Pb
0.1					120.					
0.2	1.4		28.	63.	155.					
0.5	6.4		48.	90.	164.					
0.7	9.7		55.	93.	159.					
1.0	16.	43.	61.	96.	144.	8.0	9.4	8.6		
2.0	36.	68.	62.	87.	102.	9.3	18.	20.	20.	
3.0	42.	75.	57.	77.	78.	13.	31.	31.	25.	
5.0	38.	66.	40.	56.	55.	18.	37.	34.	29.	
7.0	30.	53.	30.	42.	43.	21.	35.	29.	23.	13.
10.0	17.	24.	21.	28.	29.	20.	26.	22.	16.	14
20.0	3.1	3.5	8.3	9.4	14.	8.0	6.7	5.2	4.1	9.3
50.0	0.42	0.71	2.1		4.8	0.49		1.7	1.6	
70.0	0.22	0.47	1.2		3.0	0.19		1.3	1.0	
100.	0.11	0.32	0.71		1.6	0.11			0.52	
200.	0.028	0.19	0.23		0.25	0.09				

Table 3. Recommended values of σ_{+2s}, the cross section for electron capture into the 2s state of the hydrogen atom in collisions of protons with metal vapor atoms. Cross sections are in 10^{-16} cm^2.

E (keV/u)	Mg	Ba
0.5		
0.7		
1.0		
2.0		5.3
3.0		5.6
5.0	2.2	4.1
7.0	3.1	2.9
10.0	2.8	1.7
20.0	1.0	0.27
30.0	0.36	0.096
50.0	0.041	0.053
70.	0.007	0.044

Table 4. Recommended values for σ_{+-}, the cross section for double electron capture for collisions of protons with metal vapor atoms. Cross sections are in 10^{-16} cm^2.

E (keV/u)	Na	K	Rb	Mg	Ca	Sr	Ba	Pb
0.5		0.084	0.17	0.21				
0.7		0.105	0.21	0.21				
1.0	0.027	0.117	0.21	0.21	0.087	0.064		
2.0	0.048	0.116	0.19	0.16	0.11	0.076	0.068	
3.0	0.065	0.091	0.16	0.14	0.082	0.070	0.078	
5.0	0.086	0.064	0.10	0.30	0.062	0.054	0.079	
7.0				0.36	0.082	0.027	0.053	0.28
10.0				0.30	0.078	0.012	0.029	0.34
20.0				0.046	0.016	0.011	0.018	0.26
50.0				0.0006		0.007	0.010	
70.0				0.0002			0.006	

Table 5. Recommended values for σ_{o+}, the cross section for electron loss in collisions of hydrogen atoms with metal vapor atoms. Cross sections are in 10^{-16} cm^2.

E (keV/u)	Li	Na	K	Rb	Mg	Ca	Sr	Pb
0.5								
0.7			0.12	0.15				
1.0			0.17	0.23				
2.0		0.14	0.37	0.49		0.33	0.32	
3.0		0.24	0.61	0.79		0.72	0.57	
5.0		0.44	1.3	1.4	0.31	1.1	0.93	
7.0		0.63			0.41	1.3	1.2	
10.0		0.88			0.60	2.9	2.2	0.67
20.0		1.5			1.6	3.7	4.3	1.5
30.0	2.4	2.0	5.9	5.9	2.4	3.6	4.3	2.1
50.0	2.4	2.6	6.2	6.3	2.8		4.0	
70.0	2.3	2.9	6.1	6.2	3.1		3.7	
100.0	2.1	2.9	5.7	5.9				
200.0	1.6	2.5	4.8	5.5				

Table 6. Recommended values of σ_{o-}, the cross section for electron capture in collisions of hydrogen atoms with metal vapor atoms. Cross sections are in 10^{-16} cm^2.

E (keV/u)	Li	Na	K	Rb	Cs	Mg	Ca	Sr	Pb
0.1					3.6				
0.2			2.1	3.4	6.3				
0.5		1.7	4.1	5.4	8.1				
0.7		2.1	4.4	5.6	7.1				
1.0		2.5	4.3	5.4	5.9		2.4	2.6	
2.0		2.6	2.9	3.9	3.1		2.0	2.1	
5.0		1.5	1.1	1.6	0.83	1.04	1.5	1.2	
7.0		0.94			0.46	0.90	1.2	0.92	
10.0		0.45			0.23	0.69	0.82	0.49	0.75
20.0		0.064			0.12	0.21	0.17	0.10	0.45
30.0	0.016	0.029	0.055	0.075	0.092	0.076	0.059	0.033	0.24
50.0	0.0071	0.017	0.037	0.043	0.070	0.020		0.016	
70.0	0.0053	0.014	0.024	0.029	0.053	0.012		0.008	
100.0	0.0043	0.011	0.013	0.020	0.038				
200.0		0.006	0.004						

17 July 2023 14:50:05

Table 7. Recommended values of σ_{-0}, the cross section for electron detachment in collisions of H^- with metal vapor atoms. Cross sections are in 10^{-16} cm^2.

E (keV/u)	Li	Na	K	Rb	Cs	Mg
1		42.			30.	
2		35.			33.	
3		29.			35.	
5		25.			36.	
7		22.			36.	
10		20.			35.	23.
20		16.			31.	16.
30	14.	14.	24.	26.	28.	14.
50	12.	13.	20.	23.	24.	13.
70	10.8	12.	18.	21.	21.	12.
100	9.5	11.	16.	19.	18.	
200	7.1	8.4	13.	15.	13.	

Table 8. Recommended values of σ_{-+}, the cross section for double electron loss in collisions of H^- with metal vapor atoms. Cross sections are in 10^{-16} cm^2.

E (keV/u)	Li	Na	K	Rb	Cs
2					0.12
5					0.54
7		0.08			0.86
10		0.15			1.3
20		0.38			2.2
30	0.68	0.53	2.8	2.8	2.4
50	0.63	0.70	2.9	2.7	2.2
70	0.58	0.71	2.7	2.5	1.9
100	0.50	0.69	2.3	2.2	1.5
200	0.28	0.62	1.4	1.7	0.83

Table 9. Recommended values of F_+^∞, the H^+ equilibrium fraction for collisions of hydrogen atoms and ions with metal vapor atoms. F_+^∞ is a percent.

E (keV/u)	Na	Rb	Cs	Mg	Ca	Sr	Ba
0.3	0.055						
0.5	0.080					0.46	0.30
0.7	0.10	0.11				0.92	0.54
1.0	0.14	0.20		0.46		1.5	0.90
2.0	0.24	0.61	0.63	1.1		2.6	
3.0	0.33	1.2	1.1	1.4		3.0	
5.0	0.62		2.4	2.2		4.0	
7.0	1.2		4.4	3.3		5.8	
10.0	3.3		7.9	6.0	12.	12.	
20.0	37.		29.	29.	55.	57.	
30.0				61.	76.	74.	
50.0				87.	88.	83.	

Table 10. Recommended values of F_0^∞, the H^0 equilibrium fraction for collisions of hydrogen atoms and ions with metal vapor atoms. F_0^∞ is a percent.

E (keV/u)	Li	Na	K	Rb	Cs	Mg	Ca	Sr	Ba	Cd
0.2		96.		72.	66.	85.	68.	56.	68.	
0.3		93.		73.	68.	82.	66.	54.	71.	
0.5		92.		75.	73.	83.	77.	72.	82.	
0.7		91.		78.	77.	88.	84.	79.	88.	
1.0		91.		81.	83.	91.	89.	86.	92.	
2.0		91.		87.	92.	92.	93.	93.		
3.0		92.		90.	96.	93.	93.	94.		
5.0		93.			97.	94.	92.	93.		
7.0		94.			96.	94.	90.	90.		
10.		95.			91.	93.	86.	85.		
20.		59.	40.		69.	70.	44.	44.		88.
30.	19.	31.	32.	41.	54.	38.	22.	28.		71.
50.	9.3	15.	25.	34.	38.	12.	13.	19.		44.
70.	7.1	11.	19.	25.	28.	6.1				
100.	5.5	9.0	13.	15.	17.	4.0				
200.	2.5	5.1	2.9	2.1	2.7					

17 July 2023 14:50:05

Table 11. Recommended values of F_-^∞, the H^- equilibrium fraction for collisions of hydrogen atoms and ions with metal vapor atoms. F_-^∞ is a percent.

E (keV/u)	Li	Na	K	Rb	Cs	Mg	Ca	Sr	Ba
0.2		5.1		26.	27.	13.	32.	42.	34.
0.3		7.0		26.	26.	16.	34.	45.	29.
0.5		8.0		22.	23.	16.	22.	28.	17.
0.7		8.8		19.	19.	10.	14.	17.	11.
1.0		9.0		16.	14.	7.3	8.9	11.	7.6
2.0		8.9		10.	6.7	6.1	4.6	4.5	4.4
3.0		8.4		6.4	4.3	5.8	3.8	3.5	4.3
5.0		6.3		2.6	2.2	5.4	3.4	3.2	3.2
7.0		3.8		1.4	1.5	4.6	2.6	2.5	2.2
10.		2.0		0.61	0.96	3.4	1.8	1.6	1.2
20.		0.23		0.24	0.40	0.88	0.23	0.17	0.35
30.	0.030	0.060	0.13	0.21		0.25	0.07	0.09	0.21
50.	0.009	0.023	0.086	0.16		0.01	0.03	0.06	0.14
70.	0.005	0.016	0.054	0.08					
100.	0.003	0.011	0.022	0.02					

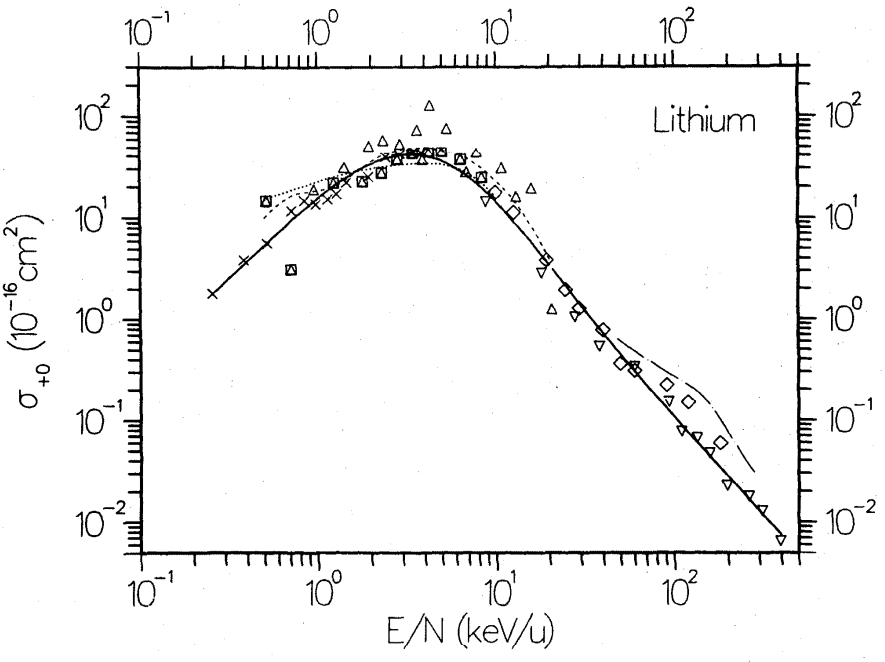

FIG. 2. Cross section σ_{+0} for single-electron capture in collisions of H^+ with Li vapor. Experimental data points: ◇, Ref. 55, c; ▽, Ref. 43, c; △, Ref. 50, H^+d; ⊠, Ref. 50, D^+ d; ×, Ref. 91, b. Theoretical curves: — · —, Ref. 79, c; - - - -, Ref. 47, b; · · · ·, Ref. 85, b. Recommended data: —.

17 July 2023 14:50:05

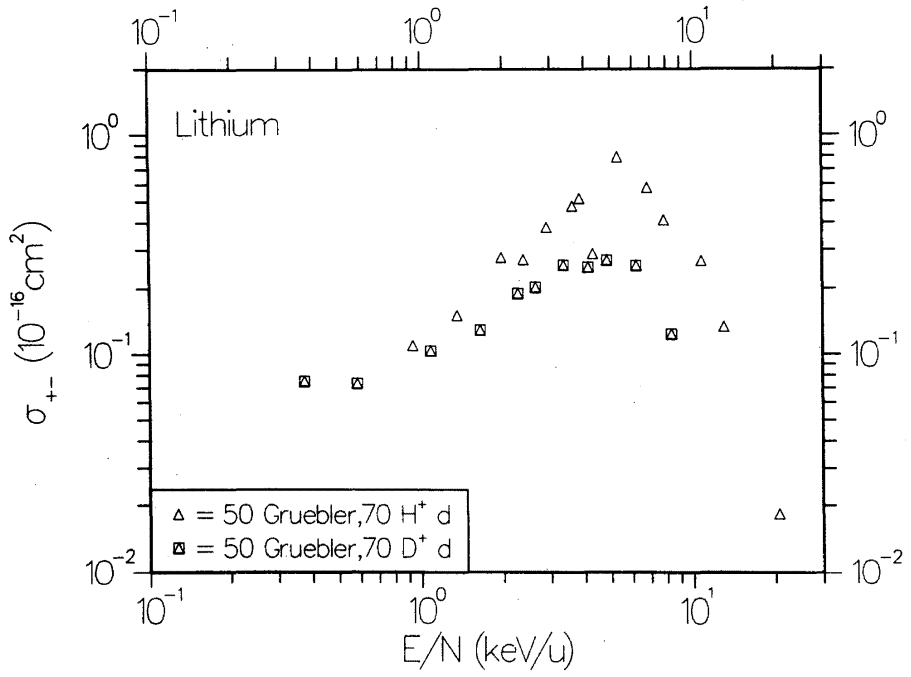

FIG. 3. Cross section σ_{+-} for double electron capture in collisions of H^+ with Li vapor.

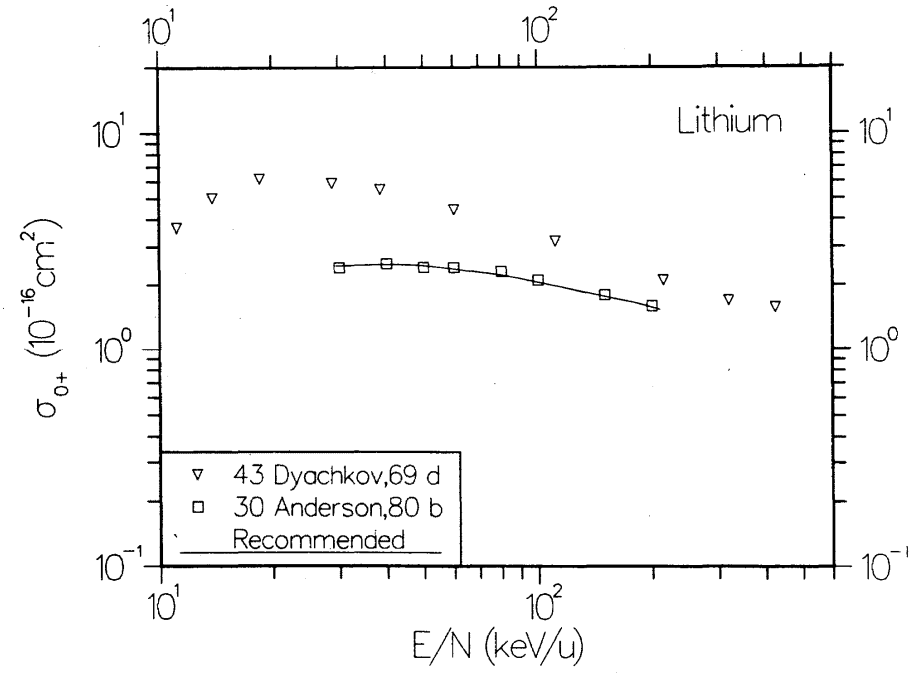

FIG. 4. Cross section σ_{0+} for electron loss in collisions of H^0 with Li vapor.

17 July 2023 14:50:05

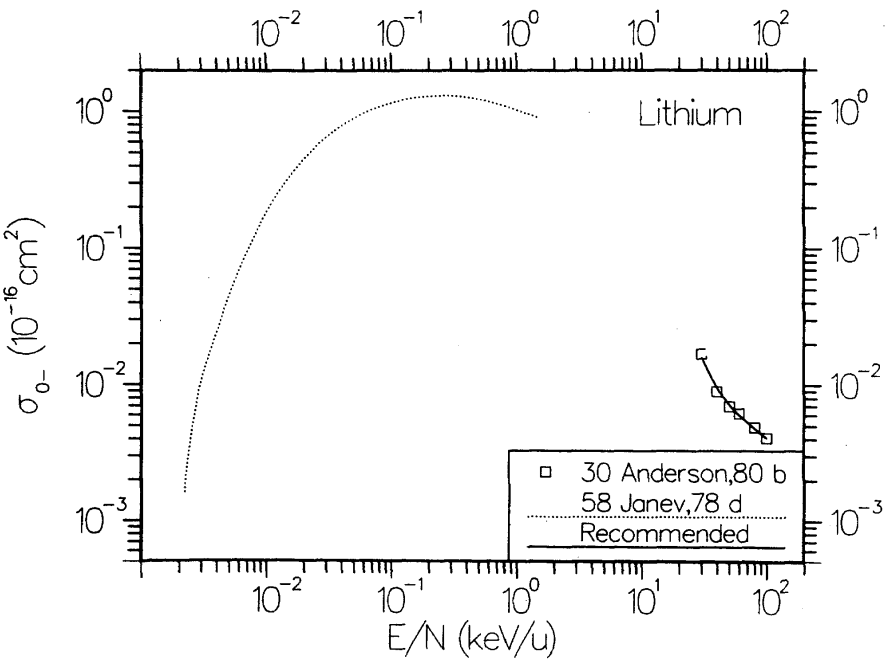

FIG. 5. Cross section σ_{0-} for electron capture in collisions of H^0 with Li vapor.

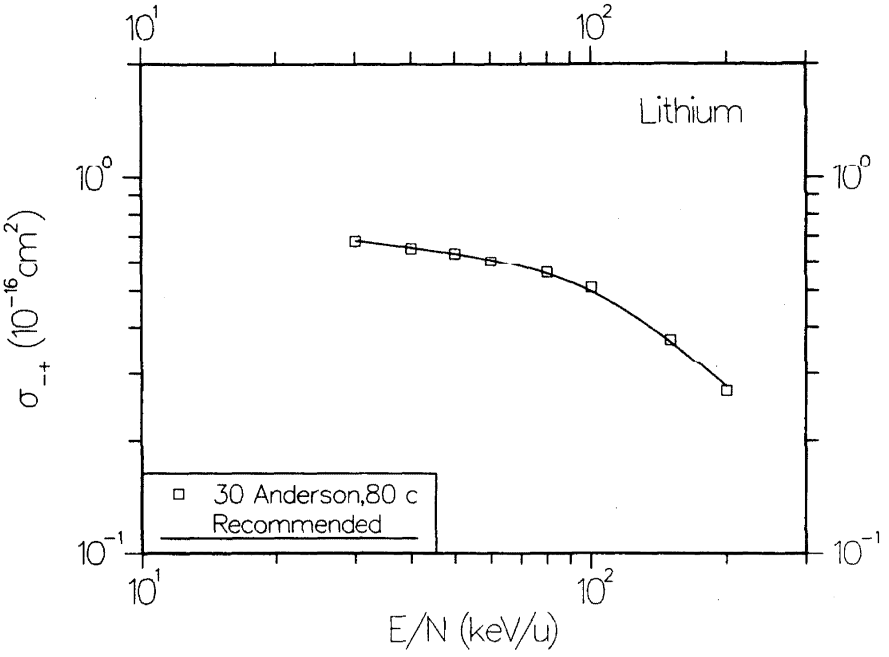

FIG. 6. Cross section σ_{-+} for double electron loss in collisions of H^- with Li vapor.

17 July 2023 14:50:05

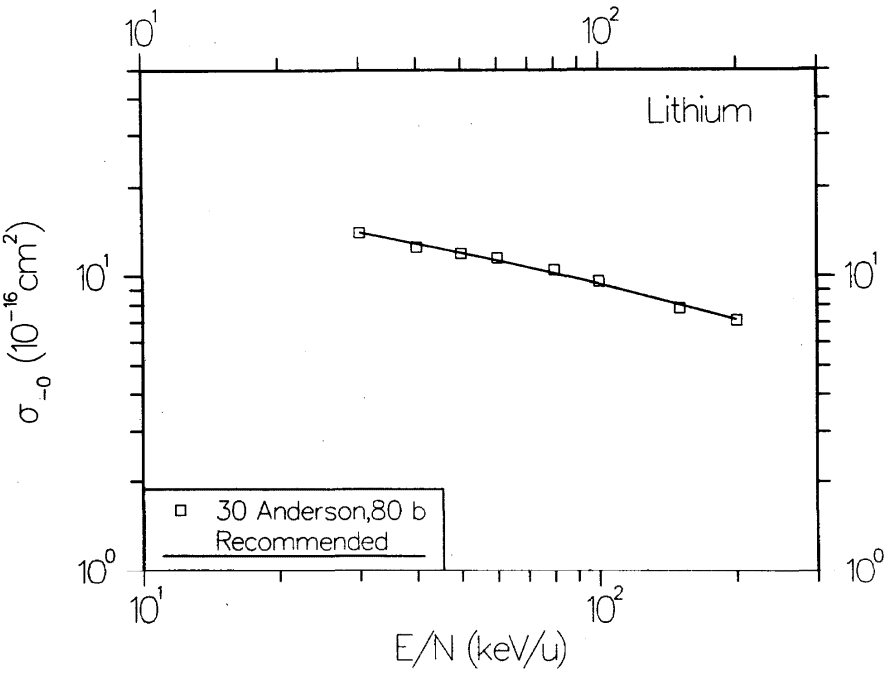

FIG. 7. Cross section σ_{-0} for detachment of electrons from H^- in collisions with Li vapor.

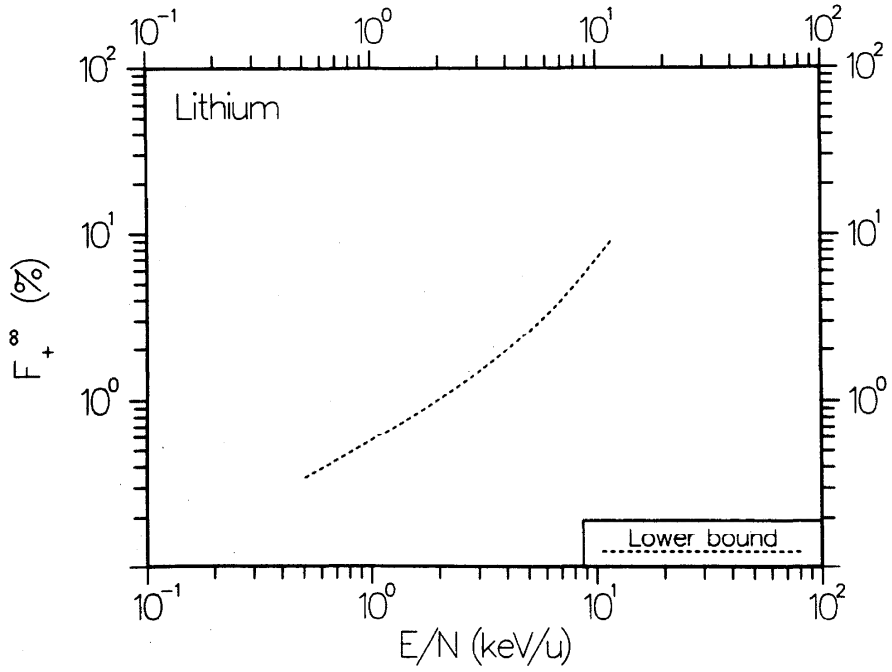

FIG. 8. Equilibrium fraction F_+^∞ for hydrogen atoms and ions incident on Li vapor. The lower bound is based on data taken from Ref. 50.

17 July 2023 14:50:05

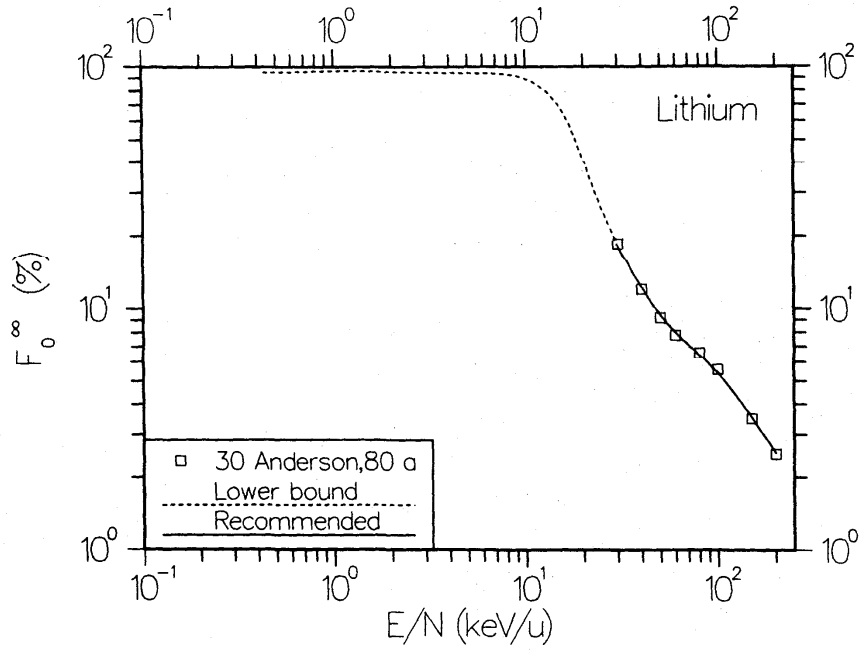

FIG. 9. Equilibrium fraction F_0^∞ for hydrogen atoms and ions incident on Li vapor. The lower bound is based on data taken from Refs. 44 and 50.

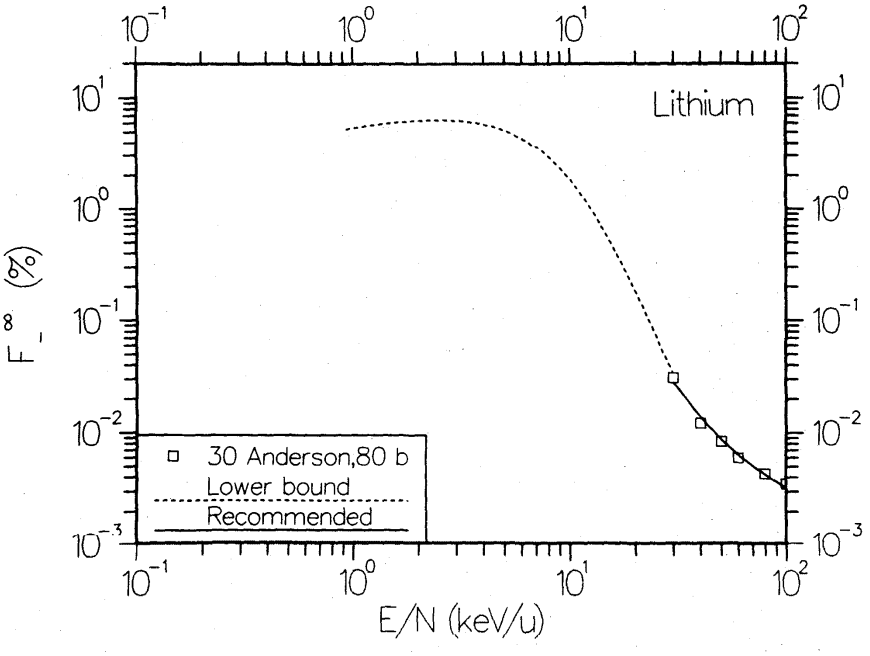

FIG. 10. Equilibrium fraction F_-^∞ for hydrogen atoms and ions incident on Li vapor. The lower bound is based on data taken from Refs. 44 and 50.

17 July 2023 14:50:05

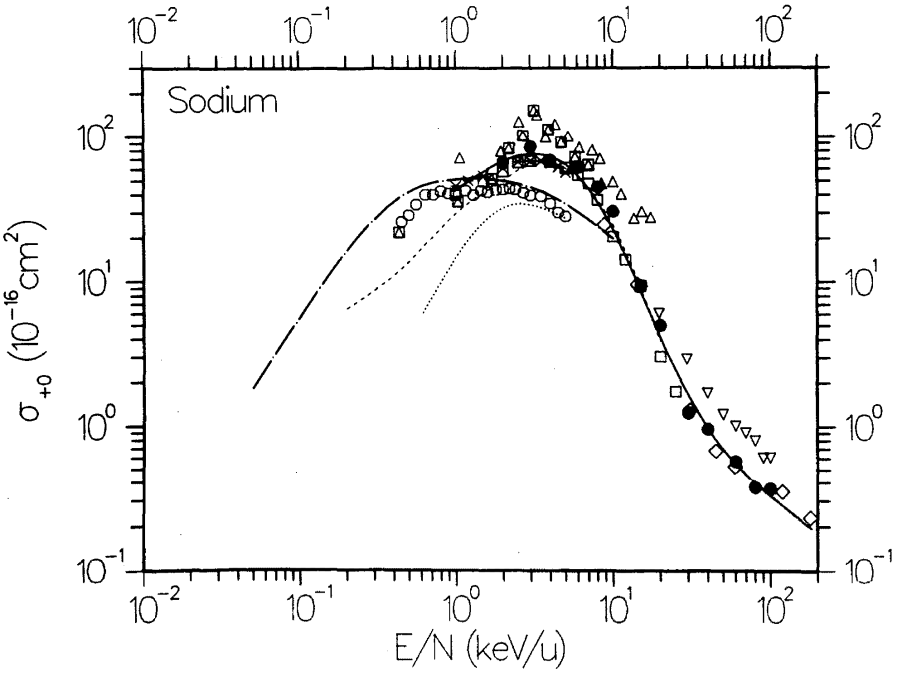

FIG. 11. Cross section σ_{+0} for electron capture into all states of the neutral hydrogen atom in collisions of H^+ with Na vapor. Experimental data points: ◇, Ref. 55, c; △, Ref. 50, H^+ d; ⊠, D^+ d; ▽, Ref. 77, c; □, Ref. 31, b; ○, Ref. 75, b; ×, Ref. 45, b; ●, Ref. 42, b. Theoretical curves: · · · ·, Ref. 61, σ_{2s+2p} d; – · – ·, Ref. 60, c; - - - -, Ref. 46, b. Recommended data: —.

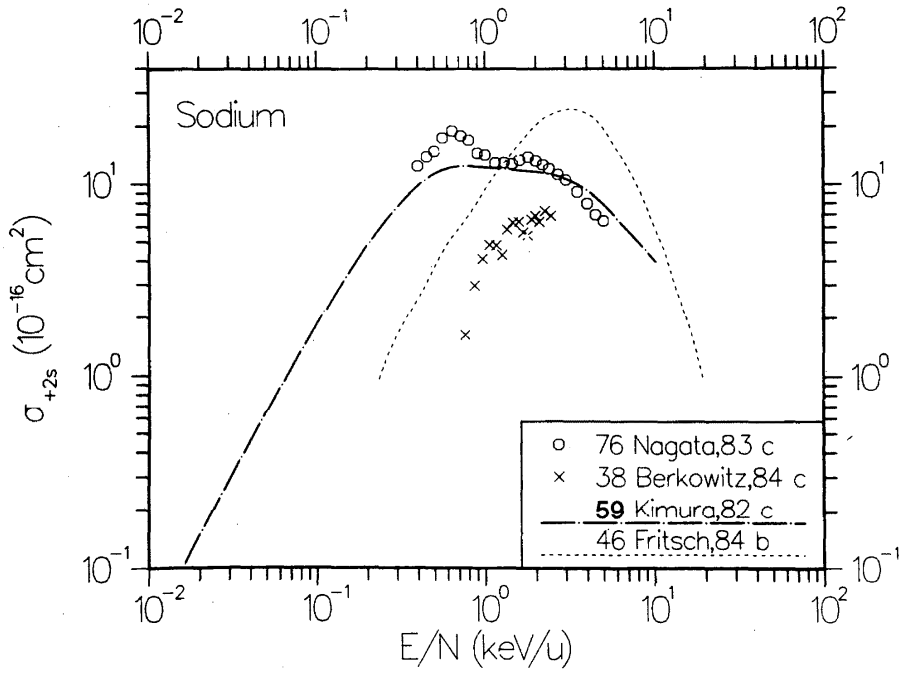

FIG. 12. Cross section σ_{+2s} for electron capture into the 2s state of the neutral hydrogen atom in collision of H^+ with Na vapor.

17 July 2023 14:50:05

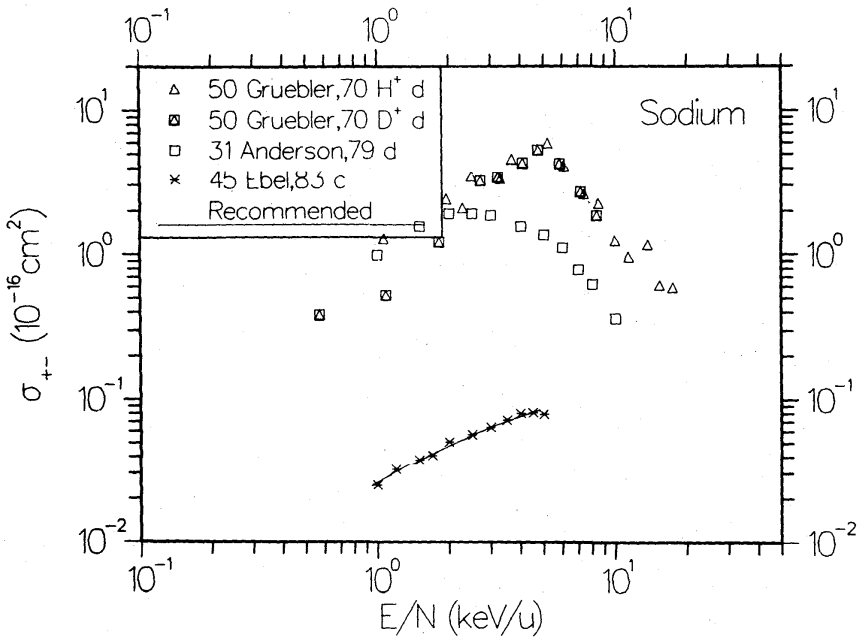

FIG. 13. Cross section σ_{+-} for double electron capture in collisions of H^+ with Na vapor.

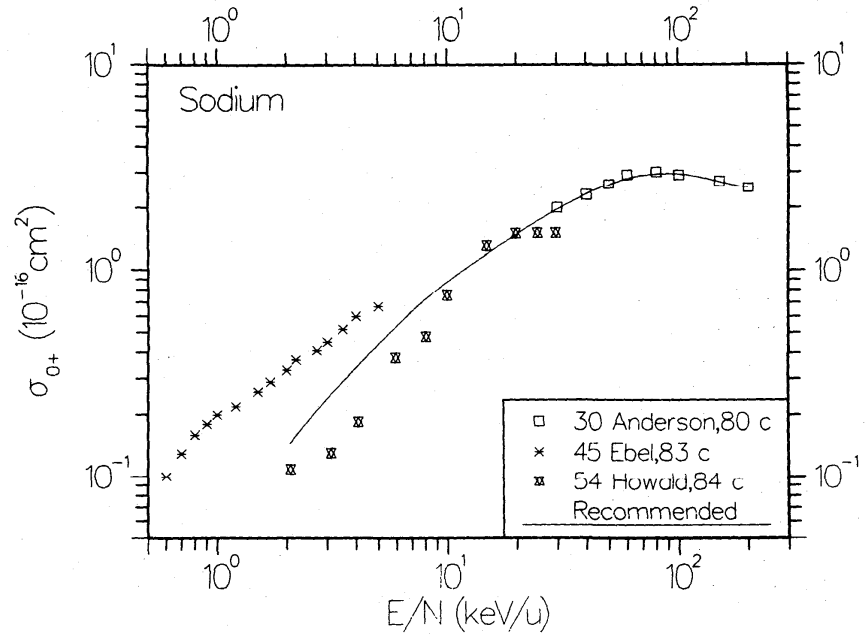

FIG. 14. Cross section σ_{0+} for electron loss in collisions of H^0 with Na vapor.

17 July 2023 14:50:05

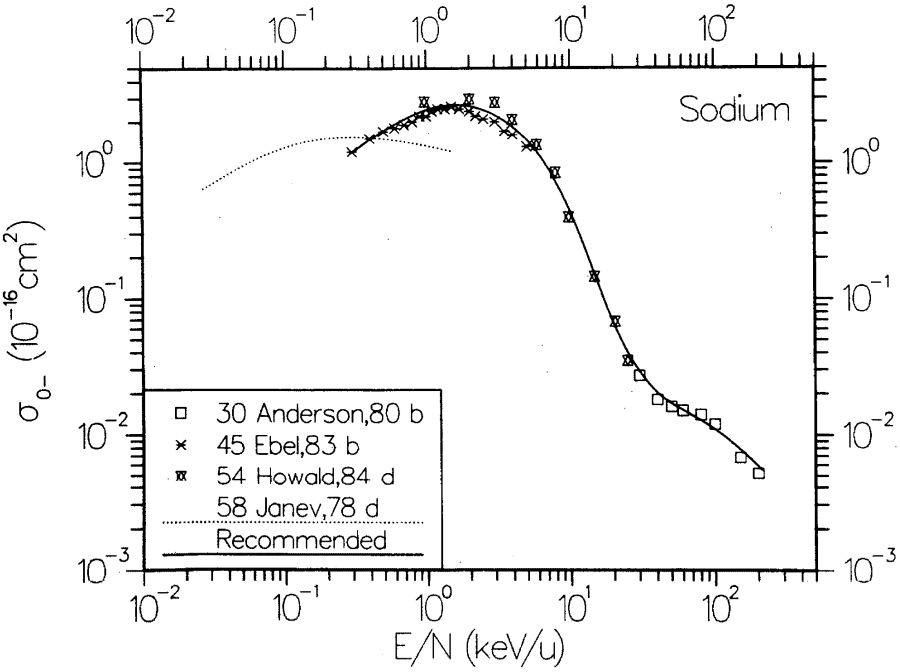

FIG. 15. Cross section σ_{0-} for electron capture in collisions of H^0 with Na vapor.

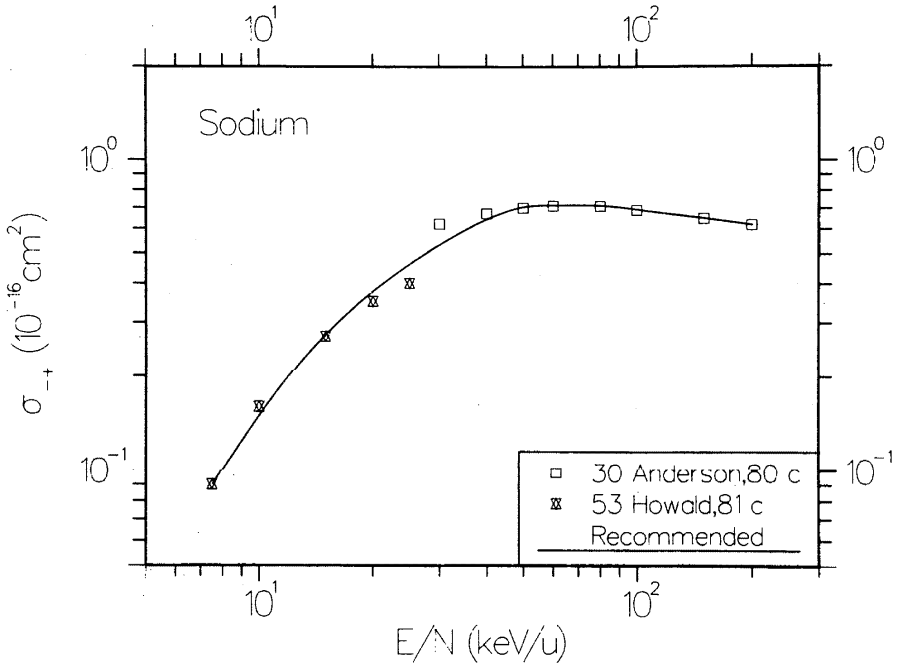

FIG. 16. Cross section σ_{-+} for double electron loss in collisions of H^- with Na vapor.

17 July 2023 14:50:05

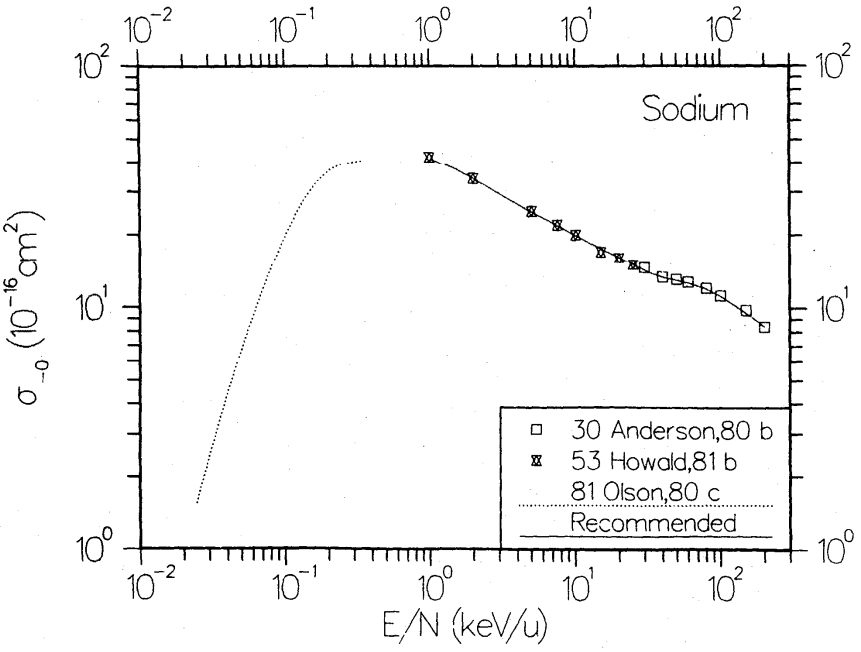

FIG. 17. Cross section σ_{-0} for detachment of electrons from H^- in collisions with Na vapor.

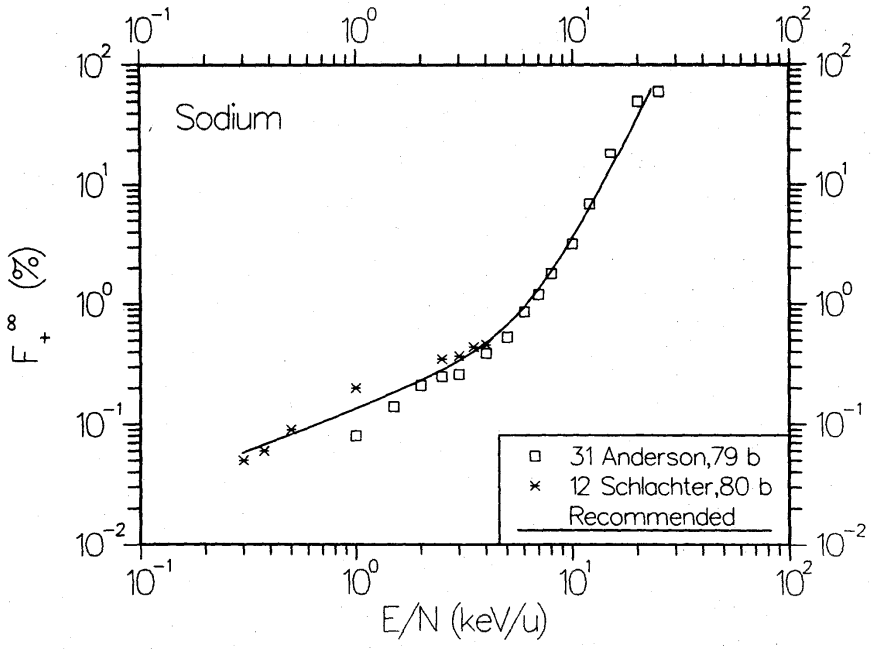

FIG. 18. Equilibrium fraction F_+^∞ for hydrogen atoms and ions incident on Na vapor.

17 July 2023 14:50:05

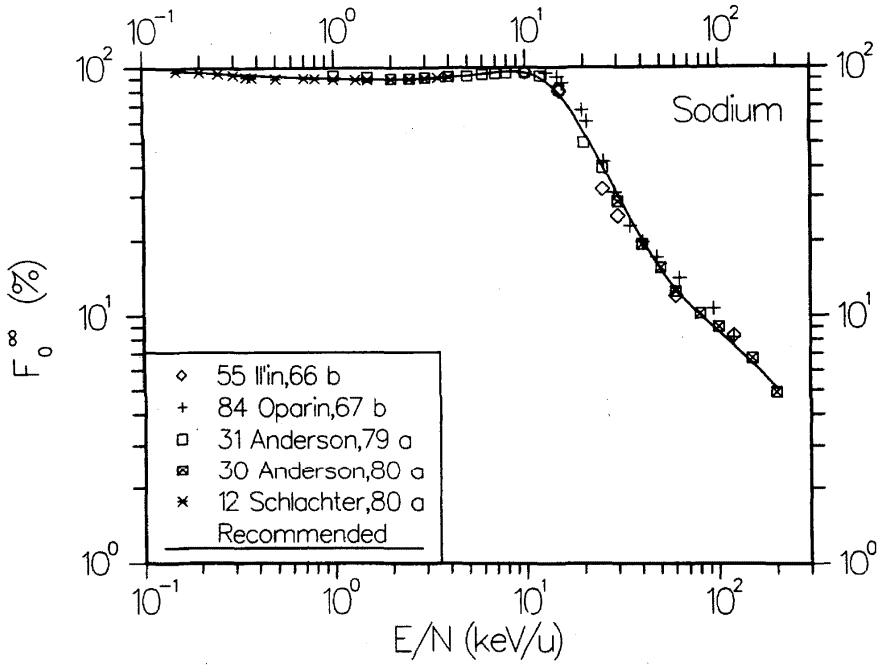

FIG. 19. Equilibrium fraction F_0^∞ for hydrogen atoms and ions incident on Na vapor.

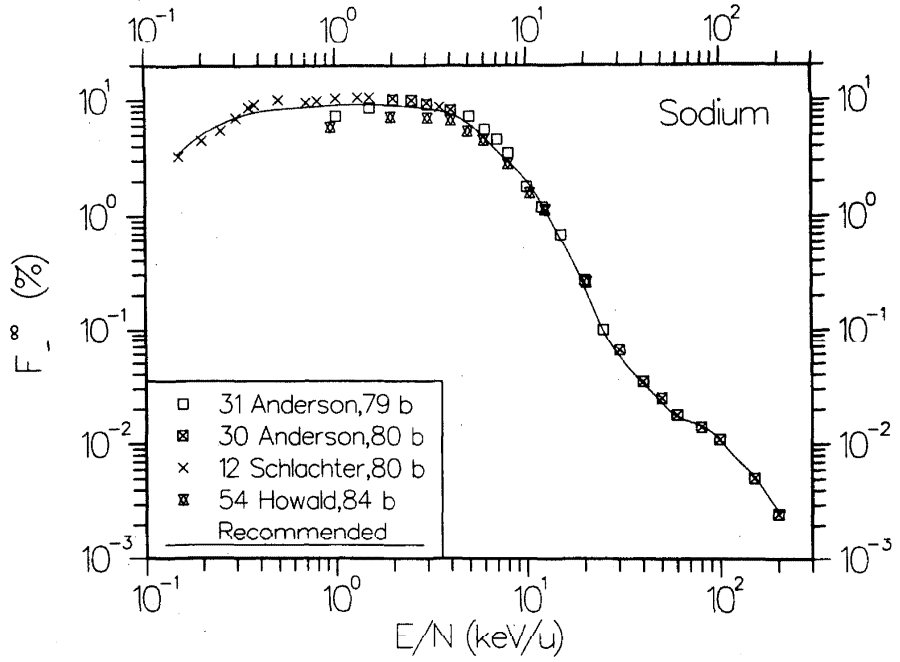

FIG. 20. Equilibrium fraction F_-^∞ for hydrogen atoms and ions incident on Na vapor.

17 July 2023 14:50:05

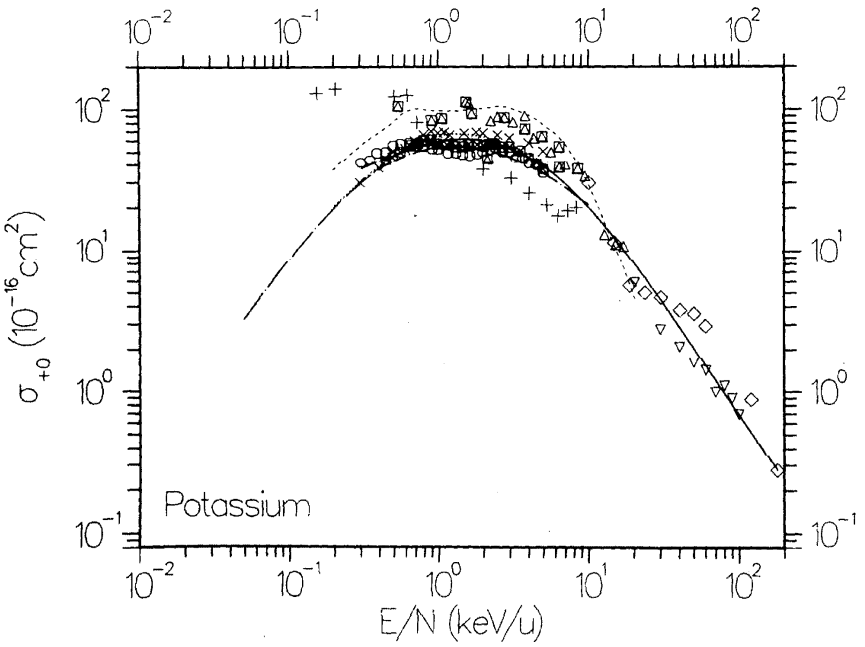

FIG. 21. Cross section σ_{+0} for electron capture into all states of the neutral hydrogen atom in collisions of H^+ with K vapor. Experimental points: ◇, Ref. 55, c; △, Ref. 50, H^+ d; ⊠, Ref. 50, D^+ d; +, Ref. 57, d; ▽, Ref. 77, c; ⊗, Ref. 74, c; ○, Ref. 75, b; ×, Ref. 45, b. Theoretical curves: · · · ·, Ref. 61, σ_{2s+2p} b; — · — ·, Ref. 60, b; - - - -, Ref. 46, b. Recommended data: —.

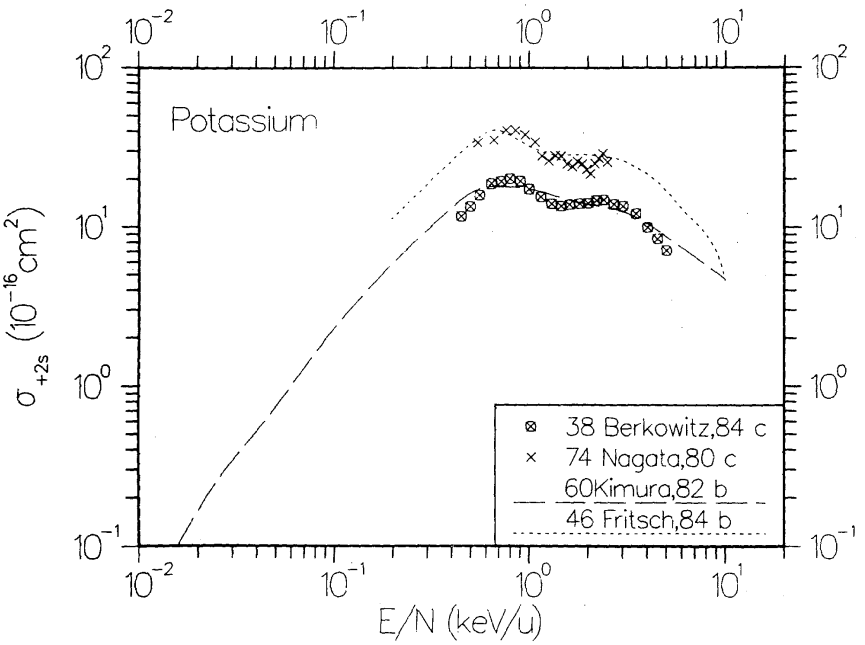

FIG. 22. Cross section σ_{+2s} for electron capture into the 2*s* state of the neutral hydrogen atom in collisons of H^+ with K vapor.

17 July 2023 14:50:05

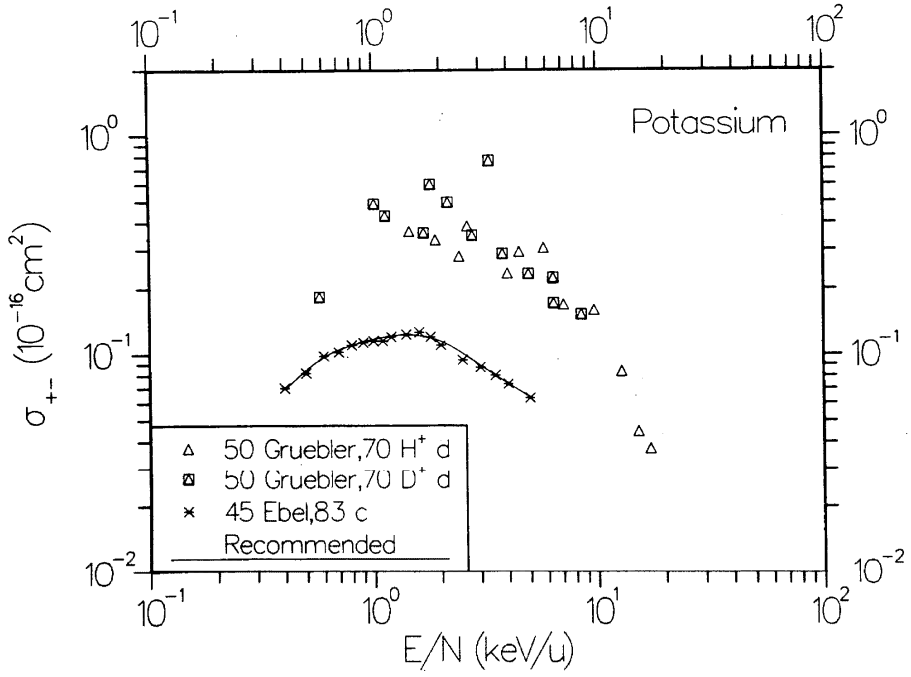

FIG. 23. Cross section σ_{+-} for double electron capture in collisions of H^+ with K vapor.

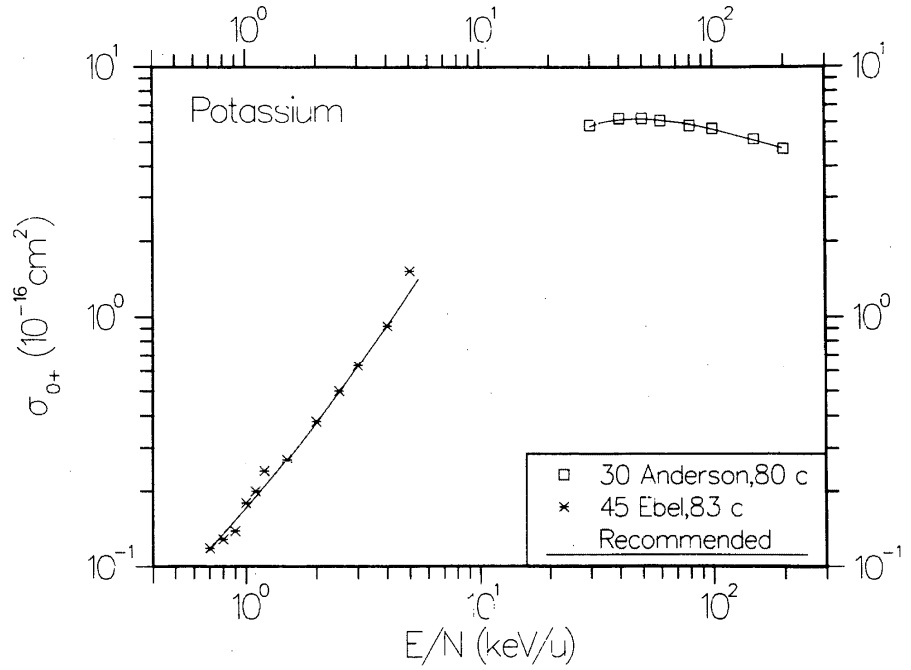

FIG. 24. Cross section σ_{0+} for electron loss in collisions of H^0 with K vapor.

17 July 2023 14:50:05

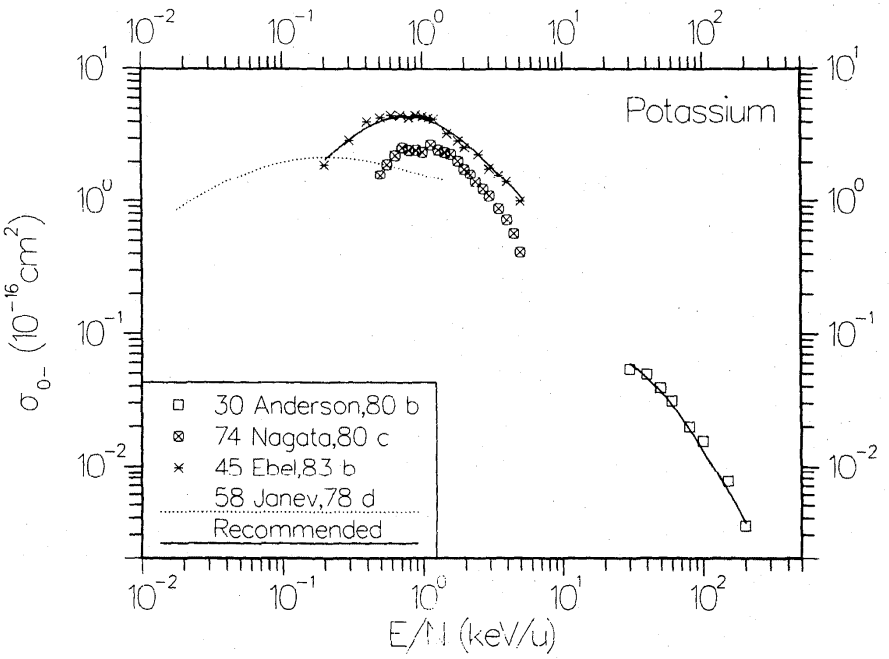

FIG. 25. Cross section σ_{0-} for electron capture in collisions of H^0 with K vapor.

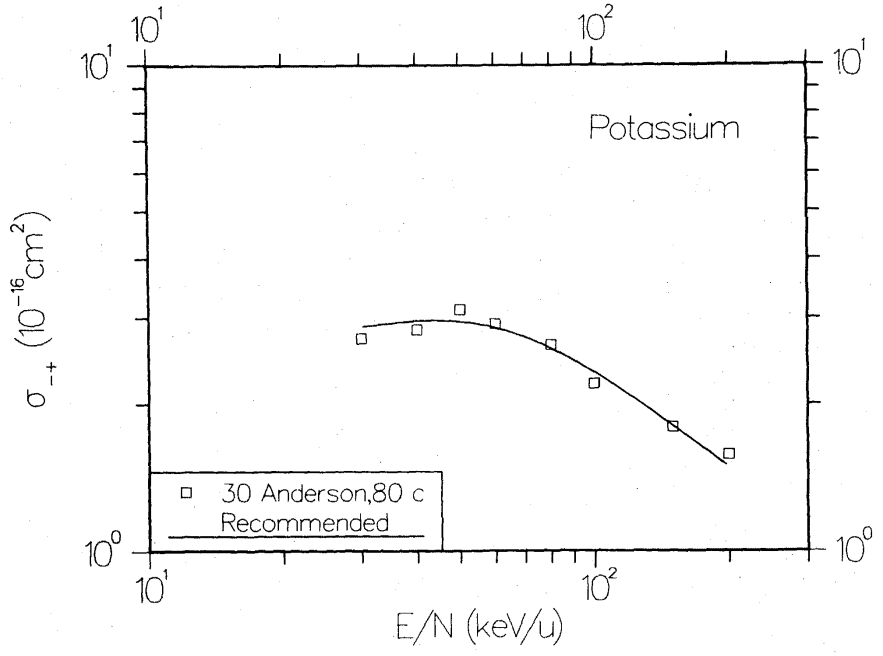

FIG. 26. Cross section σ_{-+} for double electron loss in collisions of H^- with K vapor.

17 July 2023 14:50:05

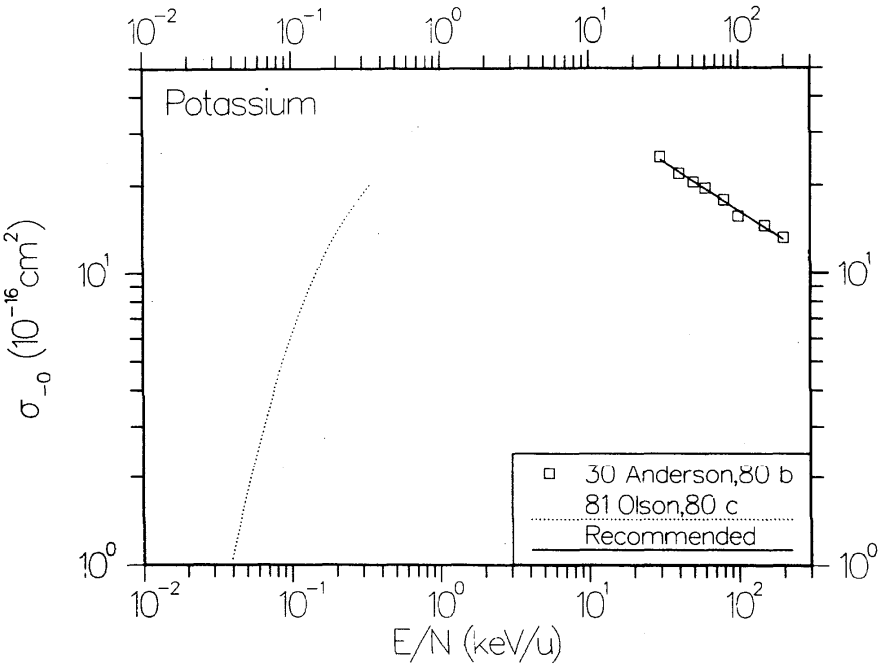

FIG. 27. Cross section σ_{-0} for detachment of electrons from H^- in collisions with K vapor.

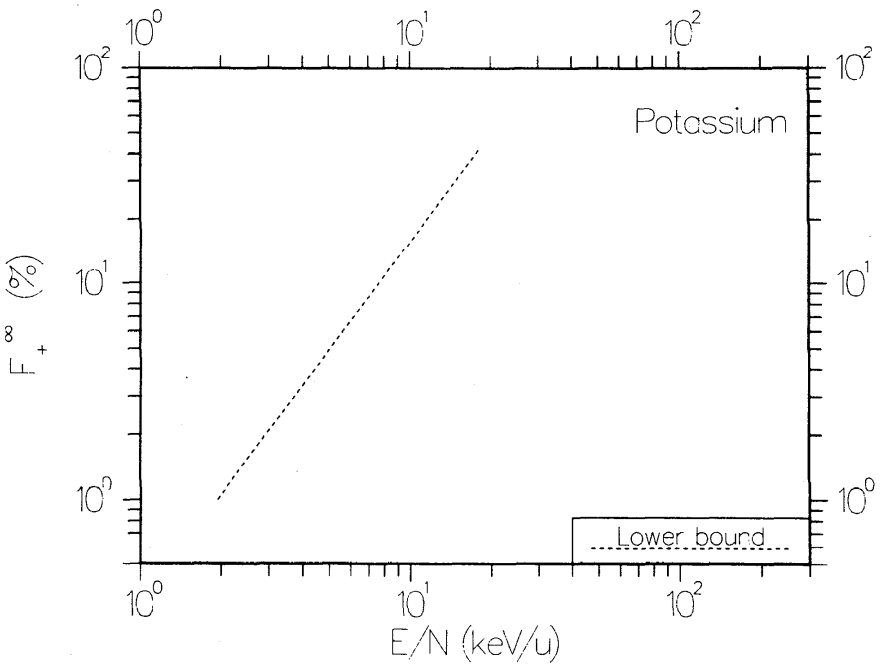

FIG. 28. Equilibrium fraction F_+^∞ for hydrogen atoms and ions incident on K vapor. The lower bound is based on data taken from Refs. 50 and 86.

17 July 2023 14:50:05

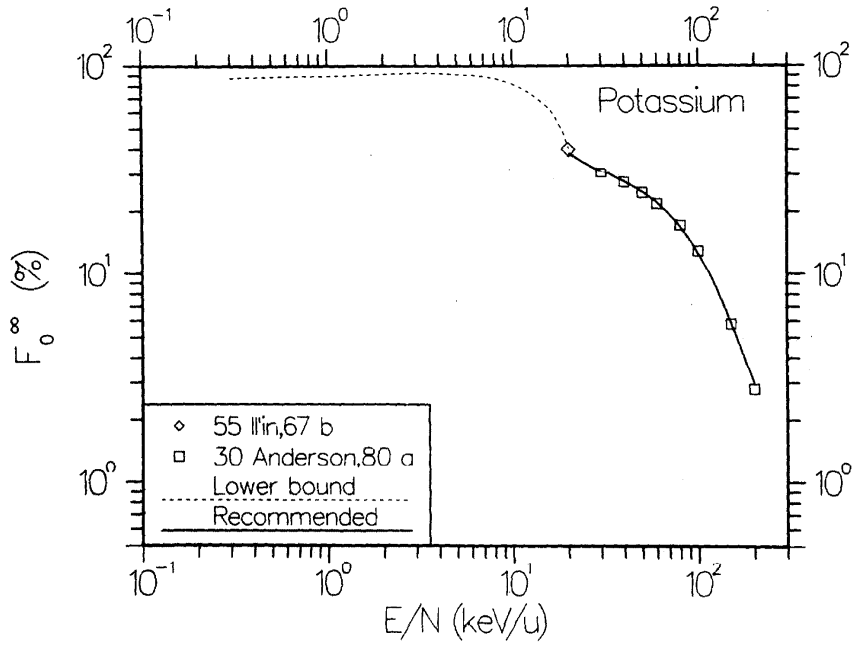

FIG. 29. Equilibrium fraction F_0^∞ for hydrogen atoms and ions incident on K vapor. The lower bound is based on data taken from Refs. 50, 55, and 86.

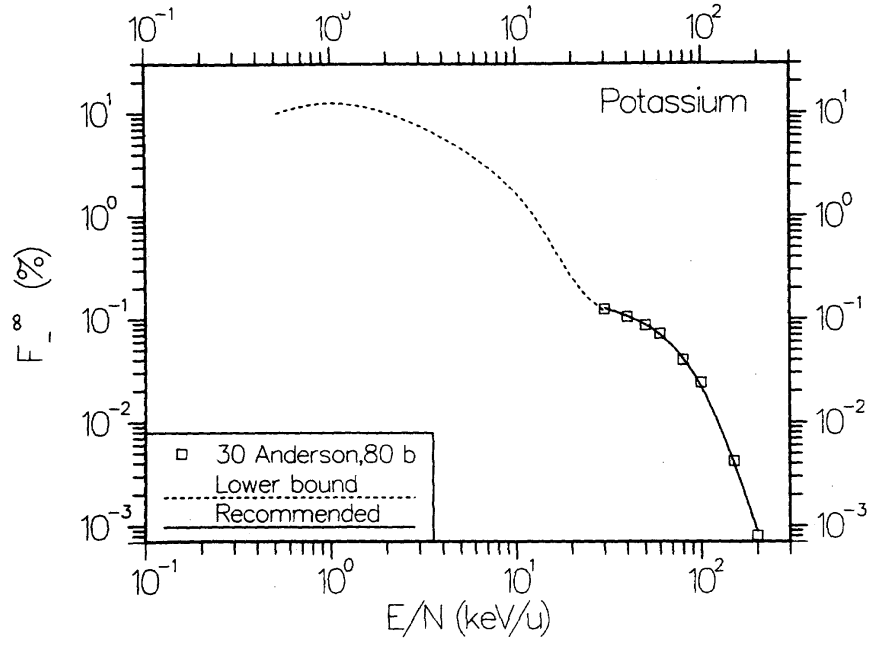

FIG. 30. Equilibrium fraction F_-^∞ for hydrogen atoms and ions incident on K vapor. The lower bound is based on data taken from Refs. 39, 50, and 86.

17 July 2023 14:50:05

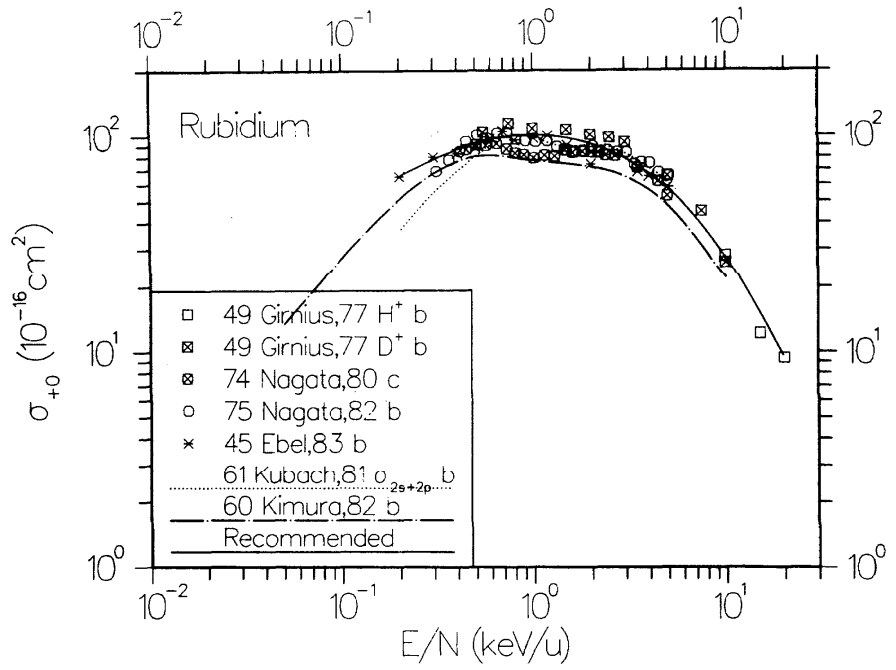

FIG. 31. Cross section σ_{+0} for electron capture into all states of the neutral hydrogen atom in collisions of H^+ with Rb vapor.

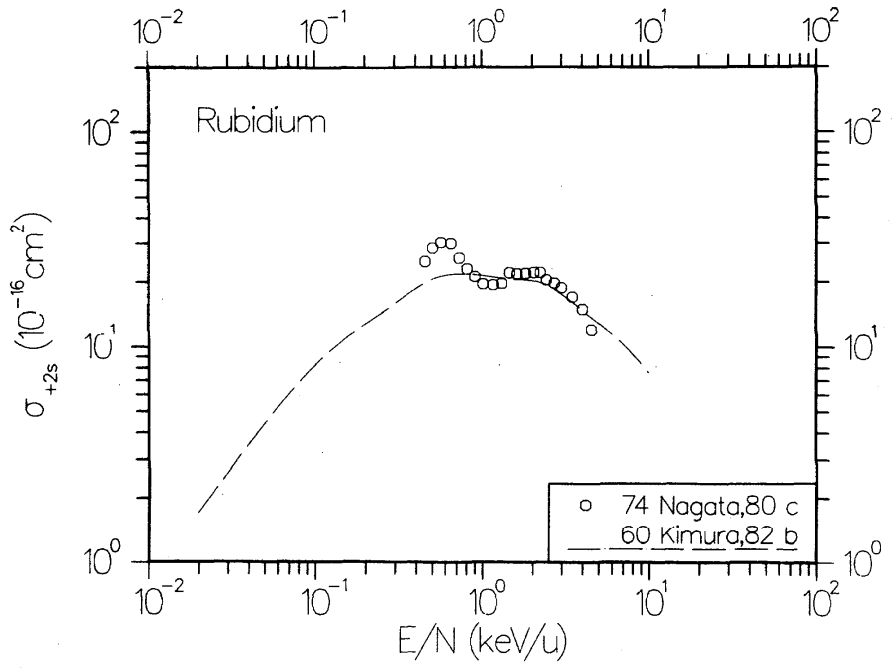

FIG. 32. Cross section σ_{+2s} for electron capture into the 2*s* state of the neutral hydrogen atom in collisions of H^+ with Rb vapor.

17 July 2023 14:50:05

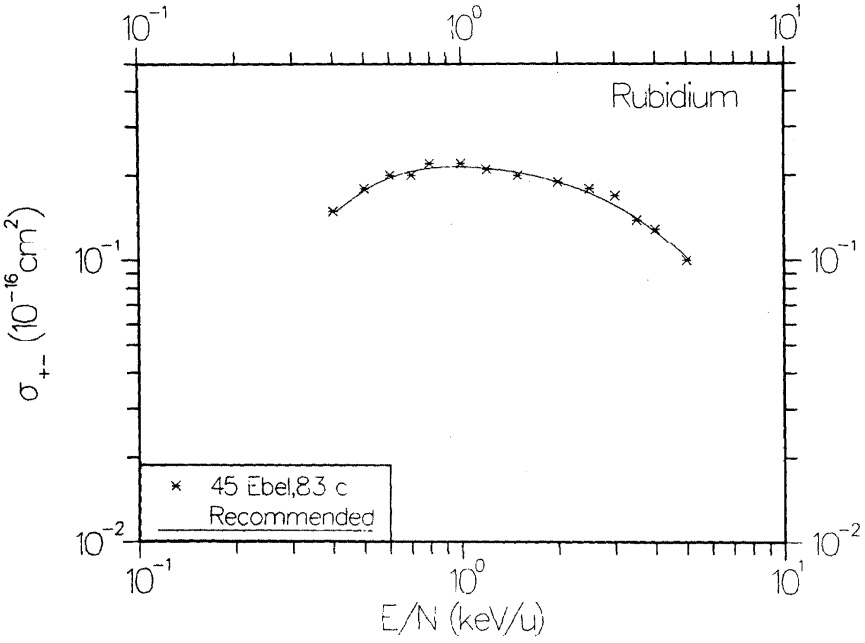

FIG. 33. Cross section σ_{+-} for double electron capture in collisions of H^+ with Rb vapor.

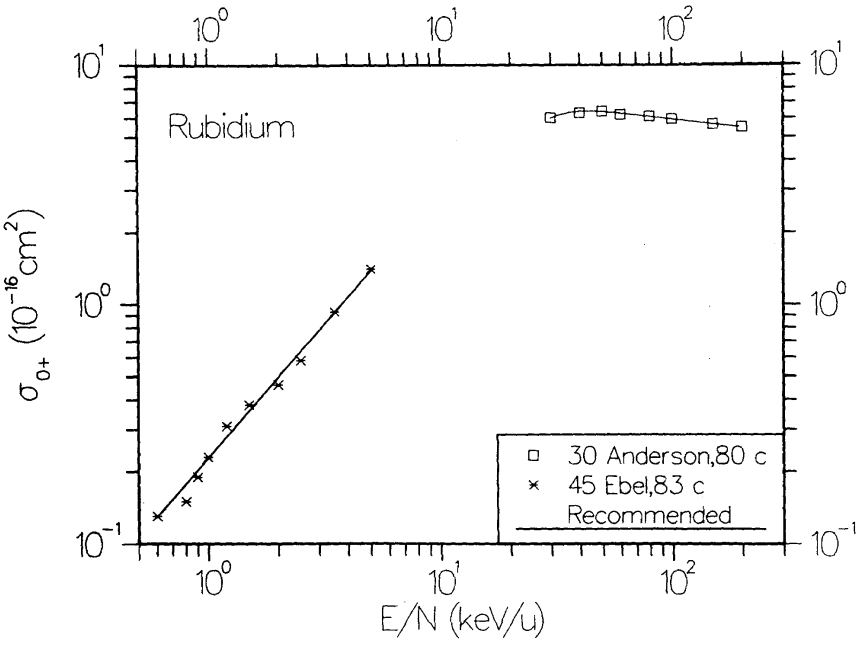

FIG. 34. Cross section σ_{0+} for electron loss in collisions of H^0 with Rb vapor.

17 July 2023 14:50:05

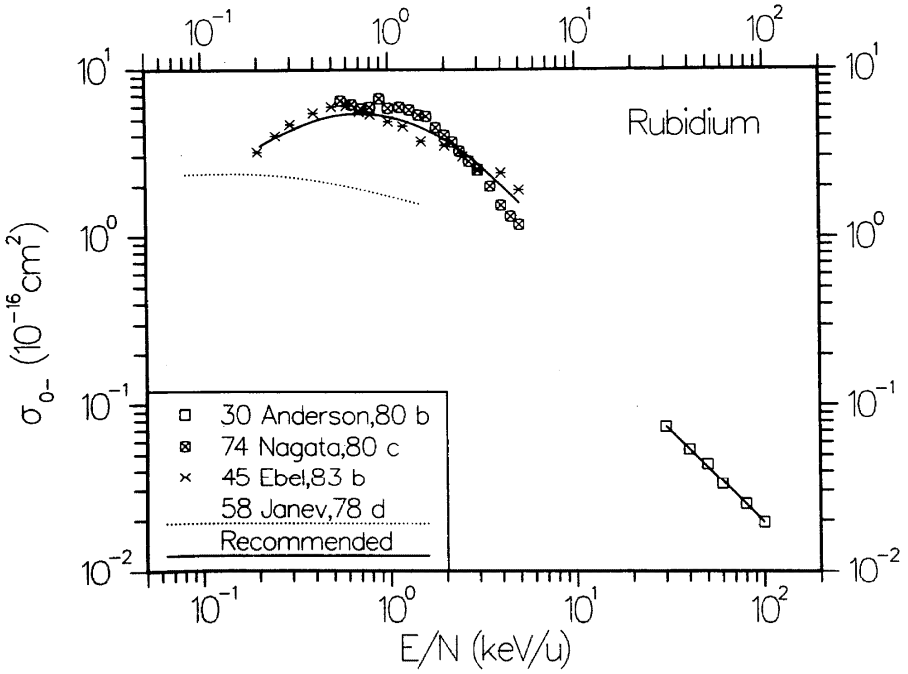

FIG. 35. Cross section σ_{0-} for electron capture in collision of H^0 with Rb vapor.

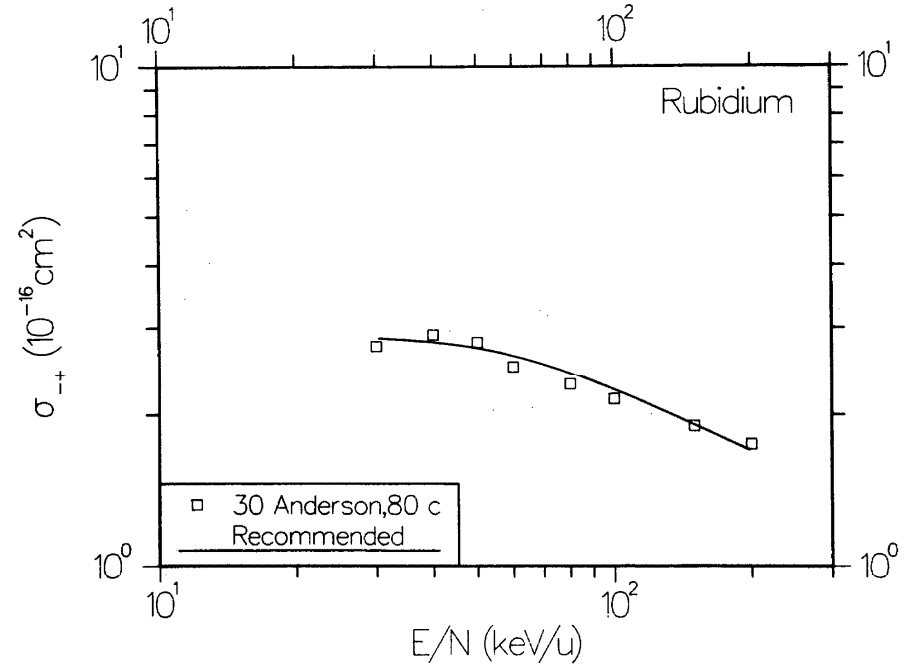

FIG. 36. Cross section σ_{-+} for double electron loss in collisions of H^- with Rb vapor.

17 July 2023 14:50:05

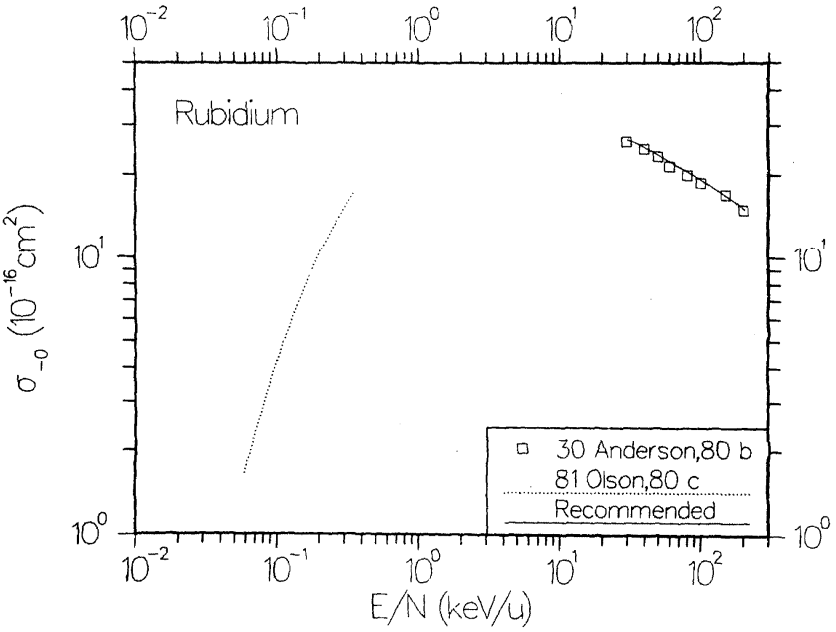

FIG. 37. Cross section σ_{-0} for detachment of electrons from H^- in collisions with Rb vapor.

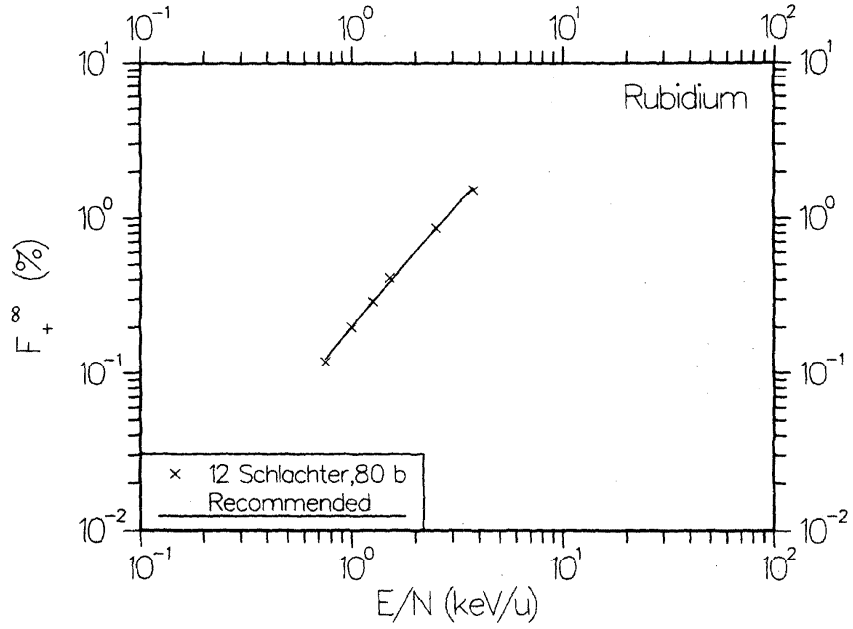

FIG. 38. Equilibrium fraction F_+^∞ for hydrogen atoms and ions incident on Rb vapor.

17 July 2023 14:50:05

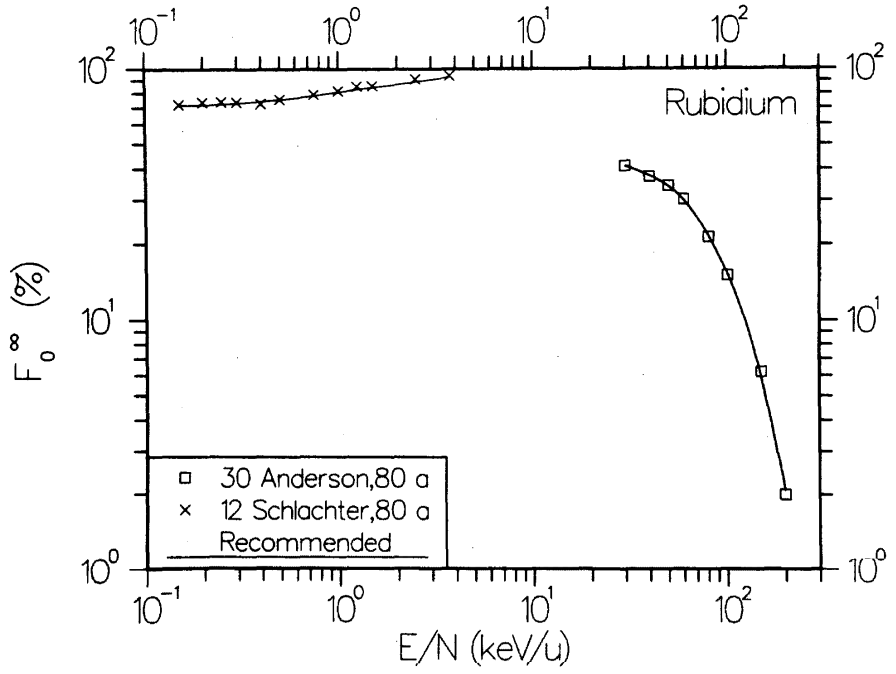

FIG. 39. Equilibrium fraction F_0^∞ for hydrogen atoms and ions incident on Rb vapor.

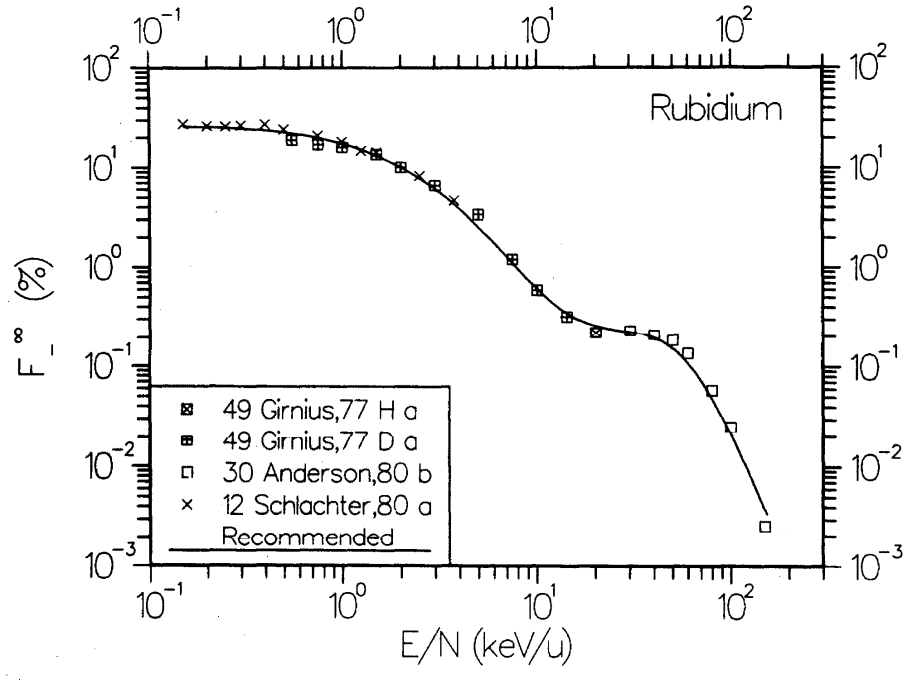

FIG. 40. Equilibrium fraction F^∞_- for hydrogen atoms and ions incident on Rb vapor.

17 July 2023 14:50:05

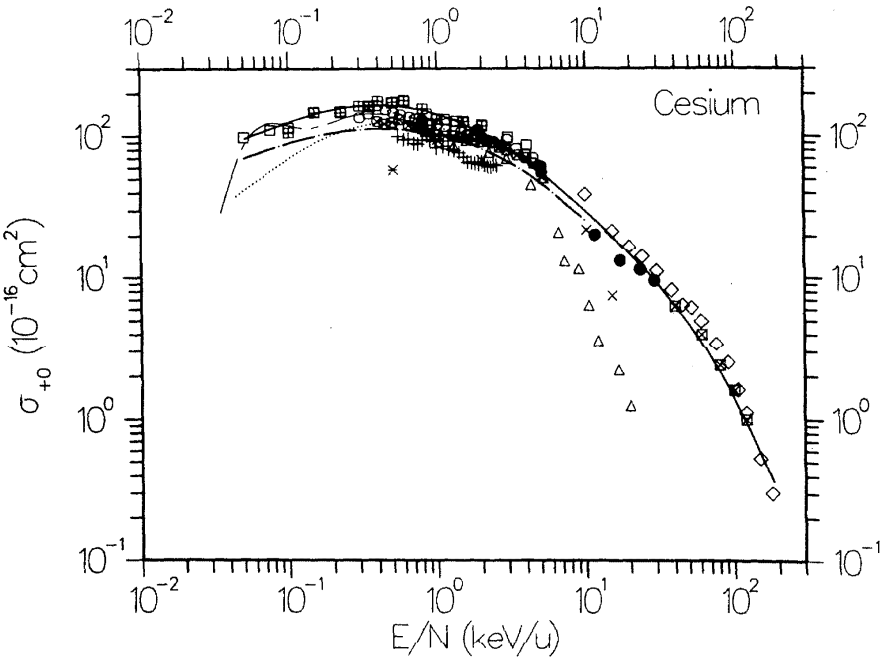

FIG. 41. Cross section σ_{+0} for electron capture into all states of the neutral hydrogen atom in collisions of H^+ with Cs vapor. Experimental data points: ◇, Ref. 55, c; ×, Ref. 17, H^+ c; ⋇, Ref. 17, D^+ c; △, Ref. 50, d; +, Ref. 89, c; ●, Ref. 69, Ref. 17, c; ⊠, Ref. 67, c; ⊞, Ref. 66, b; ⊗, Ref. 74, c; ○, Ref. 75, c; □, Ref. 32, b. Theoretical curves: · · · ·, Ref. 83, b; — · — · —, Ref. 88, b; – · – ·, Ref. 60, b. Recommended data: —.

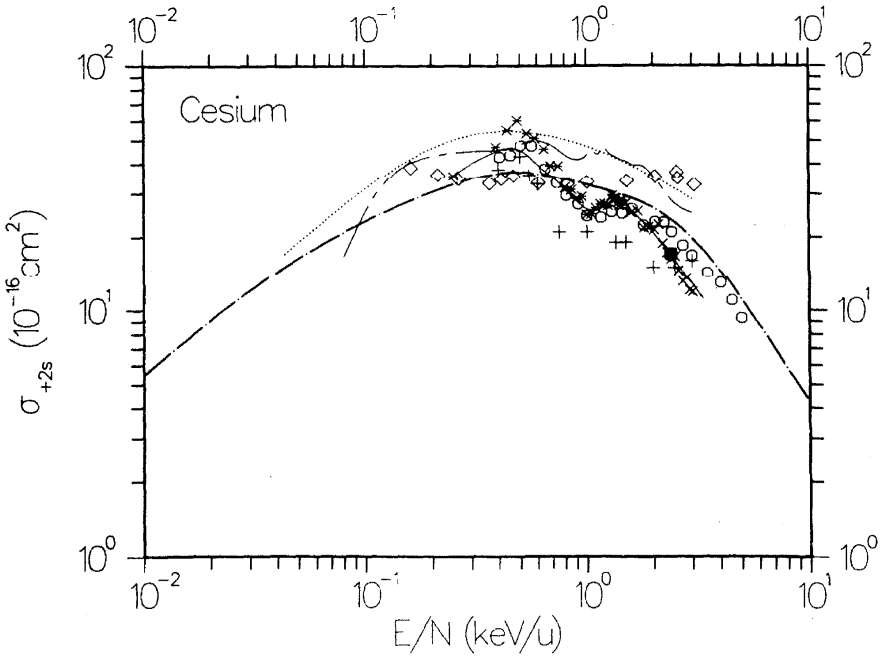

FIG. 42. Cross section σ_{+2s} for electron capture into the 2*s* state of the neutral hydrogen atom in collisions of H^+ with Cs vapor. Experimental data points: ◇, Ref. 41, d; ■, Ref. 89, c; ×, Ref. 15, H^+ b; ⋇, Ref. 15, D^+ b; +, Ref. 11, c; ○, Ref. 74, c. Theoretical data: · · · ·, Ref. 83, c; — · — · —, Ref. 88, c; – · – ·, Ref. 60, b. Recommended values: —.

17 July 2023 14:50:05

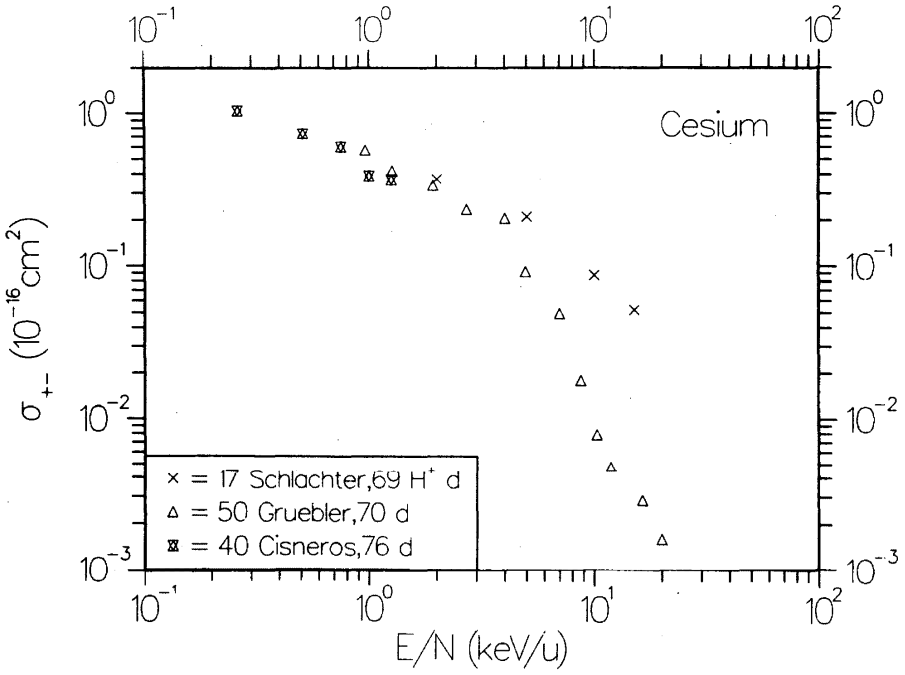

FIG. 43. Cross section σ_{+-} for double electron capture in collisions of H^+ with Cs vapor.

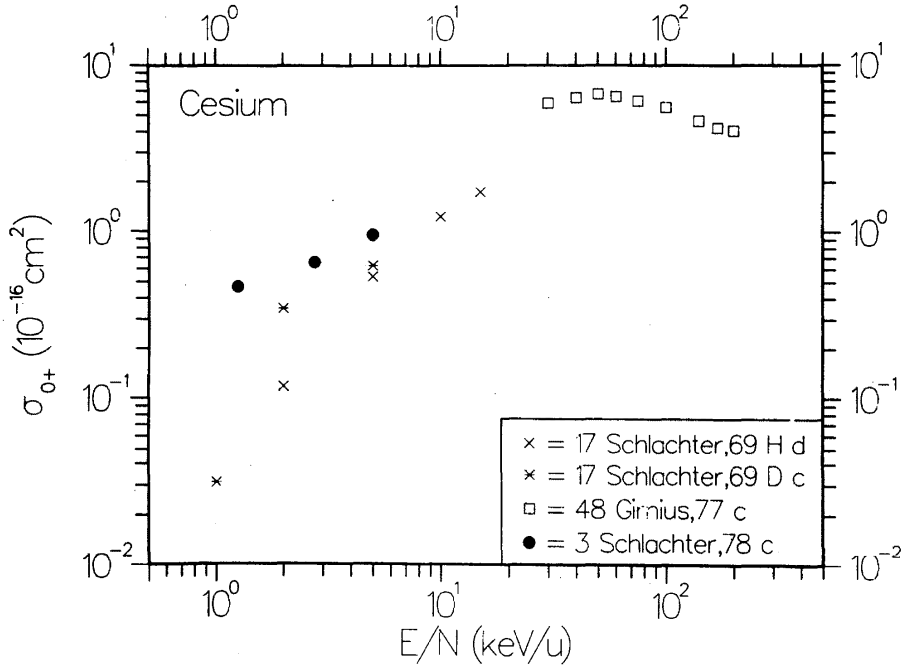

FIG. 44. Cross section σ_{0+} for electron loss in collisions of H^0 with Cs vapor.

17 July 2023 14:50:05

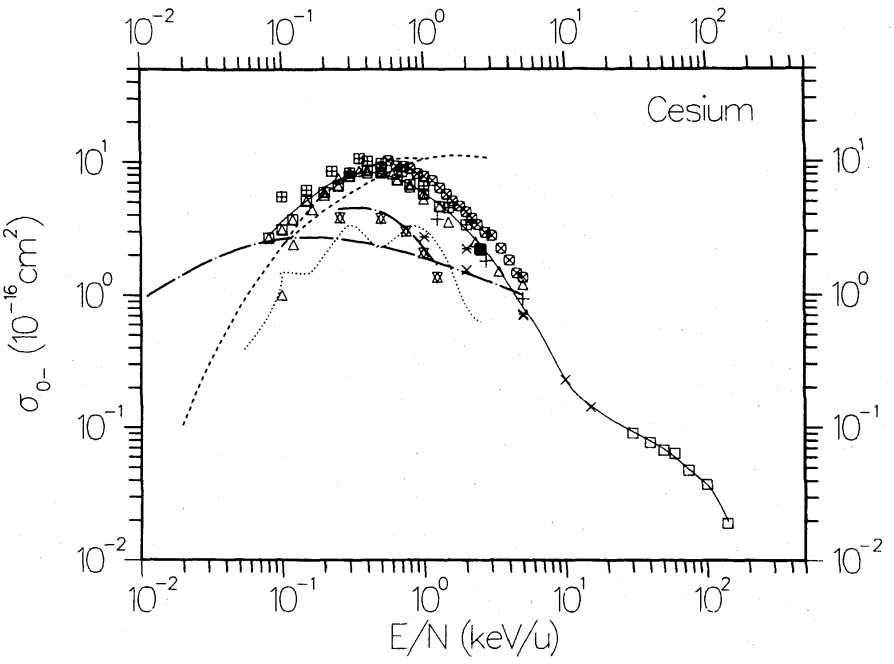

FIG. 45. Cross section σ_{0-} for electron capture in collisions of H^0 with Cs vapor. Experimental data points: ×, Ref. 17, H c; ⋊, Ref. 17, D c; ■, Ref. 90, c; ⧖, Ref. 40, c; □, Ref. 48, c; ⊗, Ref. 74, c; ⊞, Ref. 66, c; +, Ref. 12, c; △, Ref. 70, H b; ⊠, Ref. 70, D b. Theoretical data: - - - -, Ref. 83, d; – · – · (upper), Ref. 52, d; · · · ·, Ref. 51, d; – · – ·, Ref. 58, (lower), d; — · — ·, Ref. 78, b. Recommended data: —.

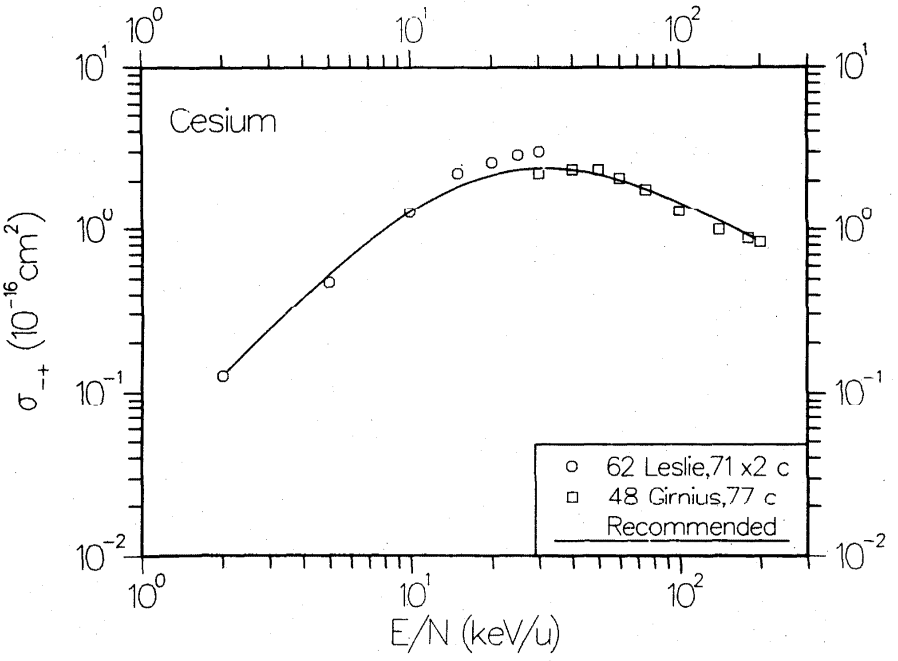

FIG. 46. Cross section σ_{-+} for double electron loss in collisions of H^- with Cs vapor.

17 July 2023 14:50:05

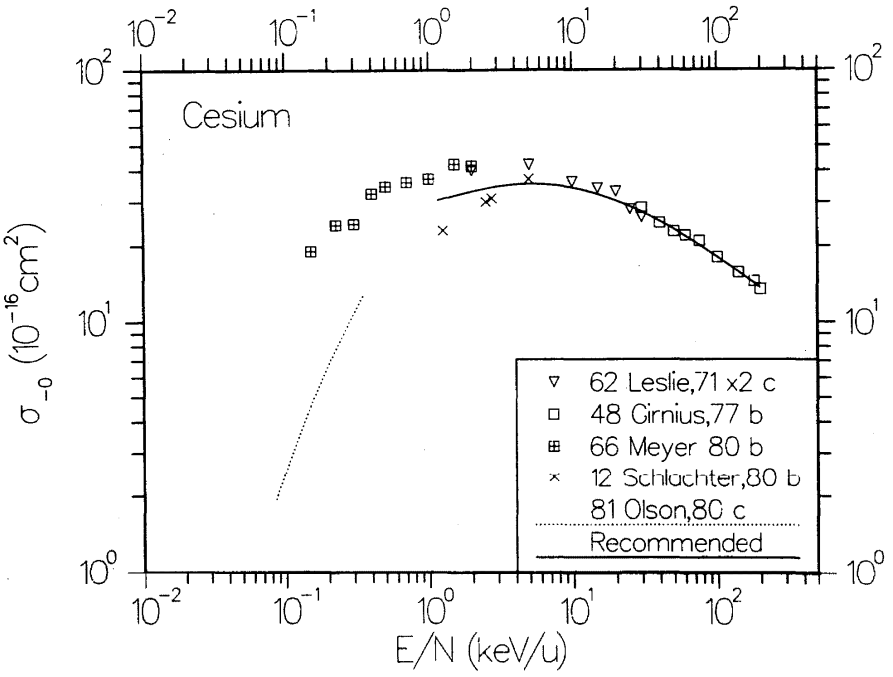

FIG. 47. Cross section σ_{-0} for detachment of electrons from H^- in collisions with Cs vapor.

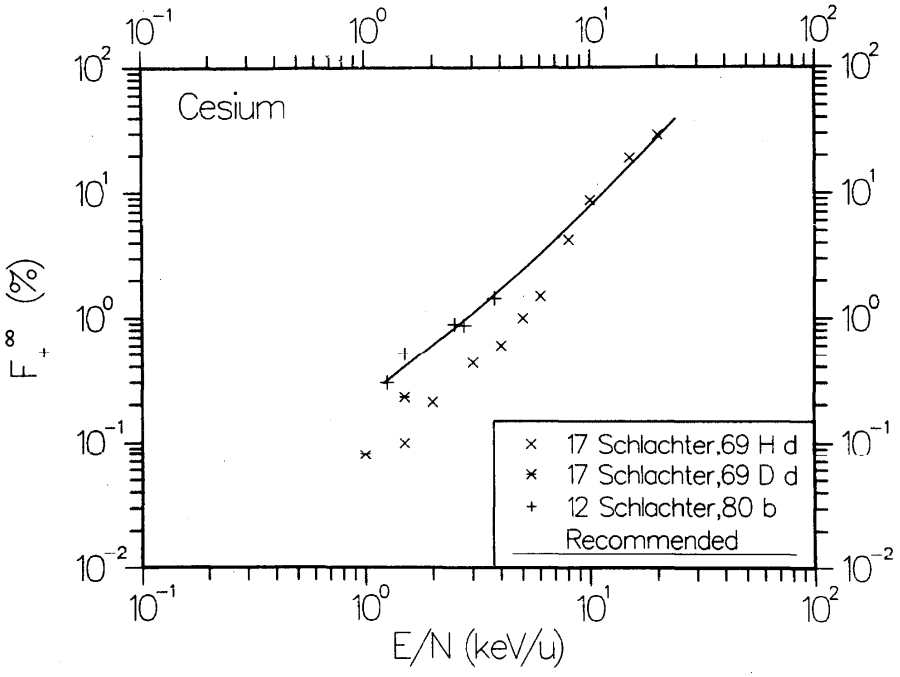

FIG. 48. Equilibrium fraction F_+^∞ for hydrogen atoms and ions incident on Cs vapor.

17 July 2023 14:50:05

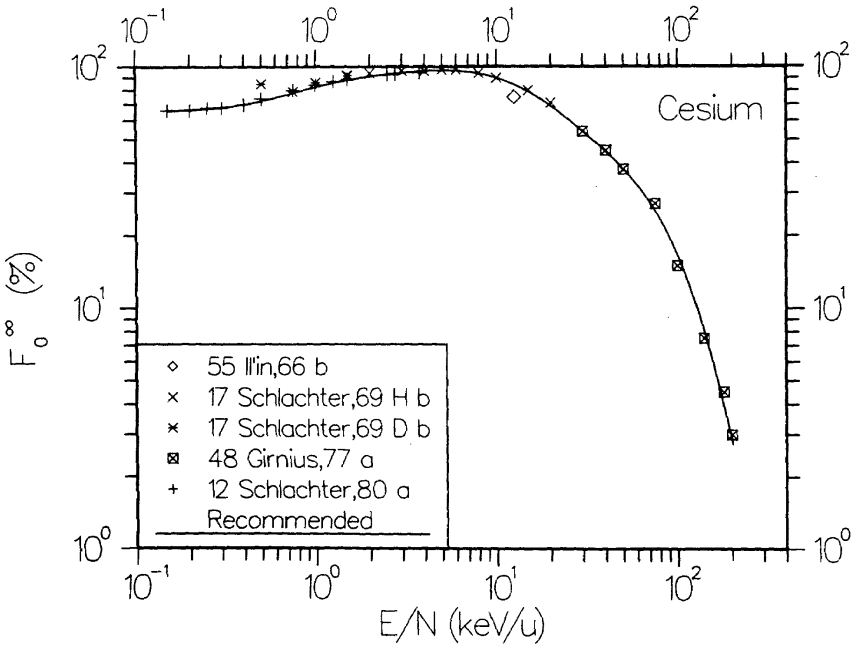

FIG. 49. Equilibrium fraction F_0^∞ for hydrogen atoms and ions incident on Cs vapor.

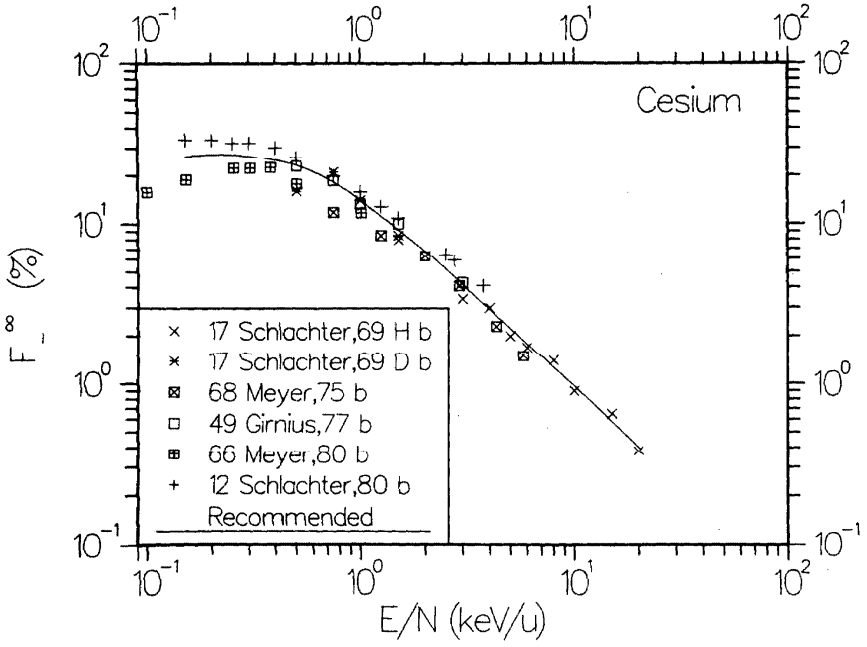

FIG. 50. Equilibrium fraction F_-^∞ for hydrogen atoms and ions incident on Cs vapor.

17 July 2023 14:50:05

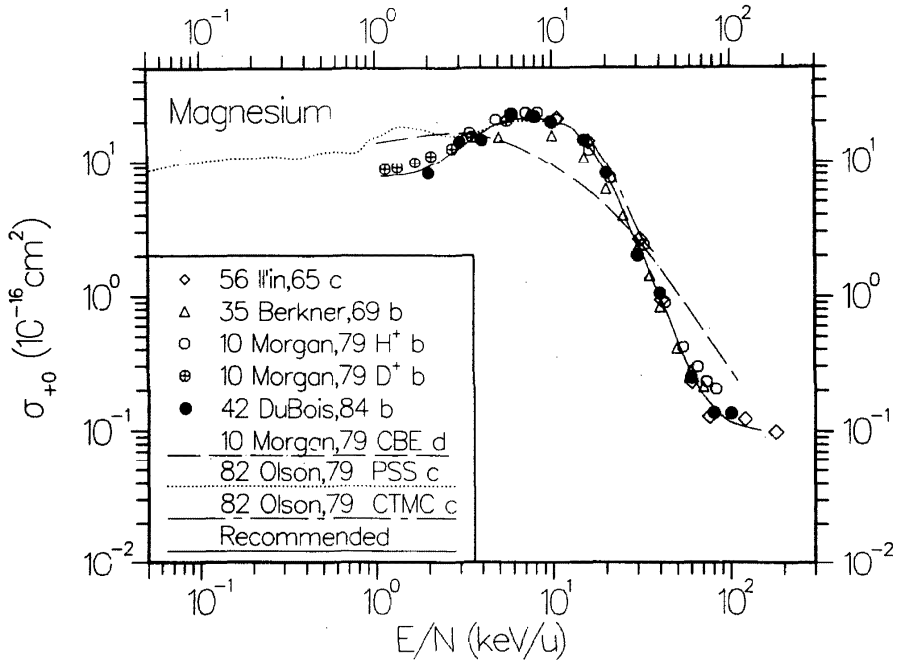

FIG. 51. Cross section σ_{+0} for electron capture into all states of the neutral hydrogen atom in collisions of H^+ with Mg vapor.

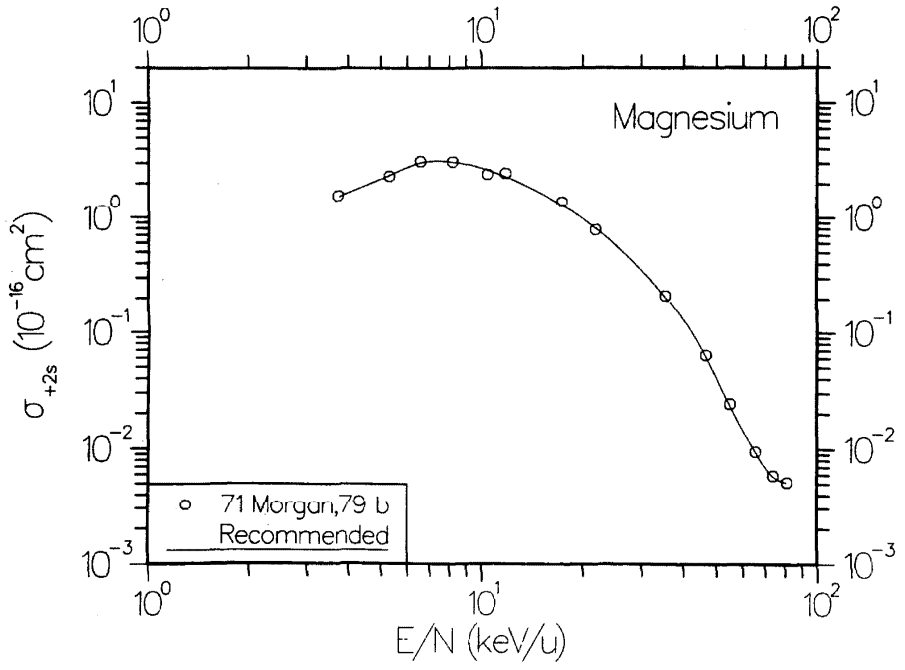

FIG. 52. Cross section σ_{+2s} for electron capture into the 2s state of the neutral hydrogen atom in collisions of H^+ with Mg vapor.

17 July 2023 14:50:05

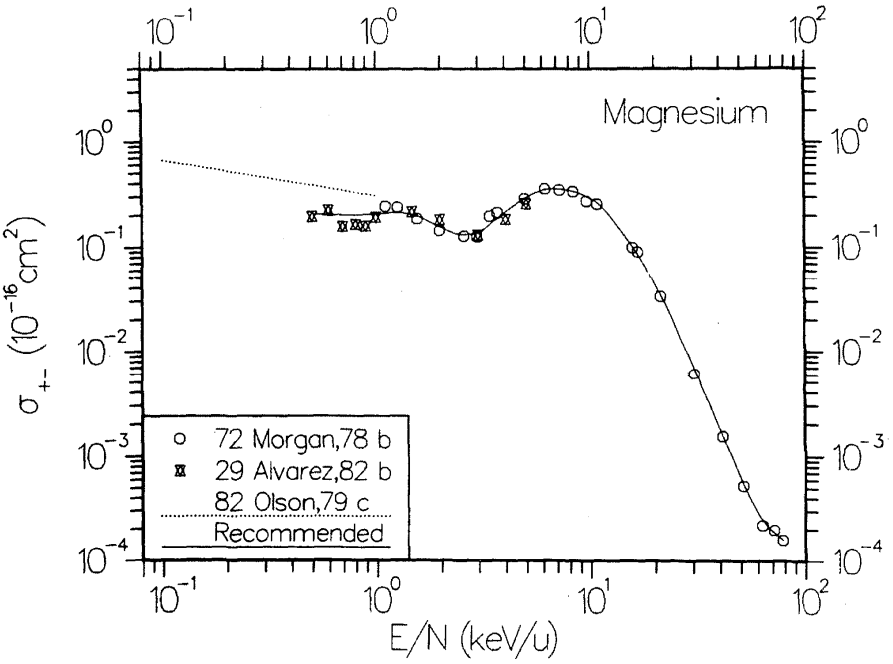

FIG. 53. Cross section σ_{+-} for double electron capture in collisions of H^+ with Mg vapor.

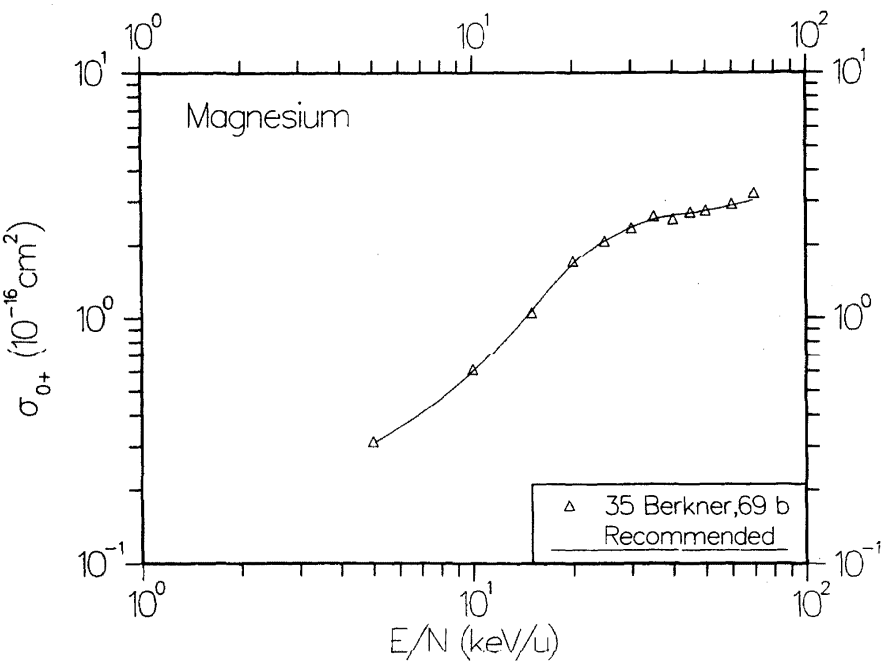

FIG. 54. Cross section σ_{0+} for electron loss in collisions of H^0 with Mg vapor.

17 July 2023 14:50:05

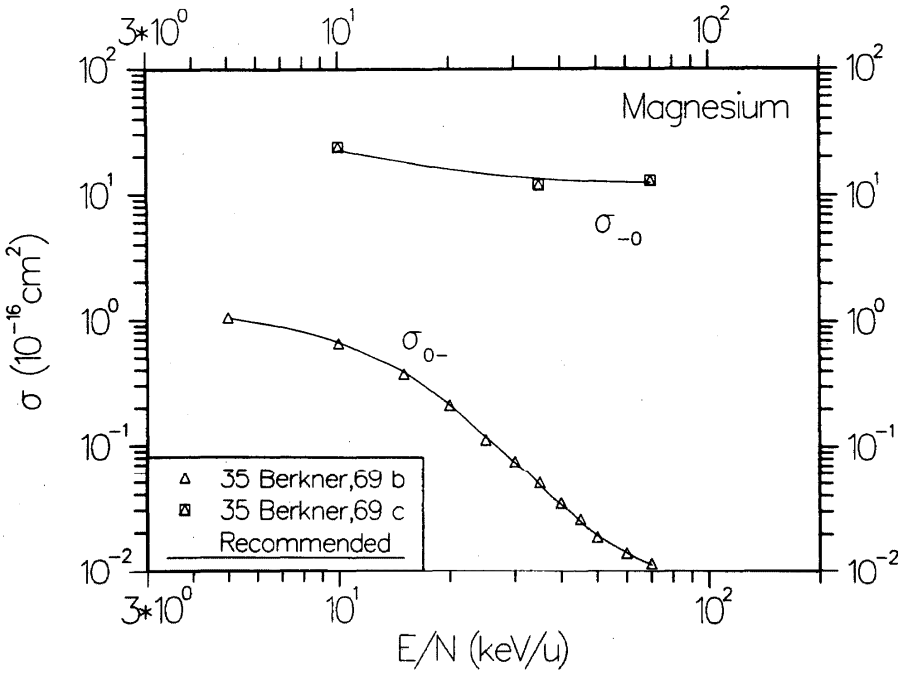

FIG. 55. Cross sections σ_{0-} for electron capture in collisions of H^0 with Mg vapor and σ_{-0} for detachment of electrons from H^- in collisions with Mg vapor.

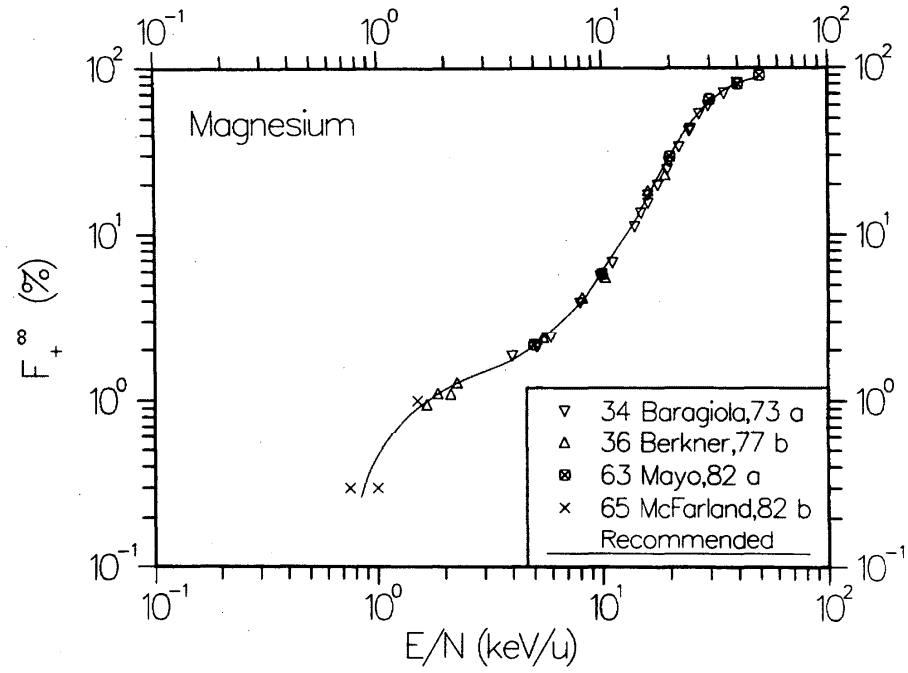

FIG. 56. Equilibrium fraction F_+^∞ for hydrogen atoms and ions incident on Mg vapor.

17 July 2023 14:50:05

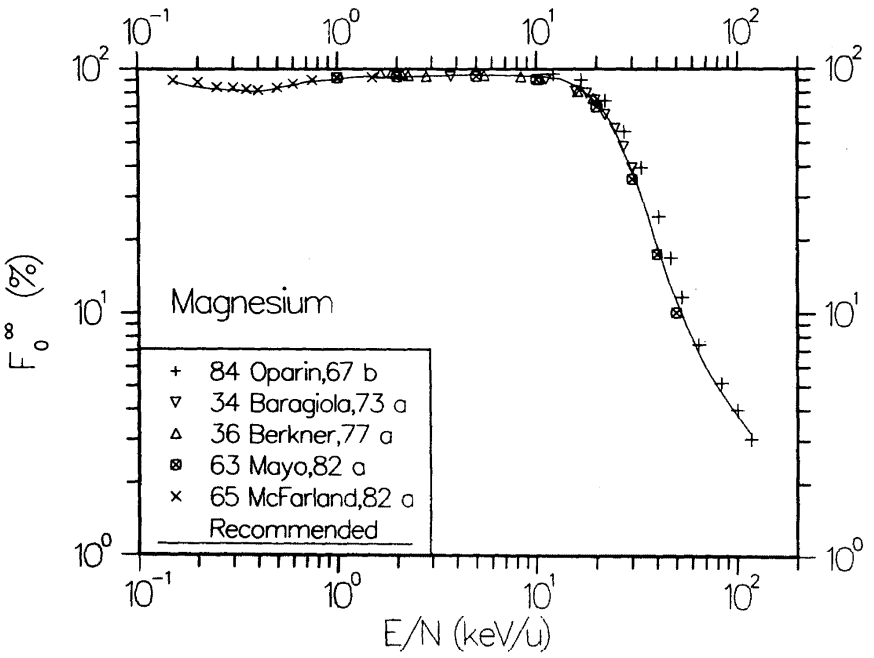

FIG. 57. Equilibrium fraction F_0^∞ for hydrogen atoms and ions incident on Mg vapor.

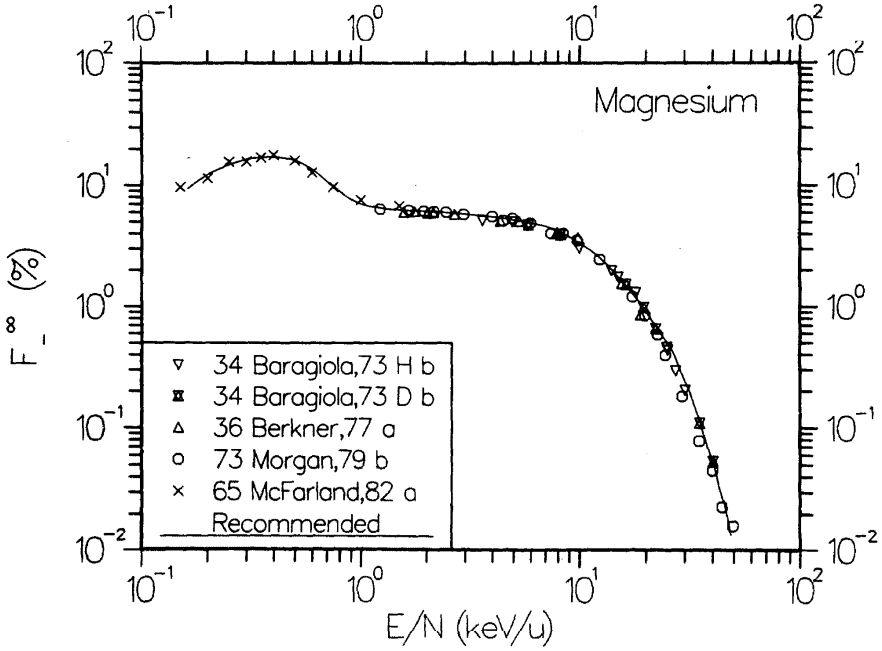

FIG. 58. Equilibrium fraction F_-^∞ for hydrogen atoms and ions incident on Mg vapor.

17 July 2023 14:50:05

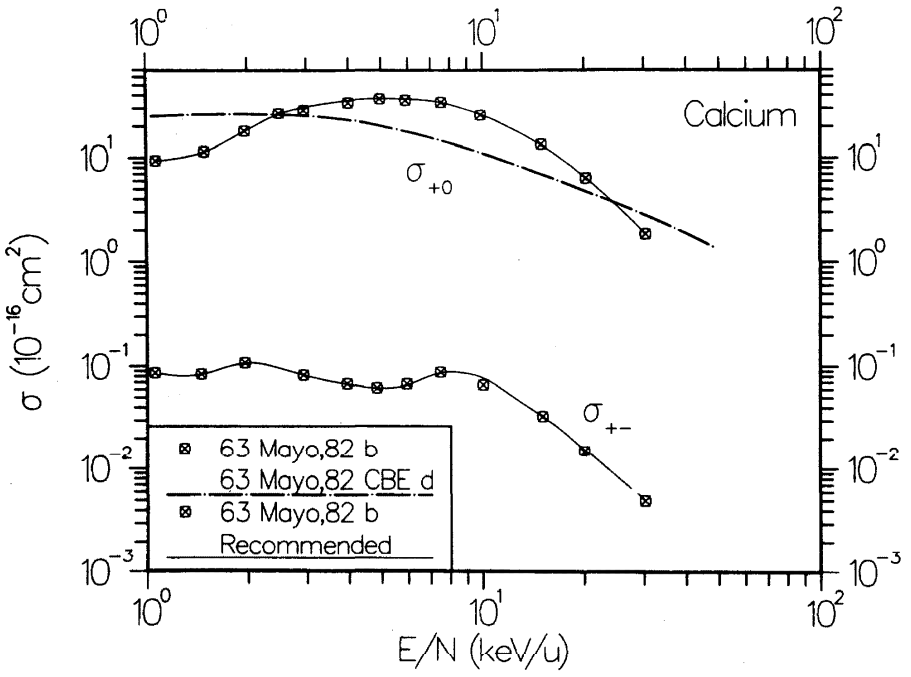

FIG. 59. Cross sections σ_{+0} for single electron capture and σ_{+-} for double electron capture in collisions of H^+ with Ca vapor.

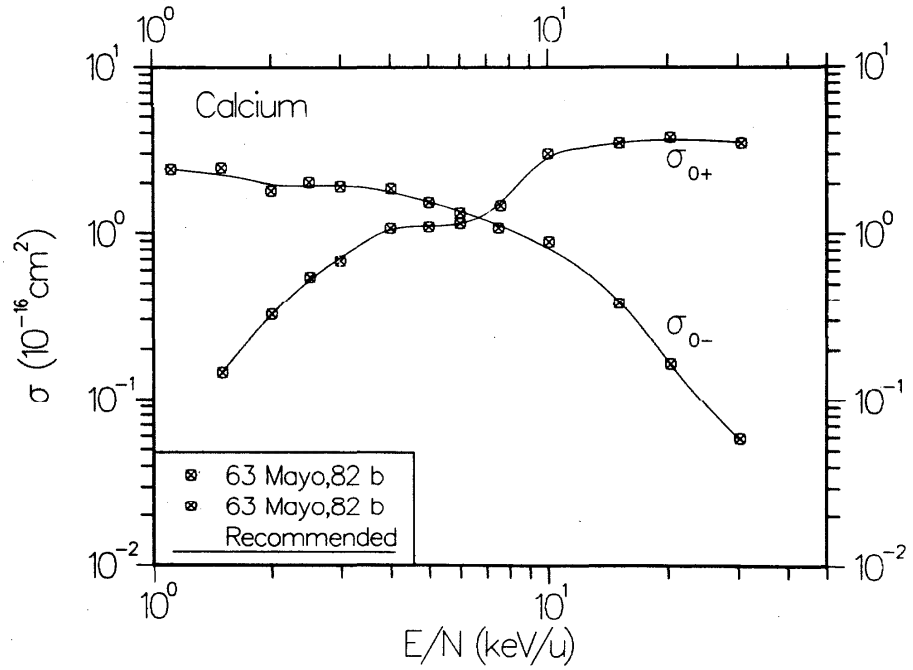

FIG. 60. Cross sections σ_{0+} for electron loss and σ_{0-} for electron capture in collisions of H^0 with Ca vapor.

17 July 2023 14:50:05

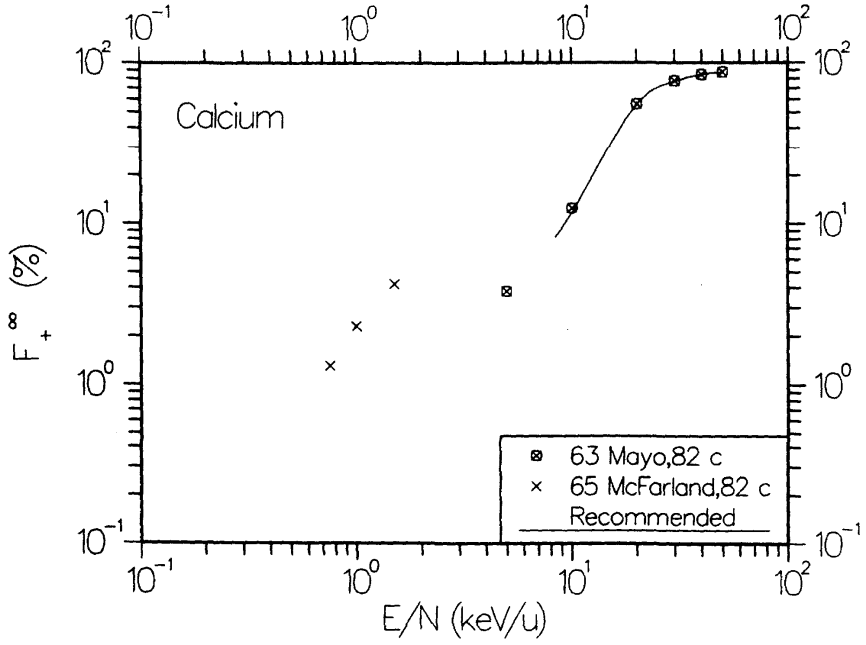

FIG. 61. Equilibrium fraction F_+^∞ for hydrogen atoms and ions incident on Ca vapor.

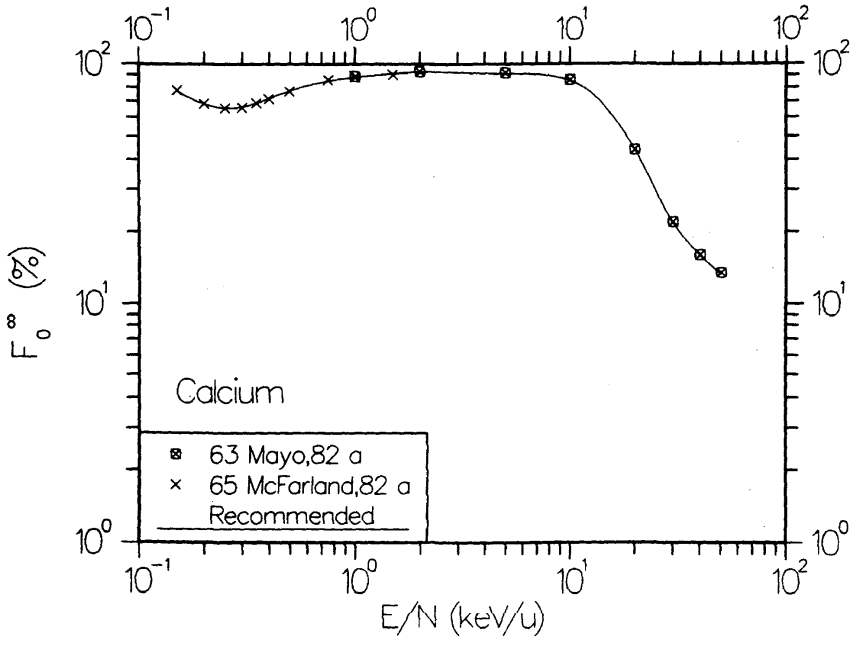

FIG. 62. Equilibrium fraction F_0^∞ for hydrogen atoms and ions incident on Ca vapor.

17 July 2023 14:50:05

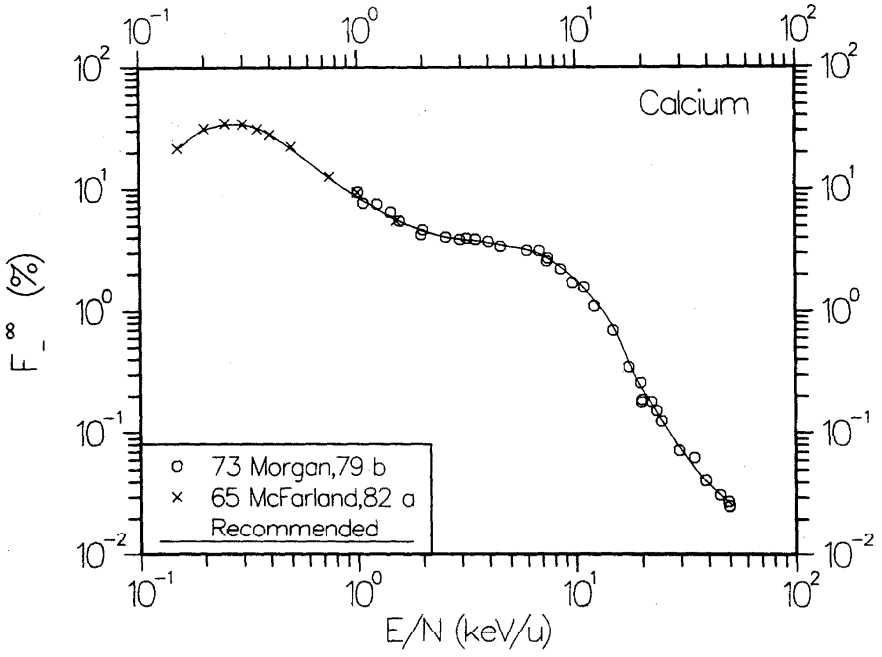

FIG. 63. Equilibrium fraction F_-^∞ for hydrogen atoms and ions incident on Ca vapor.

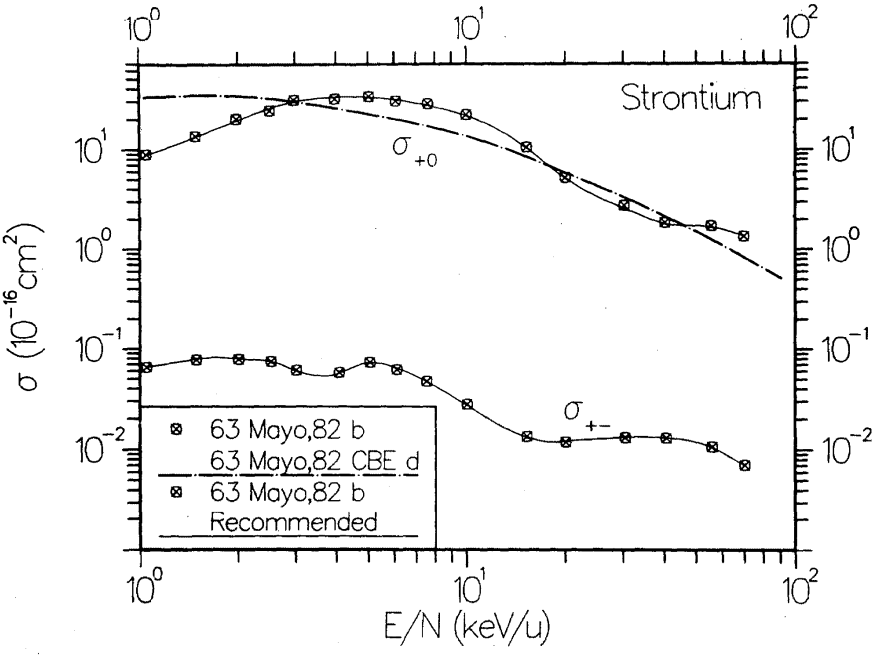

FIG. 64. Cross sections σ_{+0} for single electron capture and σ_{+-} for double electron capture in collisions of H^+ with Sr vapor.

17 July 2023 14:50:05

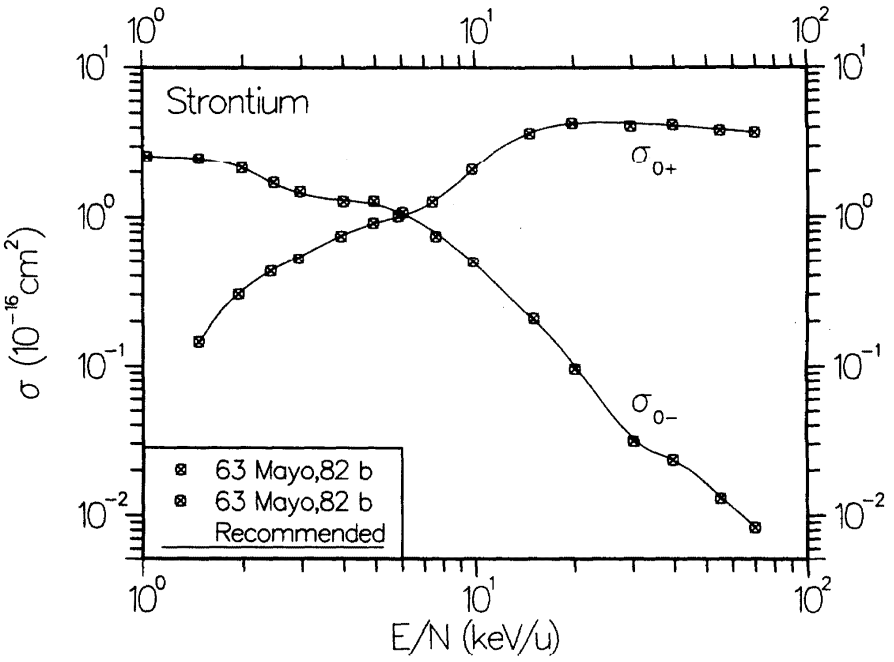

FIG. 65. Cross sections σ_{0+} for electron loss and σ_{0-} for electron capture in collisions of H^0 with Sr vapor.

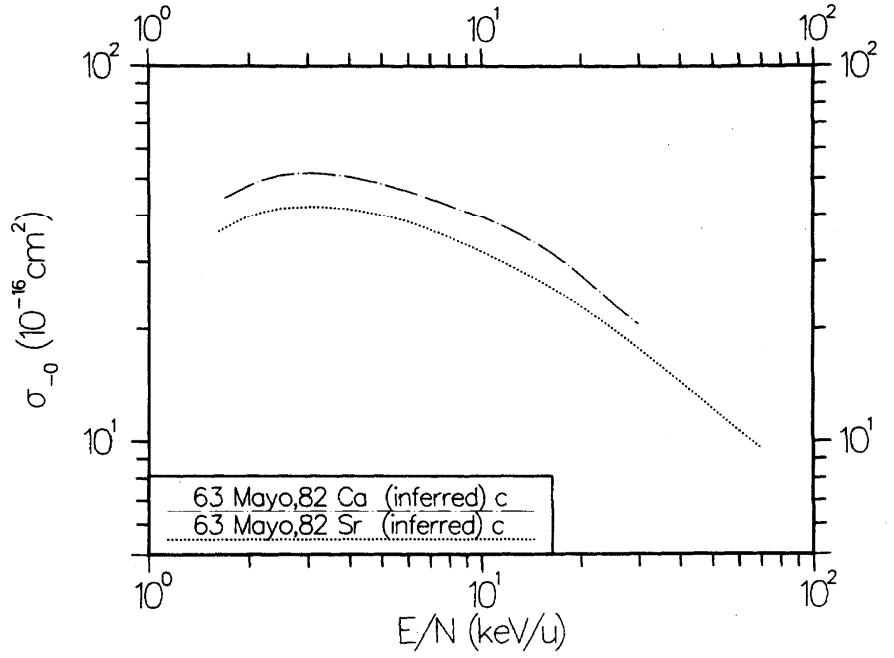

FIG. 66. Cross section σ_{-0} for detachment of electrons in collisions of H^- with Ca and Sr vapors.

17 July 2023 14:50:05

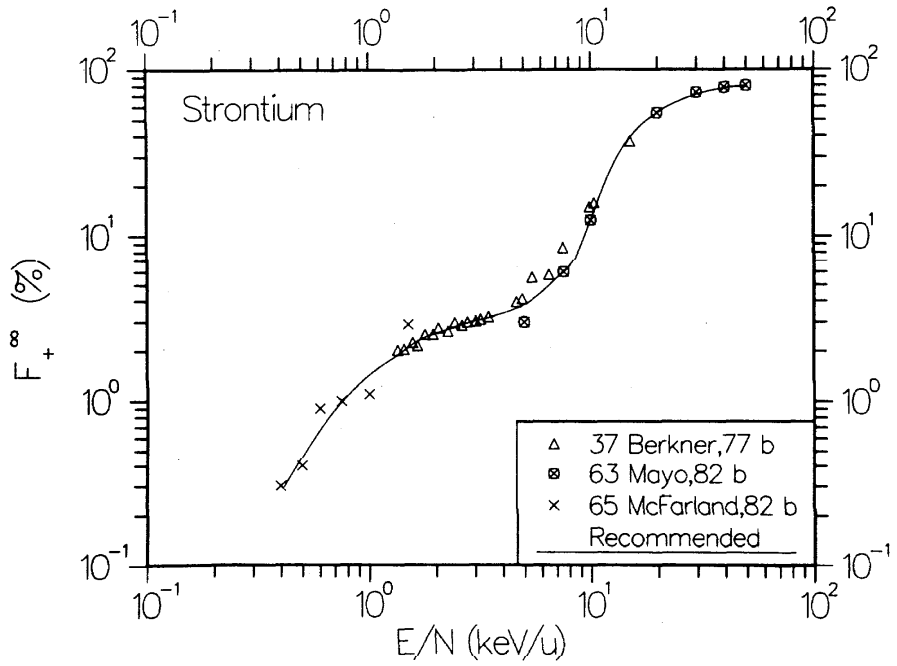

FIG. 67. Equilibrium fraction F_+^∞ for hydrogen atoms and ions incident on Sr vapor.

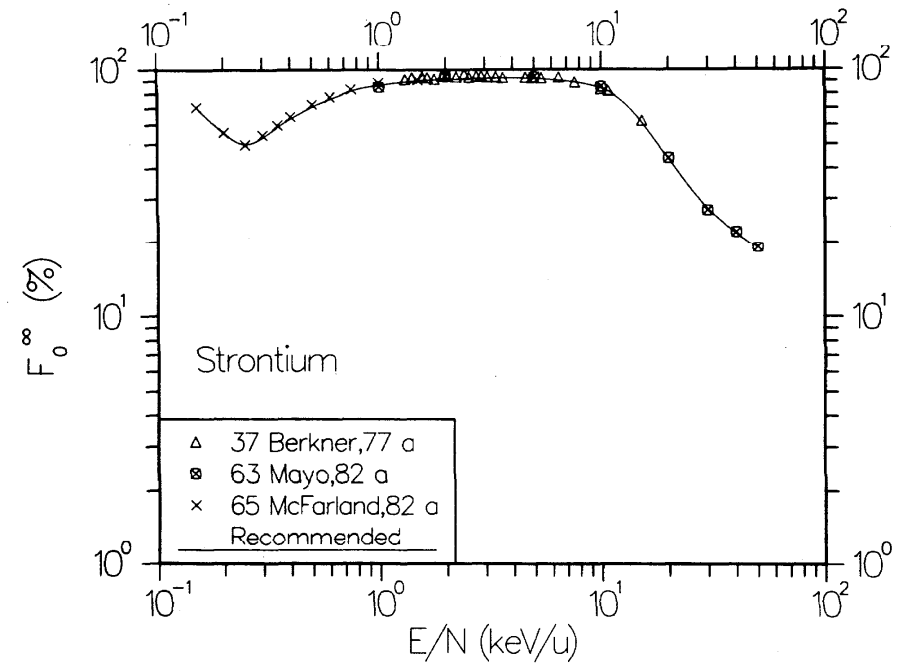

FIG. 68. Equilibrium fraction F_0^∞ for hydrogen atoms and ions incident on Sr vapor.

17 July 2023 14:50:05

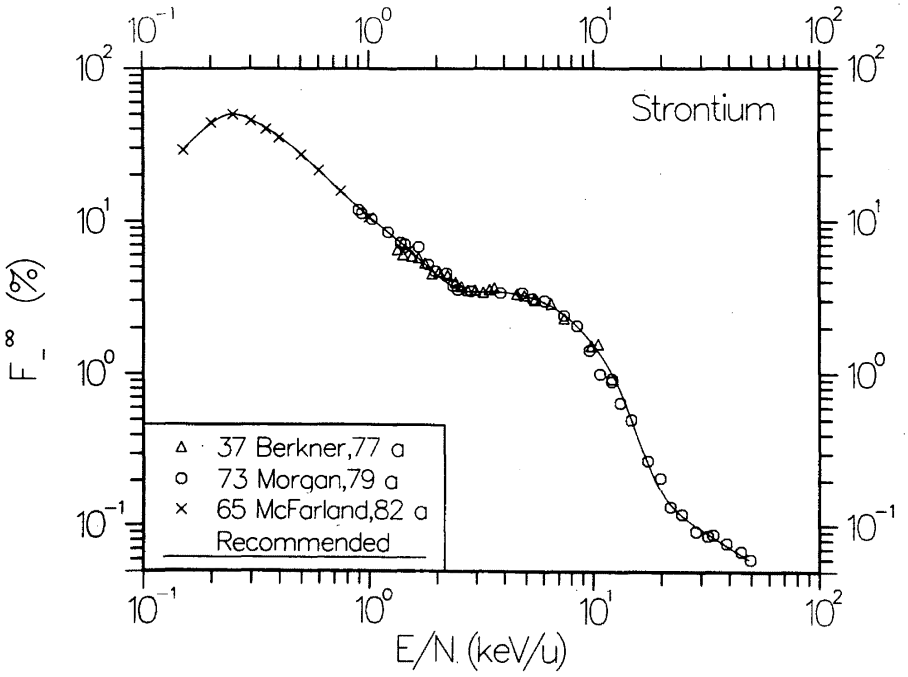

FIG. 69. Equilibrium fraction F_-^∞ for hydrogen atoms and ions incident on Sr vapor.

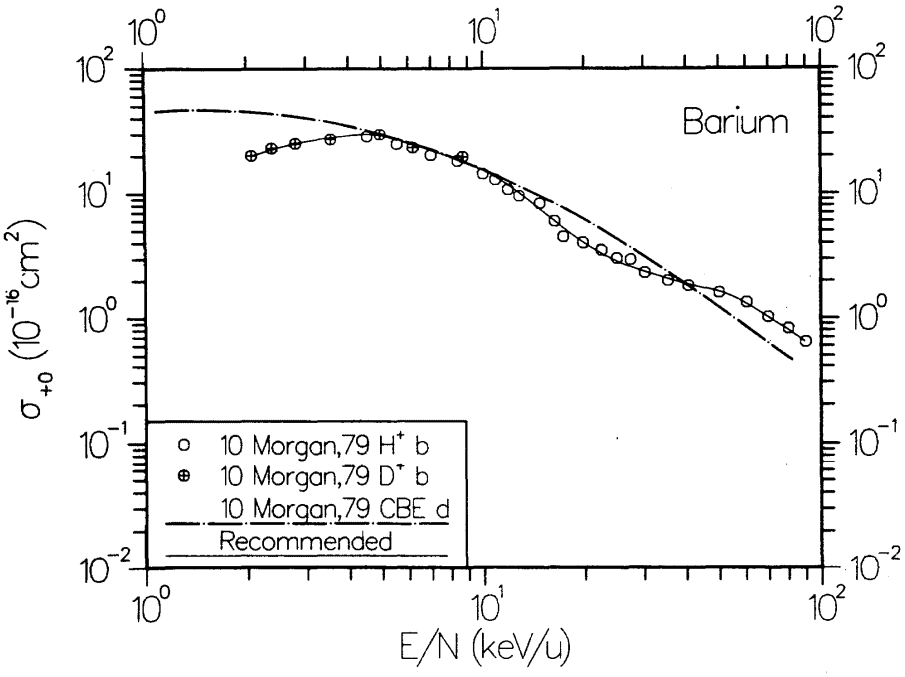

FIG. 70. Cross section σ_{+0} for electron capture into all states of the neutral hydrogen atom in collisions of H^+ with Ba vapor.

17 July 2023 14:50:05

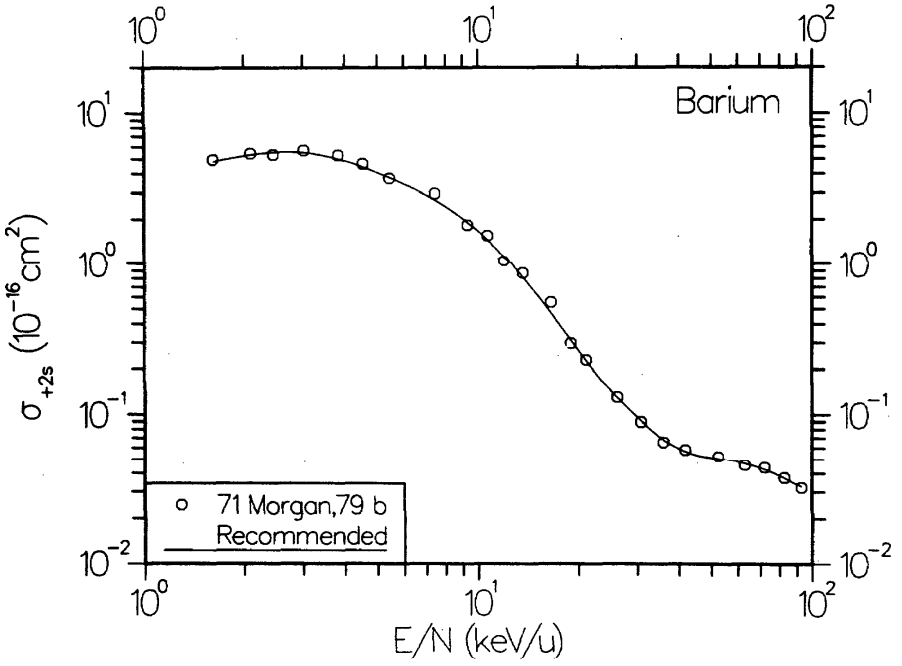

FIG. 71. Cross section σ_{+2s} for electron capture into the 2*s* state of the neutral hydrogen atom in collisions of H^+ with Ba vapor.

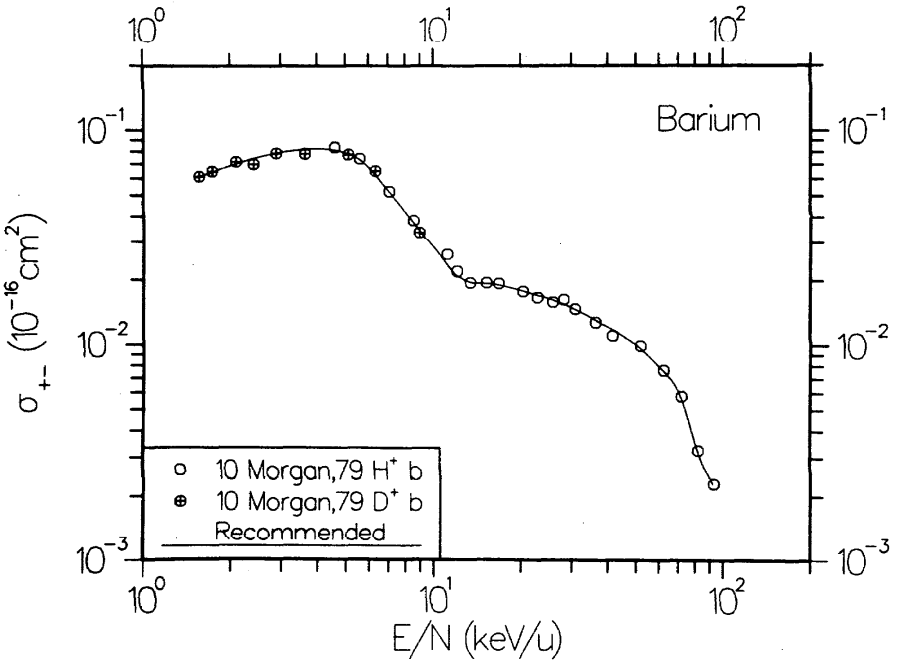

FIG. 72. Cross section σ_{+-} for double electron capture in collisions of H^+ with Ba vapor.

17 July 2023 14:50:05

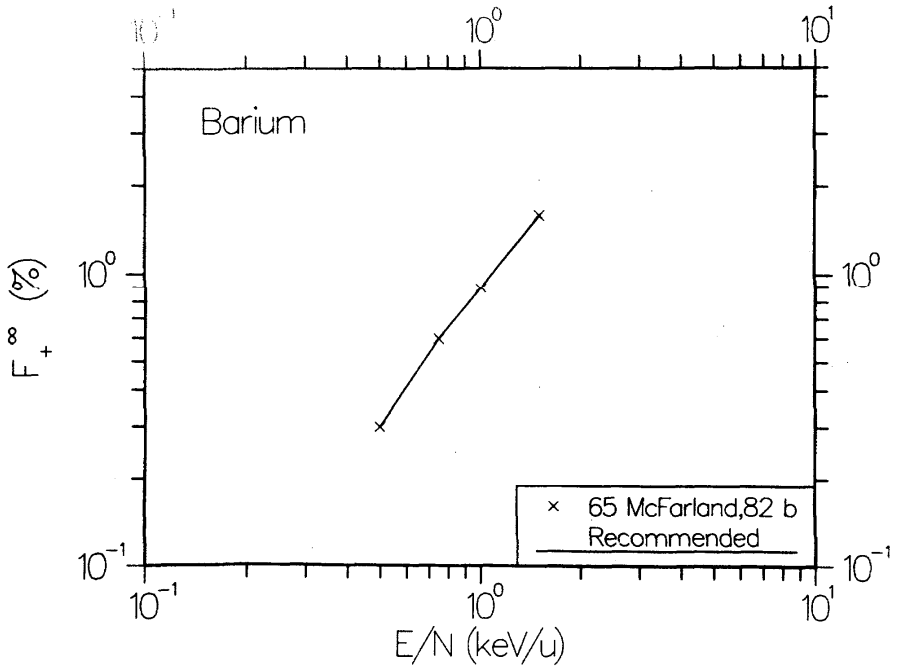

FIG. 73. Equilibrium fraction F_+^∞ for hydrogen atoms and ions incident on Ba vapor.

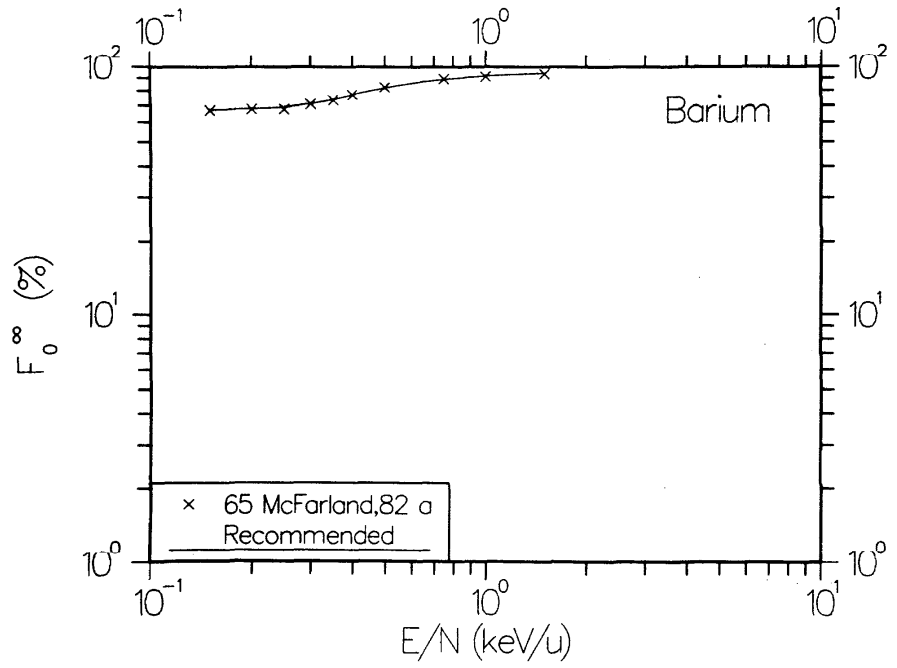

FIG. 74. Equilibrium fraction F_0^∞ for hydrogen atoms and ions incident on Ba vapor.

17 July 2023 14:50:05

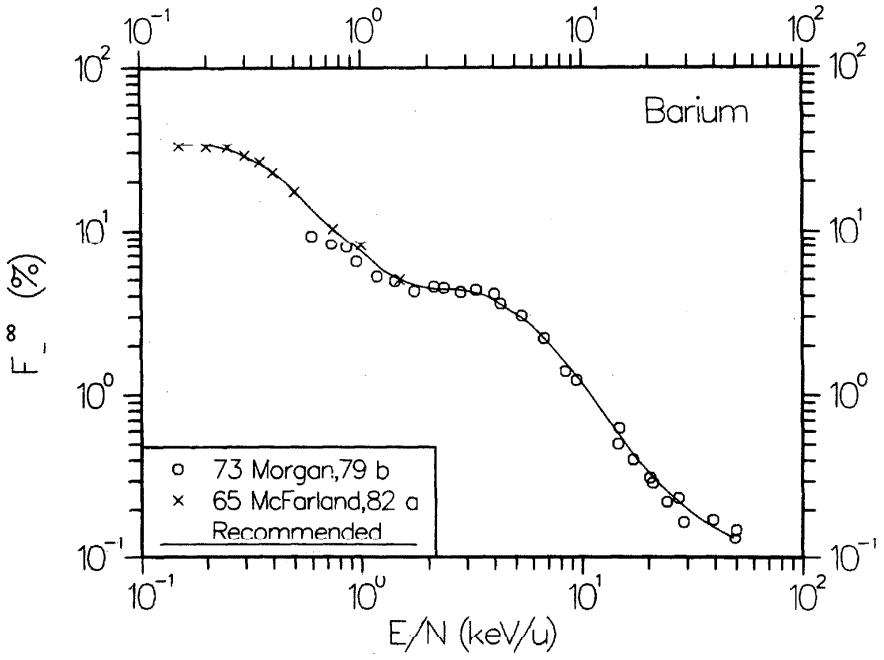

FIG. 75. Equilibrium fraction F_1^∞ for hydrogen atoms and ions incident on Ba vapor.

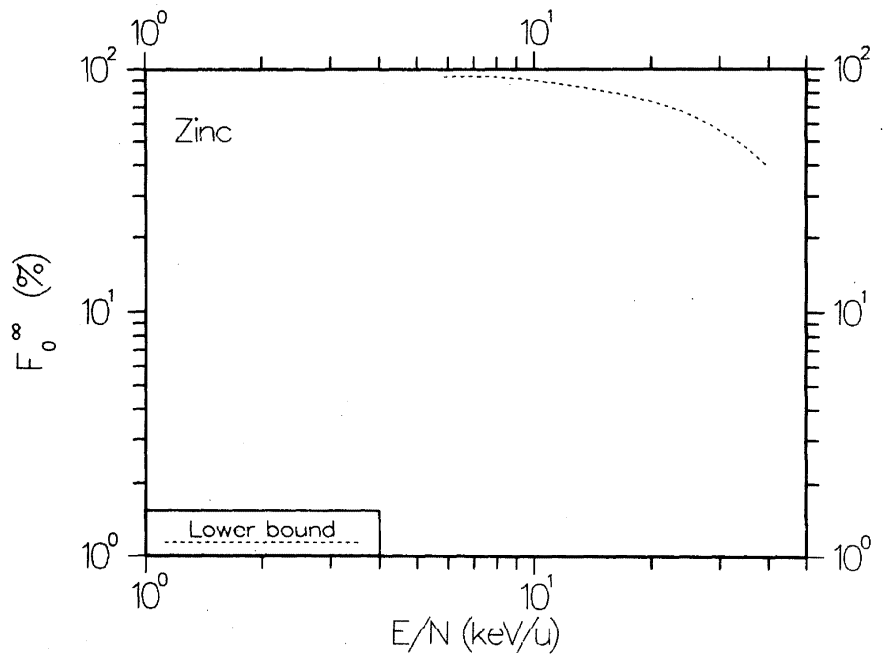

FIG. 76. Equilibrium fraction F_0^∞ for hydrogen atoms and ions incident on Zn vapor. The lower bound is based on data taken from Ref. 44.

17 July 2023 14:50:05

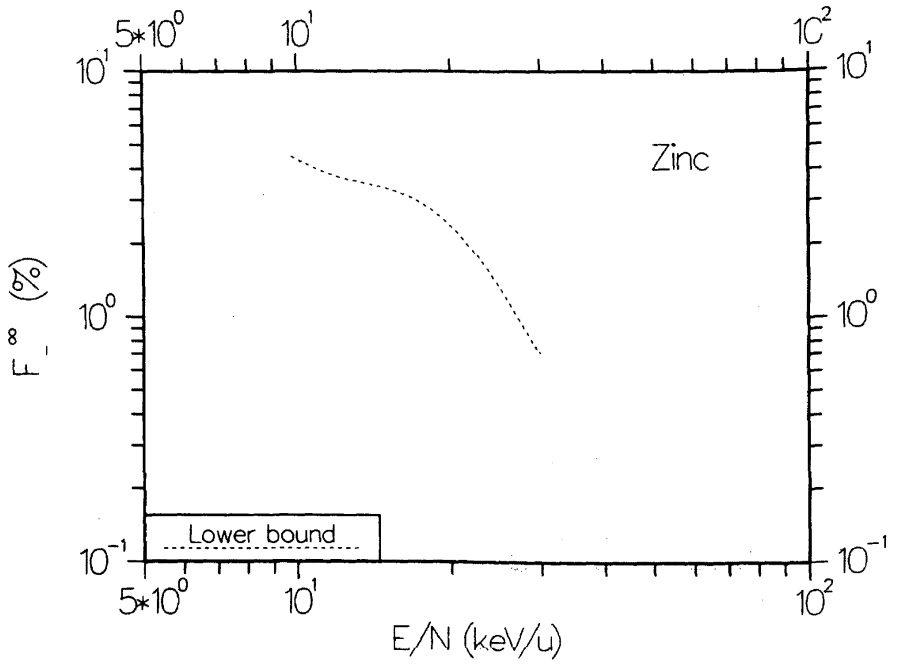

FIG. 77. Equilibrium fraction F_-^∞ for hydrogen atoms and ions incident on Zn vapor. The lower bound is based on data taken from Ref. 44.

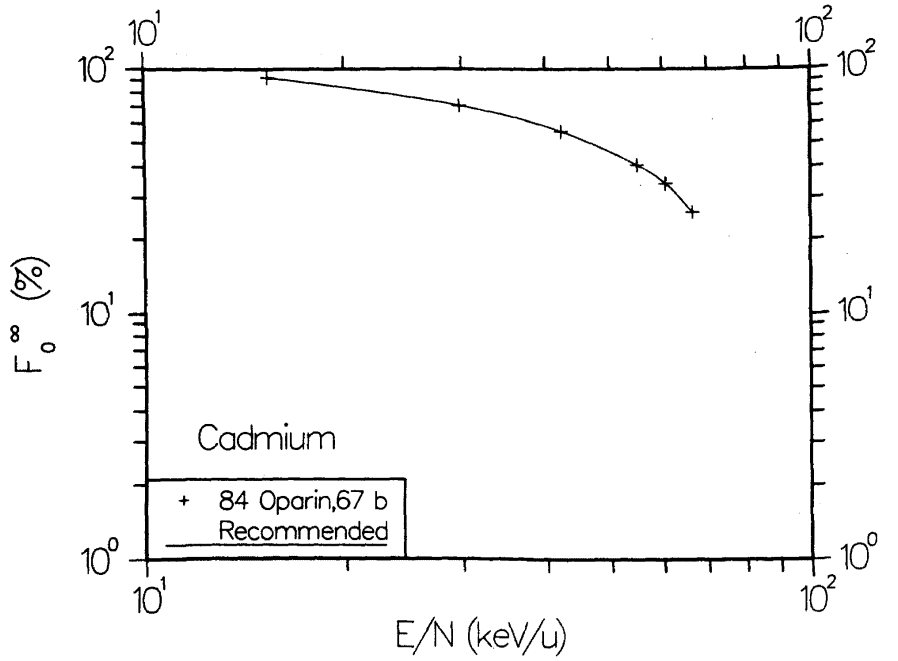

FIG. 78. Equilibrium fraction F_0^∞ for hydrogen atoms and ions incident on Cd vapor.

17 July 2023 14:50:05

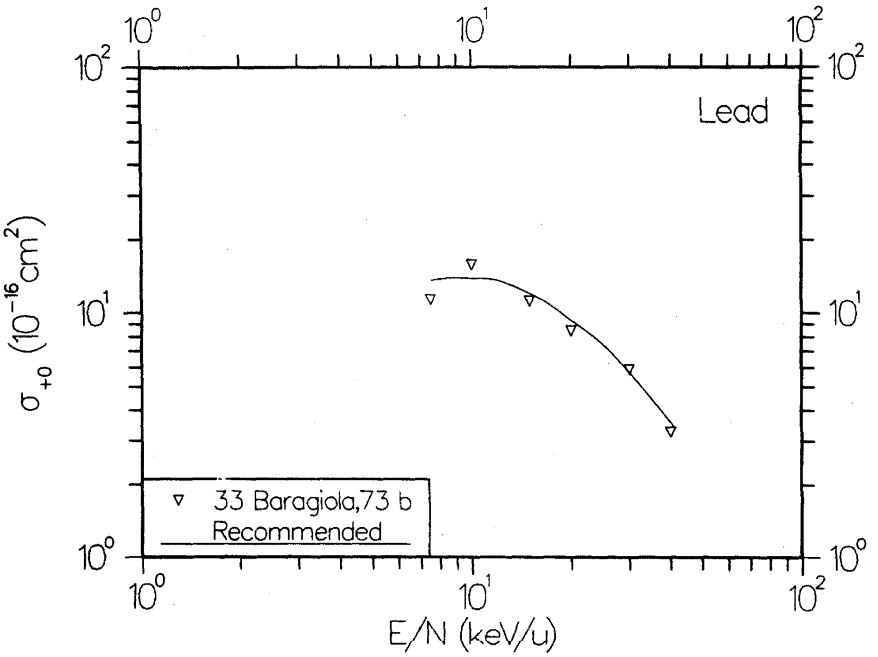

FIG. 79. Cross section σ_{+0} for single electron capture in collisions of H^+ with Pb vapor.

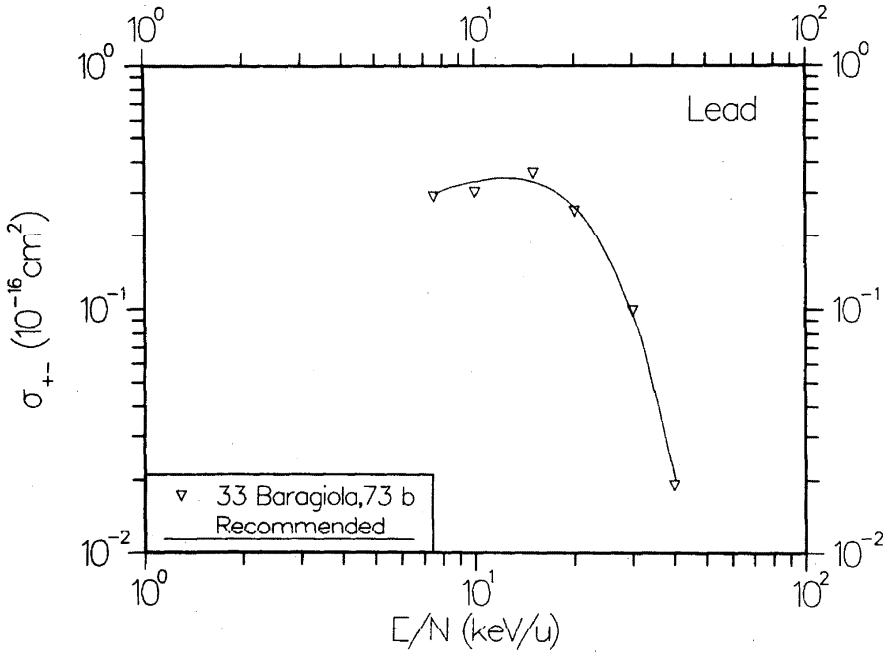

FIG. 80. Cross section σ_{+-} for double electron capture in collisions of H^+ with Pb vapor.

17 July 2023 14:50:05

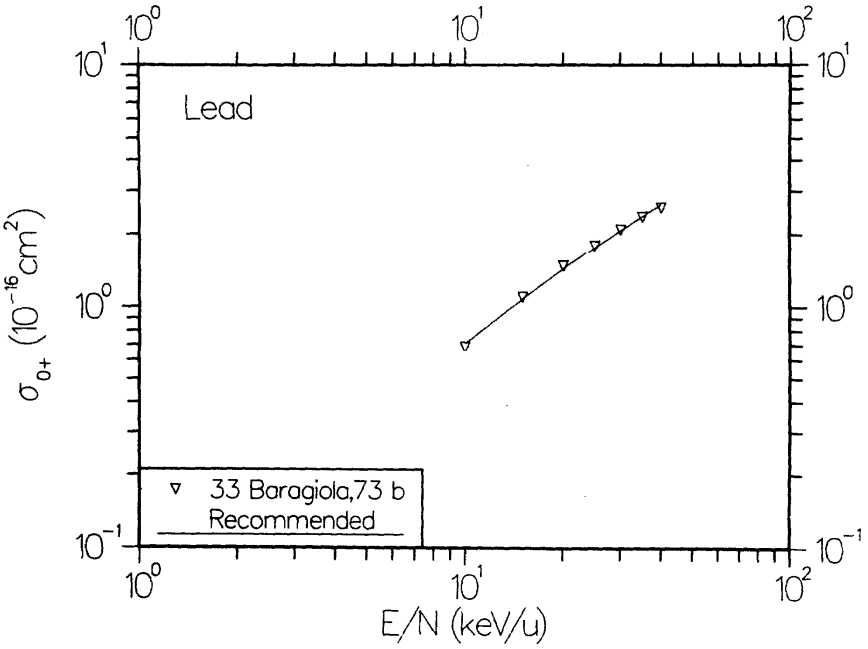

FIG. 81. Cross section σ_{0+} for electron loss in collisions of H^0 with Pb vapor.

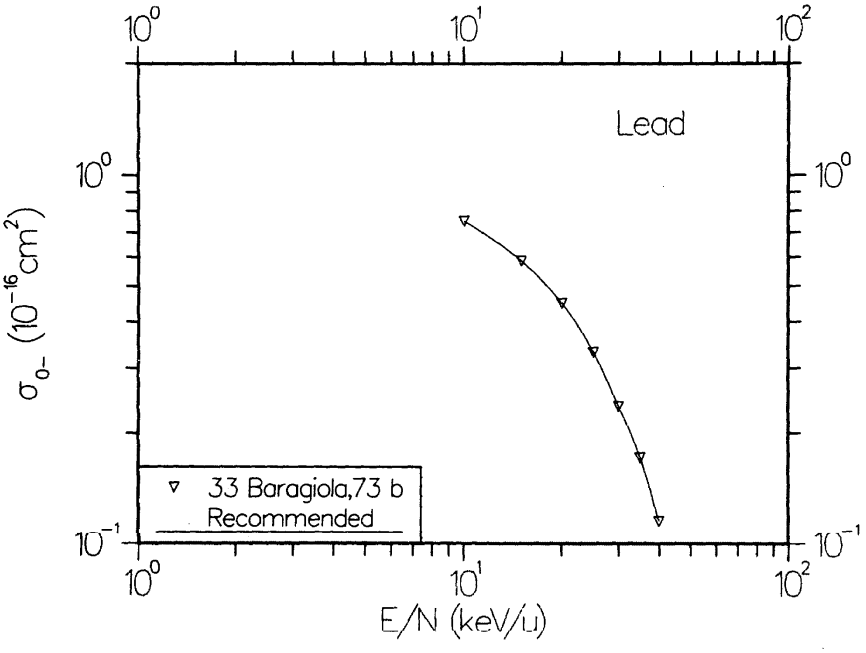

FIG. 82. Cross section σ_{0-} for electron capture in collisions of H^0 with Pb vapor.

17 July 2023 14:50:05

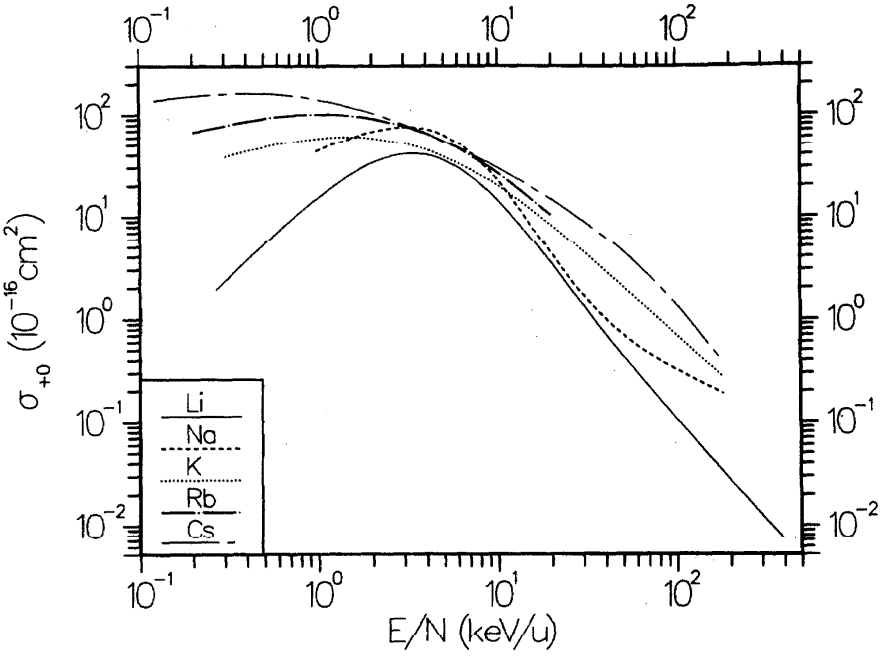

FIG. 83. Recommended values for σ_{+0}, the cross section for single electron capture, in collisions of H^+ with alkali metal vapors.

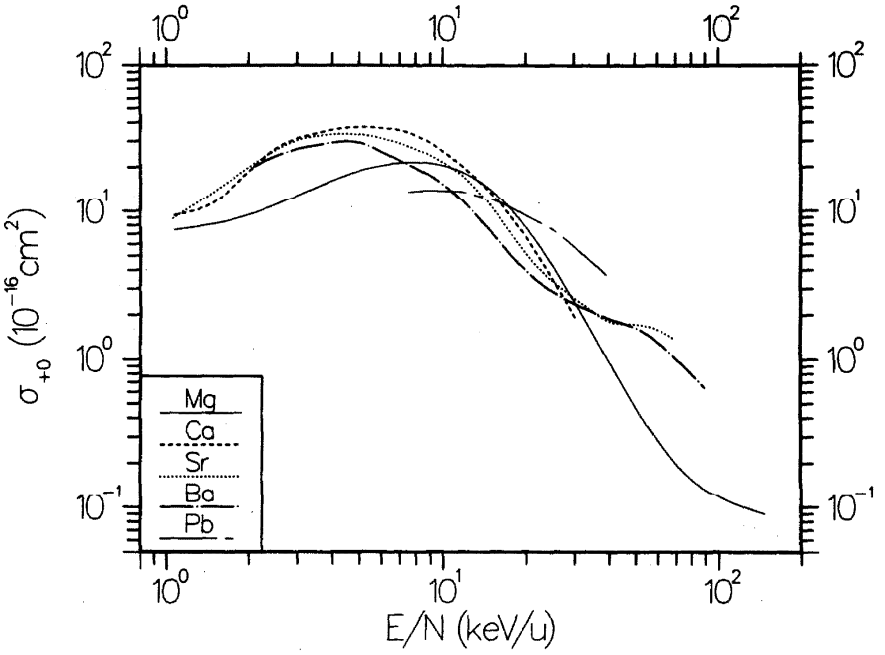

FIG. 84. Recommended values for σ_{+0}, the cross section for single electron capture, in collisions of H^+ with alkaline-earth and lead vapors.

17 July 2023 14:50:05

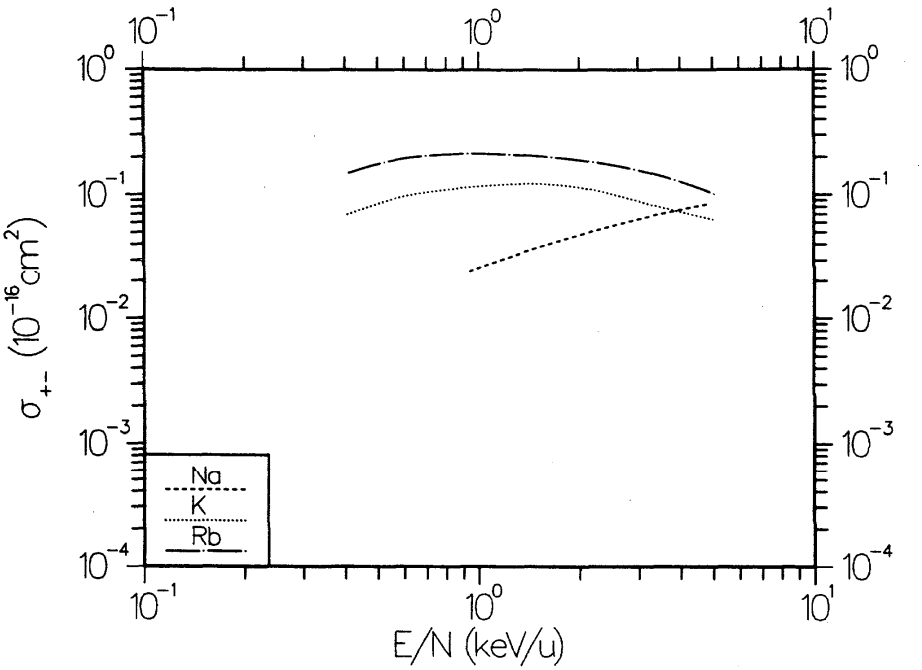

FIG. 85. Recommended values for σ_{+-}, the cross section for double electron capture, in collisions of H^+ with alkali metal vapors.

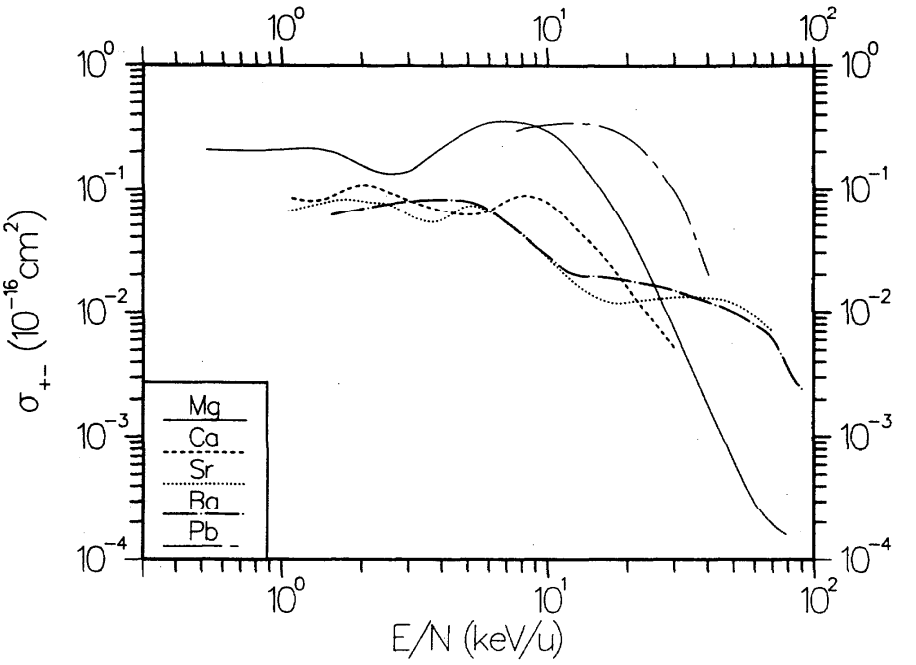

FIG. 86. Recommended values for σ_{+-}, the cross section for double electron capture, for collisions of H^+ with alkaline-earth and lead vapors.

17 July 2023 14:50:05

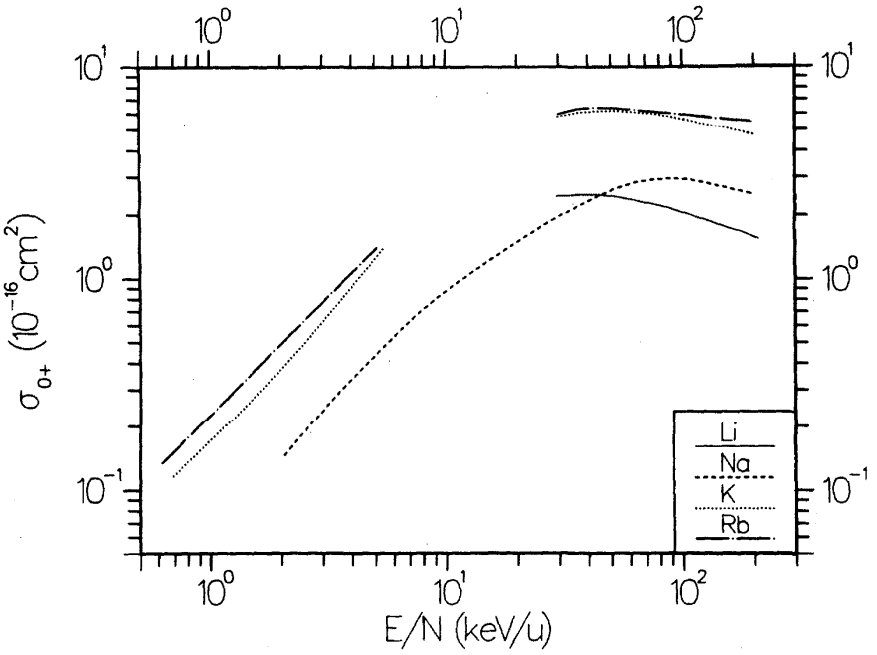

FIG. 87. Recommended values for σ_{0+}, the cross section for electron loss, for collisions of H^0 with alkali metal vapors.

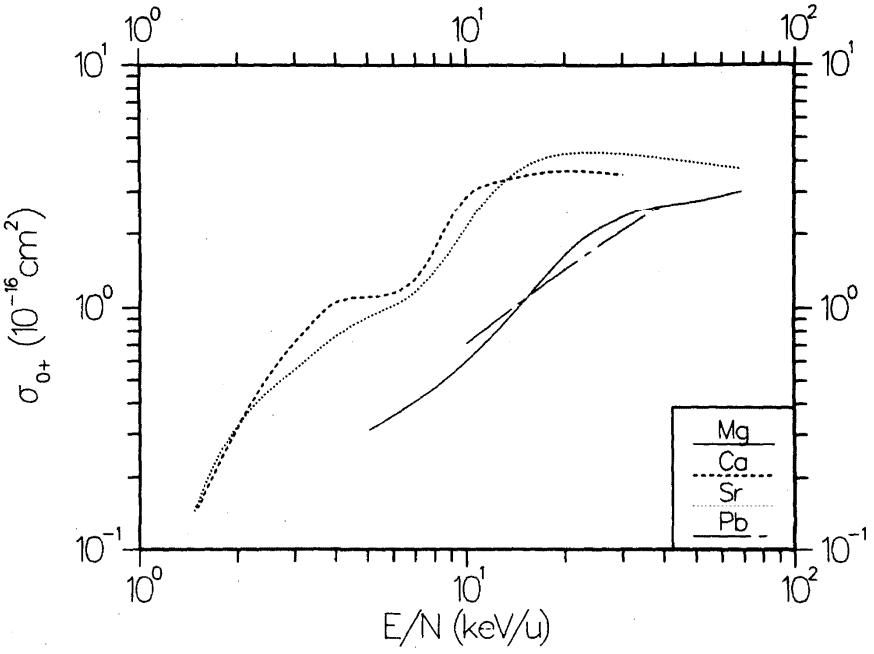

FIG. 88. Recommended values for σ_{0+}, the cross section for electron loss, for collisions of H^0 with alkaline-earth vapors and lead.

17 July 2023 14:50:05

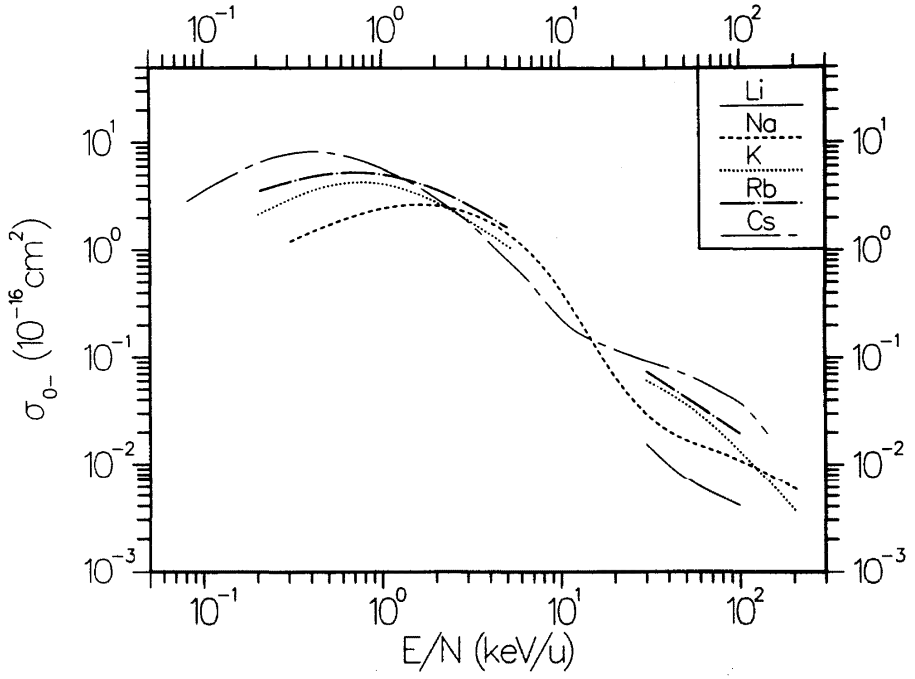

FIG. 89. Recommended values for σ_{0-}, the cross section for electron capture, in collisions of H^0 with alkali metal vapors.

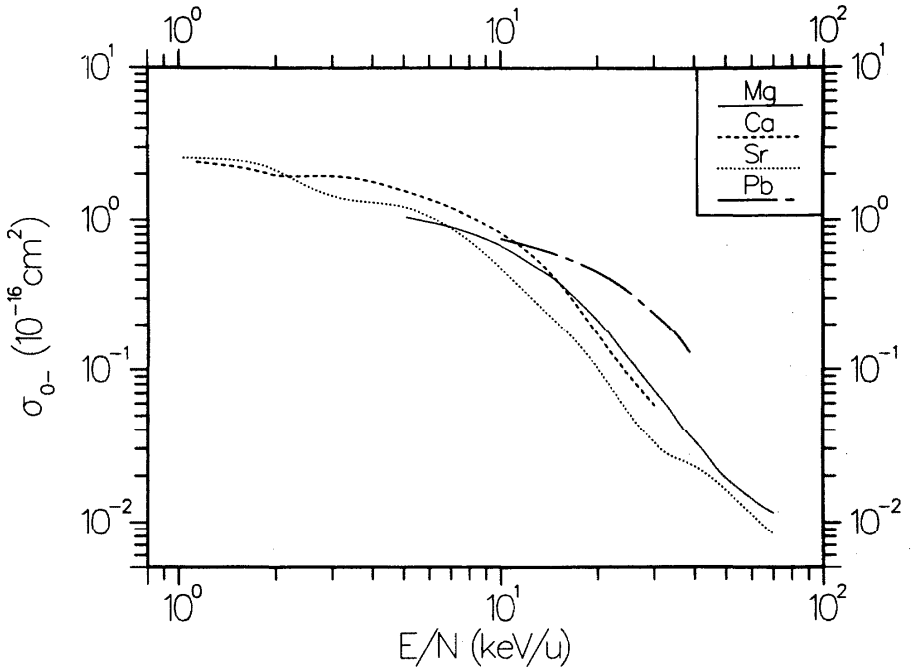

FIG. 90. Recommended values for σ_{0-}, the cross section for electron capture, in collisions of H^0 with alkaline-earth and lead vapors.

17 July 2023 14:50:05

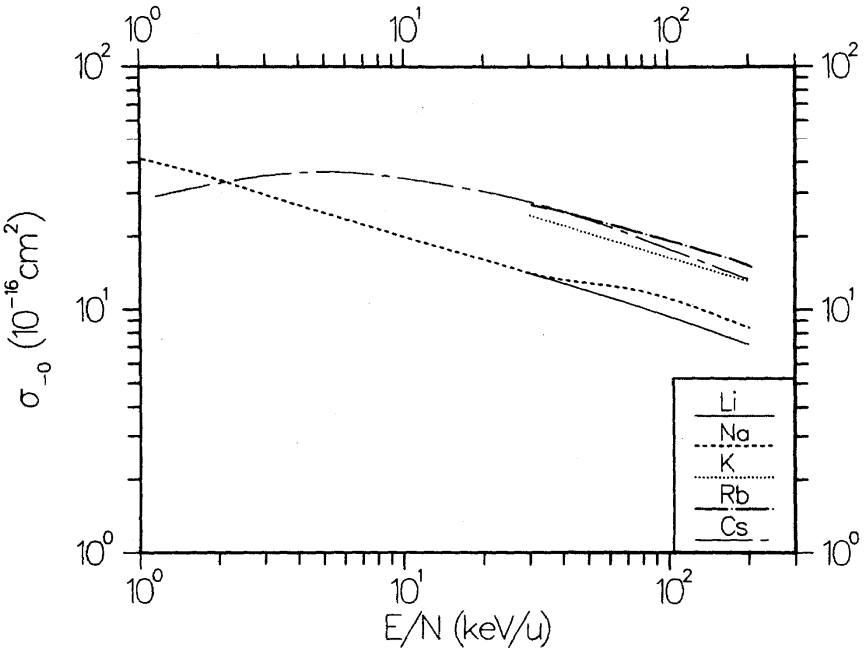

FIG. 91. Recommended values for σ_{-0}, the cross section for detachment of electrons, in collisions of H^- ions with alkali metal vapors.

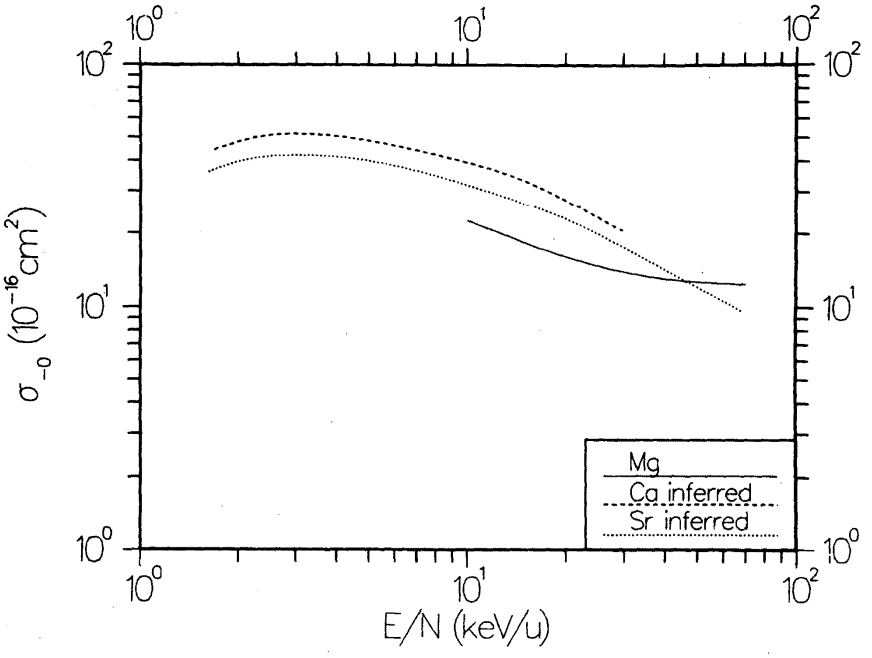

FIG. 92. Recommended values for σ_{-0}, the cross section for detachment of electrons, in collisions of H^- ions with alkaline-earth vapors.

17 July 2023 14:50:05

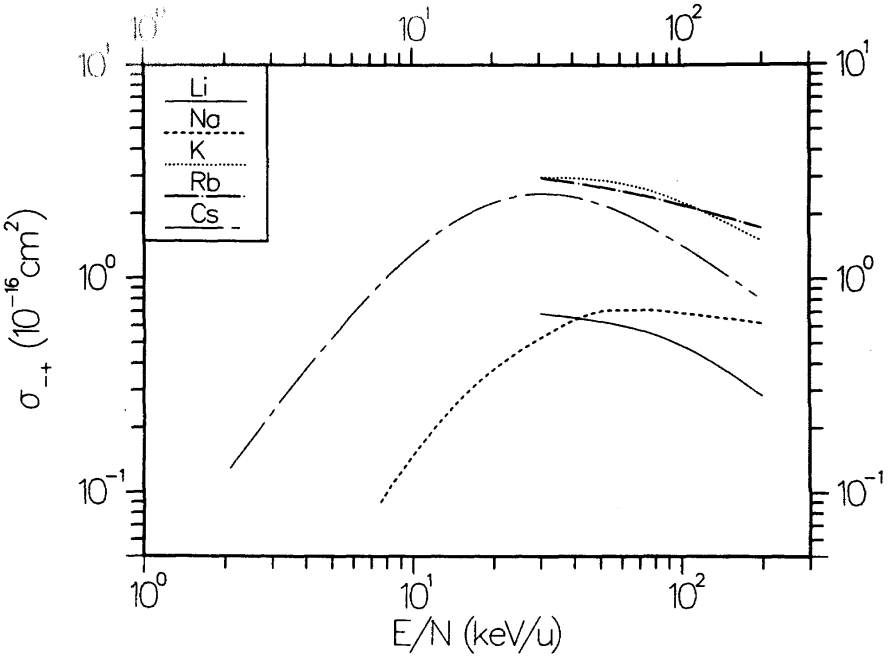

FIG. 93. Recommended values for σ_{-+}, the cross section for double electron loss, in collisions of H^- ions with alkali metal vapors.

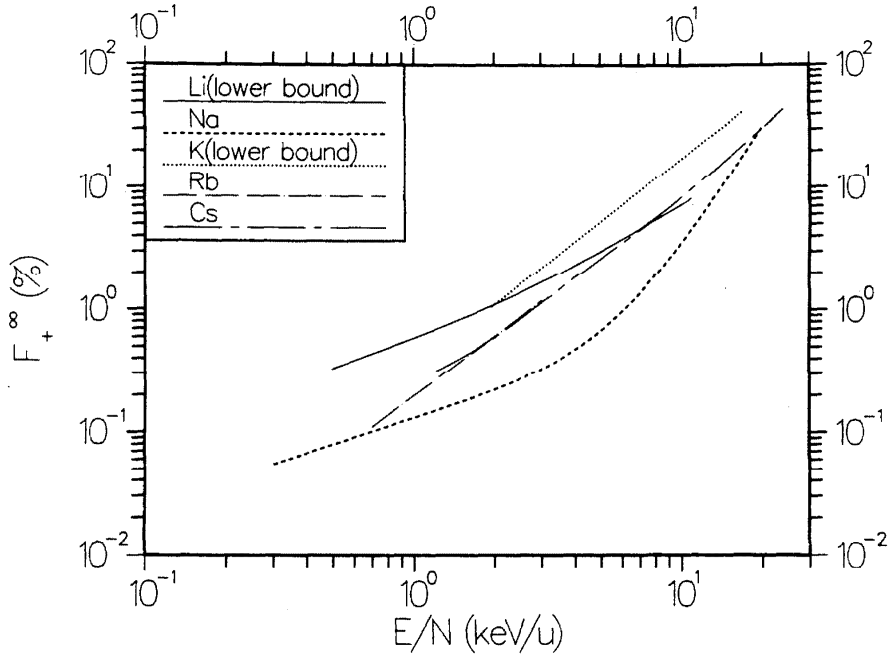

FIG. 94. Recommended values for F_+^∞, the equilibrium fraction for formation of H^+ ions, in collisions of hydrogen atoms and ions with alkali metal vapors.

17 July 2023 14:50:05

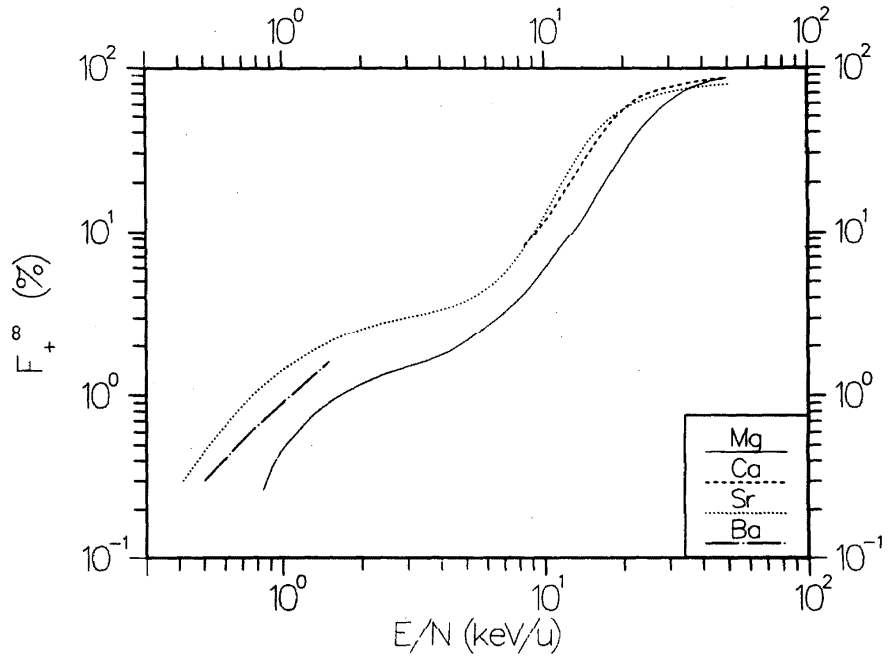

FIG. 95. Recommended values for F_+^∞, the equilibrium fraction for formation of H^+ ions, in collisions of hydrogen atoms and ions with alkaline-earth vapors.

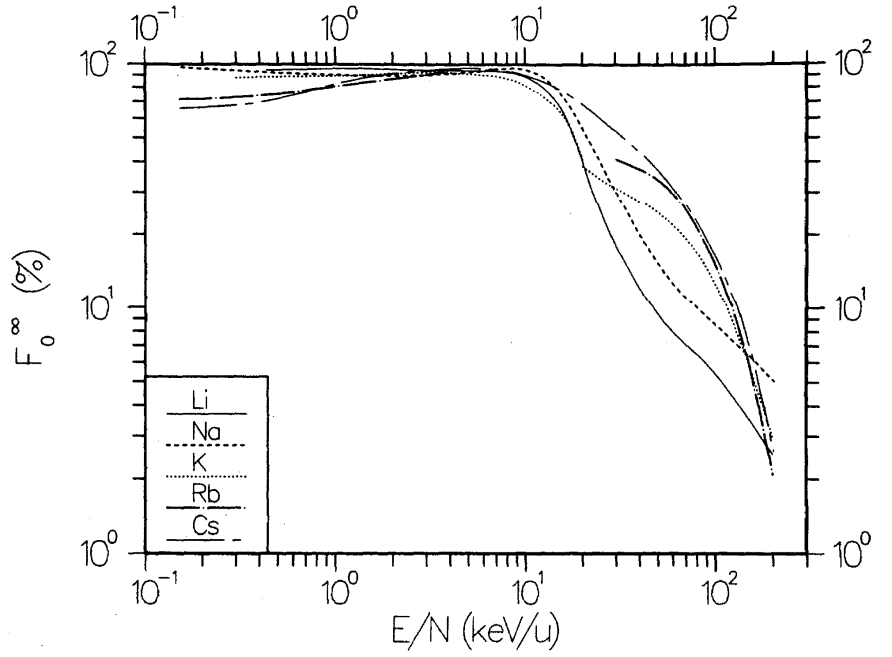

FIG. 96. Recommended values for F_0^∞, the equilibrium fraction for the formation of H^0 ions, in collisions of hydrogen atoms and ions with alkali metal vapors. For Li and $E/N \leqslant 30$ keV/u and for K and $E/N \leqslant 20$ keV/u, the values given are lower bounds.

17 July 2023 14:50:05

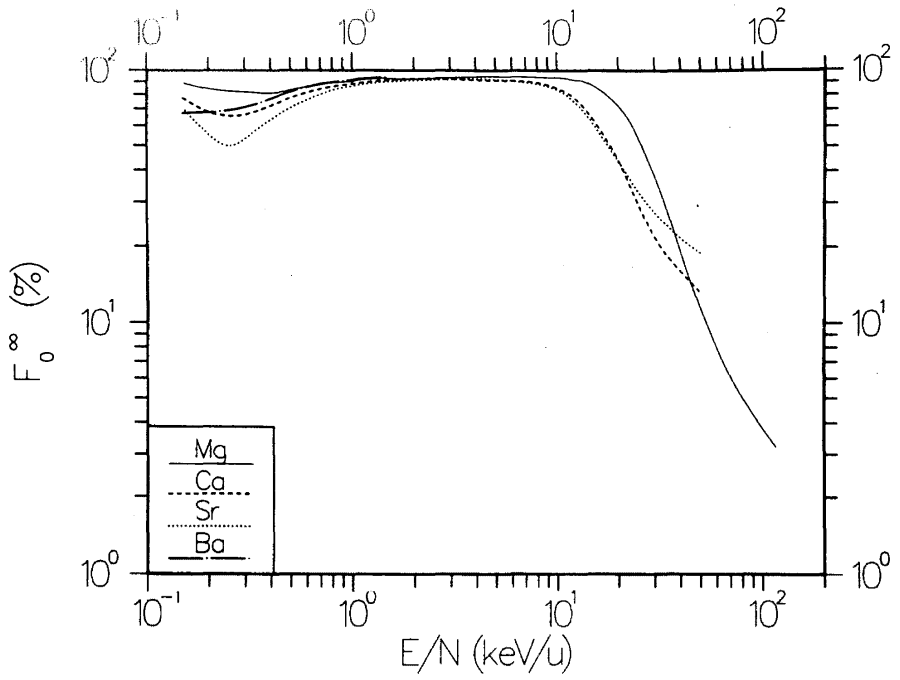

FIG. 97. Recommended values for F_0^∞, the equilibrium fraction for the formation of H^0 ions, in collisions of hydrogen atoms and ions with alkaline-earth vapors.

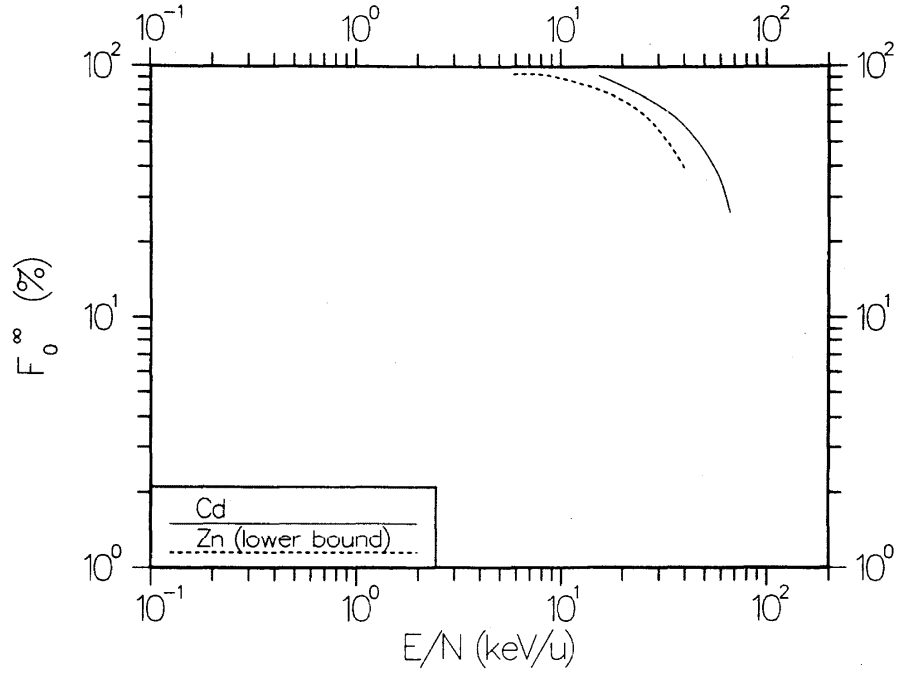

FIG. 98. Recommended values for F_0^∞, the equilibrium fraction for the formation of H^0 ions, in collisions of hydrogen atoms and ions with zinc and cadmium vapors.

17 July 2023 14:50:05

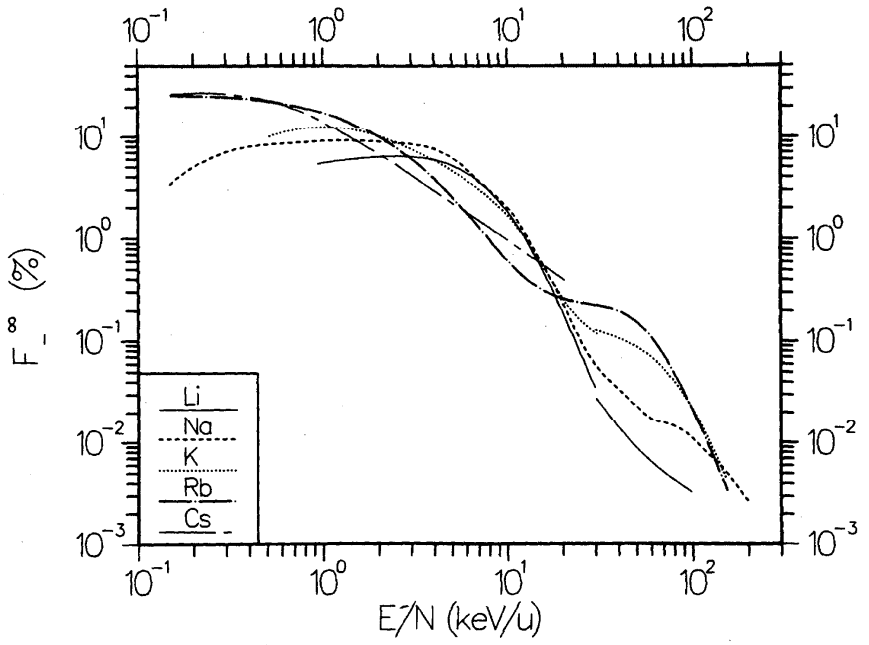

FIG. 99. Recommended values for F_{-}^{∞}, the equilibrium fraction for the formation of H^- ions, in collisions of hydrogen atoms and ions with alkali metal vapors. For Li and $E/N \lesssim 30$ keV/u and for K and $E/N \lesssim 20$ keV/u, the values given are lower bounds.

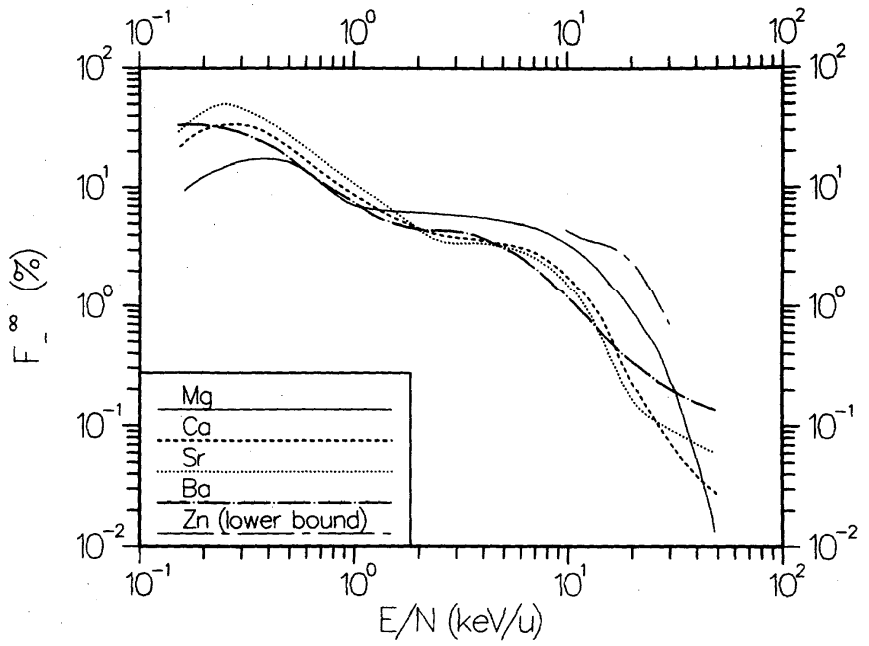

FIG. 100. Recommended values for F_{-}^{∞}, the equilibrium fraction for the formation of H^- ions, in collisions of hydrogen atoms and ions with alkaline-earth vapors.

17 July 2023 14:50:05

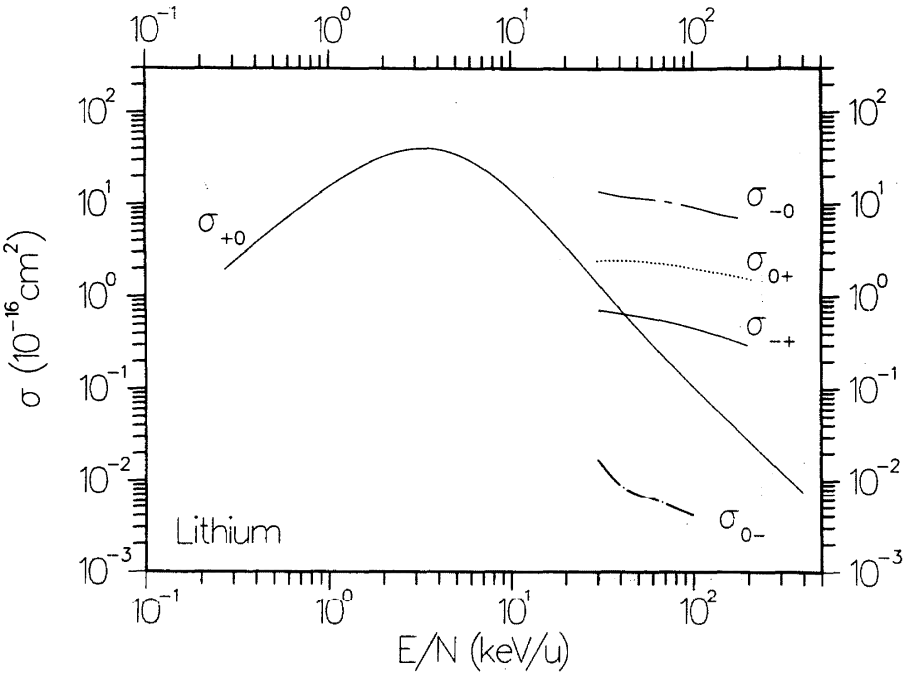

FIG. 101. Recommended values of charge transfer cross sections for hydrogen atoms and ions incident on Li vapor.

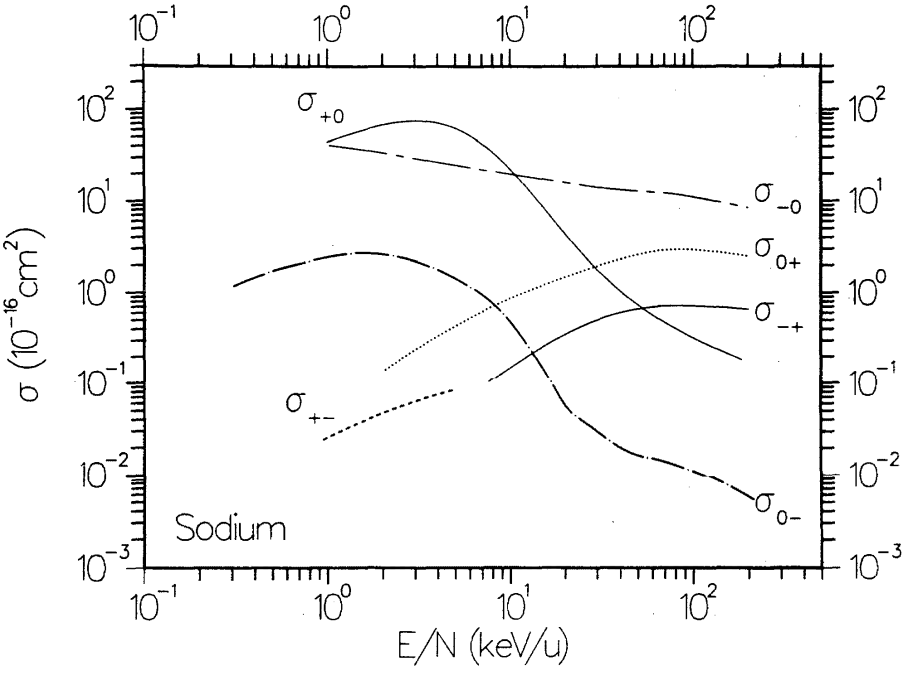

FIG. 102. Recommended values of charge transfer cross sections for hydrogen atoms and ions incident on Na vapor.

17 July 2023 14:50:05

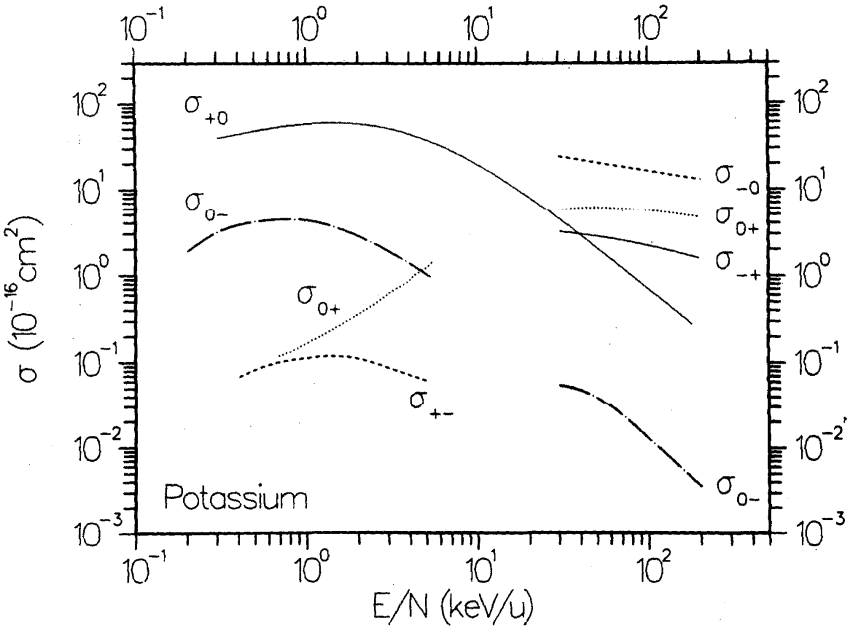

FIG. 103. Recommended values of charge transfer cross sections for hydrogen atoms and ions incident on K vapor.

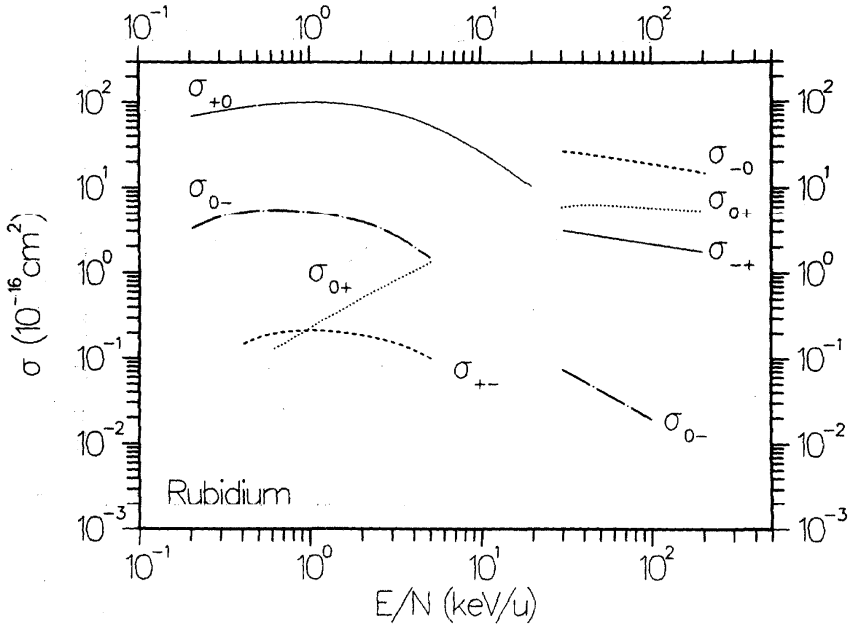

FIG. 104. Recommended values of charge transfer cross sections for hydrogen atoms and ions incident on Rb vapor.

17 July 2023 14:50:05

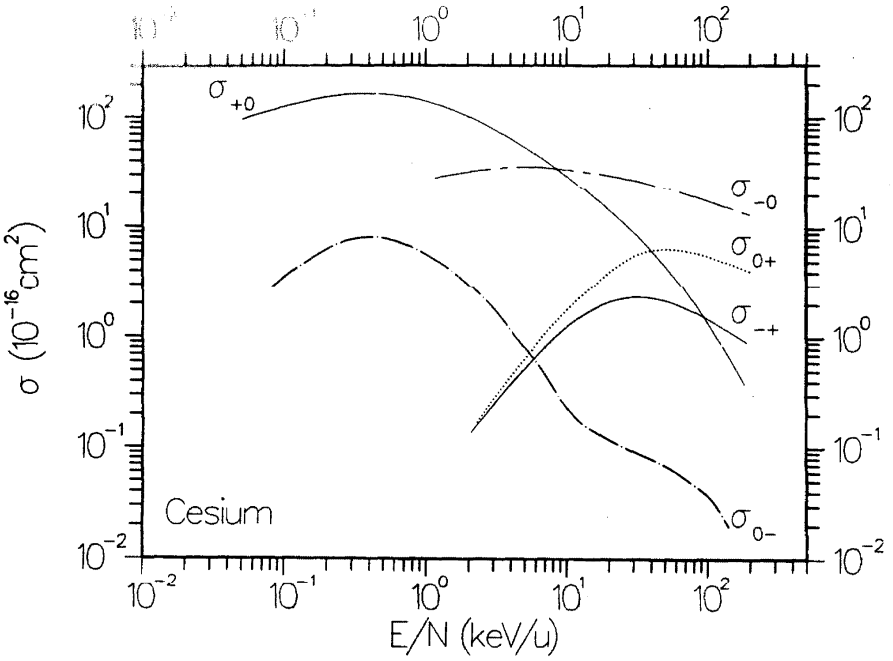

FIG. 105. Recommended values of charge transfer cross sections for hydrogen atoms and ions incident on Cs vapor.

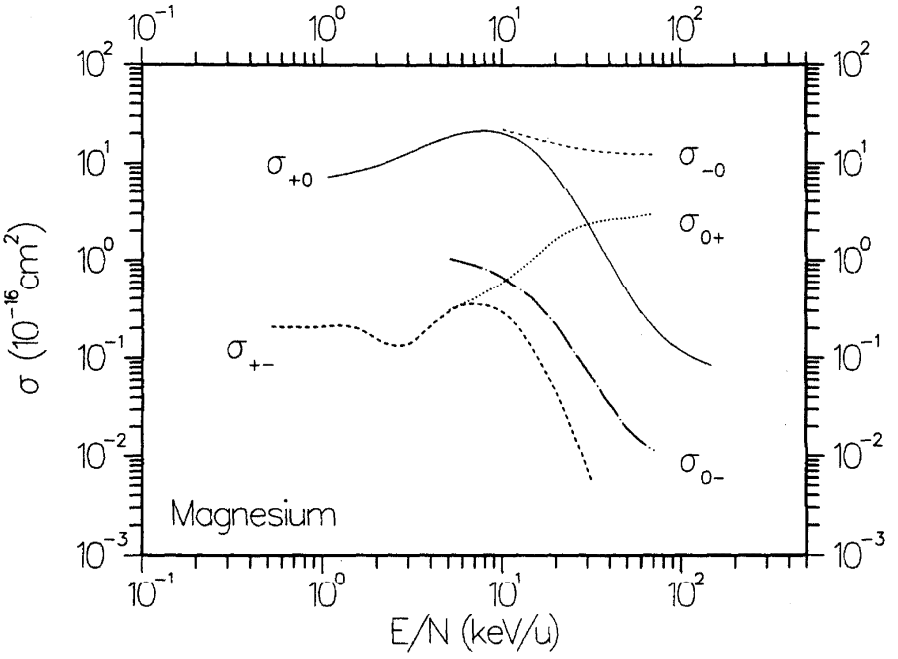

FIG. 106. Recommended values of charge transfer cross sections for hydrogen atoms and ions incident on Mg vapor.

17 July 2023 14:50:05

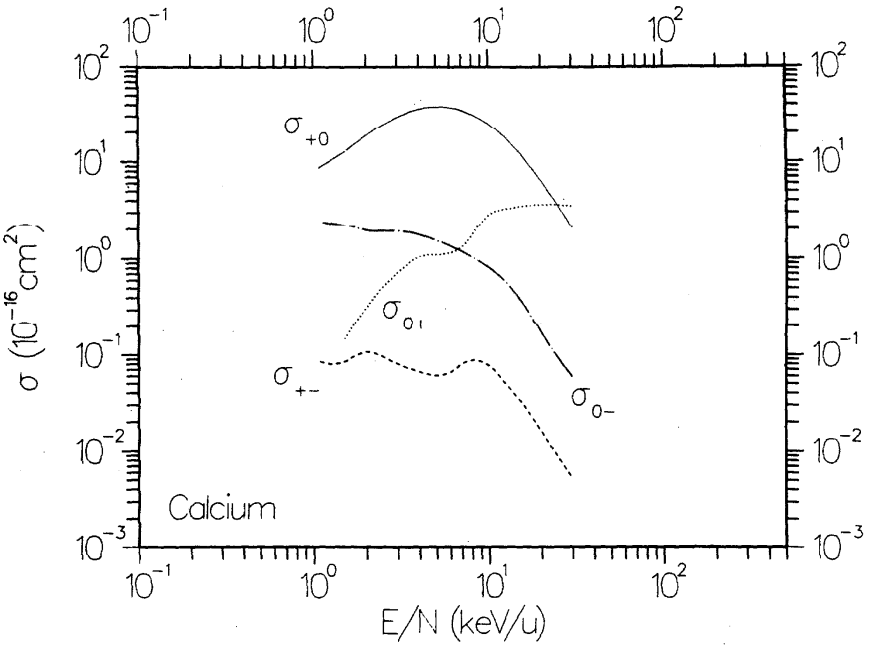

FIG. 107. Recommended values of charge transfer cross sections for hydrogen atoms and ions incident on Ca vapor.

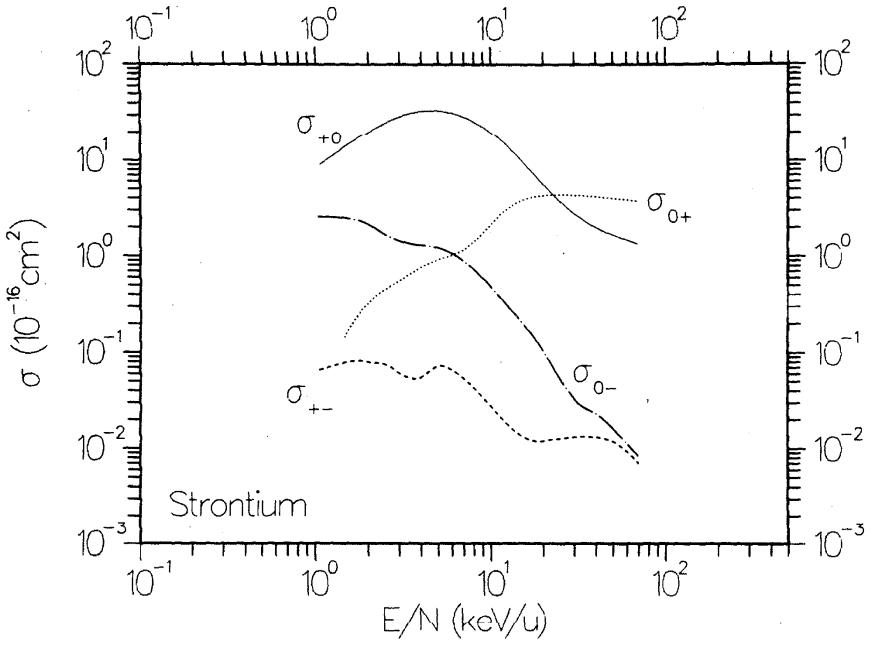

FIG. 108. Recommended values of charge transfer cross sections for hydrogen atoms and ions incident on Sr vapor.

17 July 2023 14:50:05

8. Acknowledgments

The authors wish to express appreciation to the Office of Standard Reference Data of the Bureau of Standards for support of this work. This work was also supported by the Director, Office of Energy Research, Office of Fusion Energy, Applied Plasma Physics, of the U.S. Department of Energy.

9. References

[1]S. K. Allison, Rev. Mod. Phys. **30**, 1137 (1958).
[2]H. Tawara and A. Russek, Rev. Mod. Phys. **45**, 178 (1973); H. Tawara, At. Data Nucl. Data Tables **22**, 491 (1978).
[3]A. S. Schlachter, in Proc. of Symp. on Production and Neutralization of Negative Hydrogen Ions and Beams, edited by K. Prelec, BNL No. 50727, 1978, pp. 11–23.
[4]A. S. Schlachter, in Proc. of Second Intern. Symp. on Production and Neutralization of Negative Hydrogen Ions and Beams, edited by Th. Sluyters, BNL No. 51304, 1980, pp. 42–50.
[5]A. S. Schlachter, in Proc. of the U.S.–Mexico Joint Seminar on the Atomic Physics of Negative Ions, Mexico City, 1981, edited by C. Cisneros and T. J. Morgan [Notas Fis. **5**, 481 (1982)].
[6]A. S. Schlachter and T. J. Morgan, AIP Conf. Proc. **111**, 149 (1983).
[7]Y. Nakai, T. Shirai, M. Sataka, and T. Sugiura, JAERI-M Report No. 84-169, 1984, pp. 1–123.
[8]A. S. Schlachter, AIP Conf. Proc. **117**, 180 (1984).
[9]L. W. Anderson, S. N. Kaplan, R. V. Pyle, L. Ruby, A. S. Schlachter, and J. W. Stearns, J. Phys. B **17**, L229 (1984).
[10]T. J. Morgan and F. J. Eriksen, Phys. Rev. A **19**, 1448 (1979).
[11]V. N. Tuan, G. Gautherin, and A. S. Schlachter, Phys. Rev. A **9**, 1242 (1974).
[12]A. S. Schlachter, K. R. Stalder, and J. W. Sterns, Phys. Rev. A **22**, 2494 (1980).
[13]R. Hultgren, P. D. Desai, D. T. Hawkins, M. Gleiser, K. K. Kelley, and D. D. Wagman, *Selected Values of Thermodynamic Properties of the Elements* (American Society for Metals, Cleveland, 1973).
[14]P. Pradel, F. Roussel, and G. Spiess, Rev. Sci. Instrum. **45**, 45 (1974).
[15]P. Pradel, F. Roussel, A. S. Schlachter, G. Spiess, and A. Valence, Phys. Rev. A **10**, 797 (1974).
[16]J. B. Taylor and I. Langmuir, Phys. Rev. **51**, 753 (1937).
[17]A. S. Schlachter, P. J. Bjorkholm, D. H. Loyd, L. W. Anderson, and W. Haeberli, Phys. Rev. **177**, 184 (1969).
[18]J. A. Ray, C. F. Barnett, and B. Van Zyl, J. Appl. Phys. **50**, 6516 (1979).
[19]K. H. Berkner, B. R. Myers, and R. V. Pyle, Rev. Sci. Instrum. **39**, 1204 (1968).
[20]M. W. Geis, K. A. Smith, and R. D. Rundel, J. Phys. E **8**, 1011 (1975).
[21]D. R. Bates, H. S. W. Masey, and A. L. Steward, Proc. R. Soc. London A **216**, 437 (1953).
[22]C. Kubach and V. Sidis, Phys. Rev. A **14**, 152 (1976).
[23]L. Landau, J. Phys. (Moscow) **2**, 46 (1932).
[24]C. Zener, Proc. R. Soc. London A **137**, 696 (1933).
[25]E. C. G. Stueckelberg, Helv. Phys. Acta **5**, 369 (1932).
[26]D. R. Bates and R. McCarroll, Proc. R. Soc. London A **245**, 175 (1958).
[27]R. E. Olson, F. T. Smith, and E. Bauer, Appl. Opt. **10**, 1848 (1971).
[28]W. Fritsch and C. D. Lin, J. Phys. B **16**, 1595 (1984).
[29]I. Alvarez, C. Cisneros, and A. Russek, Phys. Rev. A **26**, 77 (1982).
[30]C. J. Anderson, R. J. Girnius, A. M. Howald, and L. W. Anderson, Phys. Rev. A **22**, 822 (1980).
[31]C. J. Anderson, A. M. Howald, and L. W. Anderson, Nucl. Instrum. Methods **165**, 583 (1979).
[32]Y. K. Bae, M. Cogiolla, and J. R. Peterson, Phys. Rev. A **30**, 2807 (1984).
[33]R. A. Baragiola and E. R. Salvatelli, Nucl. Instrum. Methods **110**, 503 (1973).
[34]R. A. Baragiola, E. R. Salvatelli, and E. Alonso, Nucl. Instrum. Methods **110**, 507 (1973).
[35]K. H. Berkner, W. S. Cooper III, S. N. Kaplan, and R. V. Pyle, Phys. Rev. **182**, 103 (1969).
[36]K. H. Berkner, D. Leung, R. V. Pyle, A. S. Schlachter, and J. W. Stearns, Nucl. Instrum. Methods **143**, 157 (1977).
[37]K. H. Berkner, D. Leung, R. V. Pyle, A. S. Schlachter, and J. W. Stearns, Phys. Lett. A **64**, 217 (1977).
[38]J. K. Berkowitz and J. C. Zorn, Phys. Rev. A **29**, 611 (1984).
[39]H. Bohlen, G. Clausmitzer, and H. Wilsch, Z. Phys. **208**, 159 (1968).
[40]C. Cisneros, I. Alvarez, C. F. Barnett, and J. A. Ray, Phys. Rev. A **14**, 76 (1976).
[41]B. L. Donnally, T. Clapp, W. Sawyer, and M. Schultz, Phys. Rev. Lett. **12**, 502 (1964).
[42]R. DuBois, unpublished cross sections (private communication) (1984).
[43]B. A. Dyachkov, At. Energ. **27**, 220 (1969) [Sov. J. At. Energy **27**, 958 (1969)].
[44]B. A. Dyachkov and V. I. Zinenko, At. Energ. **24**, 18 (1968) [Sov. J. At. Energy **24**, 16 (1968)].
[45]F. Ebel, thesis (University of Giessen, West Germany, 1983).
[46]W. Fritsch, Phys. Rev. A **30**, 1135 (1984).
[47]W. Fritsch and C. D. Lin, J. Phys. B **16**, 1595 (1983).
[48]R. J. Girnius, C. J. Anderson, and L. W. Anderson, Phys. Rev. A **16**, 2225 (1977).
[49]R. J. Girnius, L. W. Anderson, and E. Staab, Nucl. Instrum. Methods **143**, 505 (1977).
[50]W. Gruebler, P. A. Schmelzbach, V. Konig, and P. Marmier, Helv. Phys. Acta **43**, 254 (1970).
[51]J. R. Hiskes, A. M. Karo, P. A. Willmann, and W. J. Stevens, Phys. Lett. A **68**, 221 (1978).
[52]E. B. Hooper, Jr. and P. A. Willmann, J. Appl. Phys. **48**, 1041 (1977).
[53]A. M. Howald, L. W. Anderson, and C. C. Lin, Phys. Rev. A **24**, 44 (1981).
[54]A. M. Howald, R. E. Miers, J. S. Allen, L. W. Anderson, and C. C. Lin, Phys. Rev. A **29**, 1083 (1984).
[55]R. N. Il'in, V. A. Oparin, E. S. Solovev, and N. V. Fedorenko, Zh. Tekh. Fiz. **36**, 1241 (1966) [Sov. Phys. Tech. Phys. **11**, 921 (1967)].
[56]R. N. Il'in, V. A. Oparin, E. S. Solovev, and N. V. Fedorenko, Pis'ma Zh. Eksp. Teor. Fiz. **2**, 310 (1965) [JETP Lett. **2**, 197 (1965)].
[57]N. Inoue, Nucl. Fusion **12**, 130 (1972).
[58]R. K. Janev and Z. M. Radulovic, Phys. Rev. A **17**, 889 (1978).
[59]M. Kimura, R. E. Olson, and J. Pascale, Phys. Rev. A **26**, 1138 (1982).
[60]M. Kimura, R. E. Olson, and J. Pascale, Phys. Rev. A **26**, 3113 (1982).
[61]C. Kubach and V. Sidis, Phys. Rev. A **23**, 110 (1981).
[62]T. E. Leslie, K. P. Sarver, and L. W. Anderson, Phys. Rev. A **4**, 408 (1971).
[63]M. R. Mayo, thesis (Wesleyan University, 1982).
[64]M. Mayo, J. A. Stone, and T. J. Morgan, Phys. Rev. A **28**, 1315 (1983).
[65]R. H. McFarland, A. S. Schlachter, J. W. Stearns, B. Liu, and R. E. Olson, Phys. Rev. A **26**, 775 (1982).
[66]F. W. Meyer, J. Phys. B **13**, 3823 (1980).
[67]F. W. Meyer, C. J. Anderson, and L. W. Anderson, Phys. Rev. A **15**, 455 (1977).
[68]F. W. Meyer and L. W. Anderson, Phys. Rev. A **11**, 589 (1975).
[69]F. W. Meyer and L. W. Anderson, Phys. Lett. A **54**, 333 (1975).
[70]K. Miethe, T. Dreiseidler, and E. Salzborn, J. Phys. B **15**, 3069 (1982).
[71]T. J. Morgan and F. J. Eriksen, Phys. Rev. A **19**, 2185 (1979).
[72]T. J. Morgan and F. J. Eriksen, Phys. Lett. A **66**, 198 (1978).
[73]T. J. Morgan, J. Stone, M. Mayo, and J. Kurose, Phys. Rev. A **20**, 54 (1979).
[74]T. Nagata, J. Phys. Soc. Jpn. **48**, 2068 (1980).
[75]T. Nagata, Mass. Spectrosc. (Japan) **30**, 153 (1982).
[76]T. Nagata, J. Phys. Soc. Jpn. **54**, 4 (1983).
[77]B. G. O'Hare, R. W. McCullough, and H. B. Gilbody, J. Phys. B **8**, 2968 (1975).
[78]R. E. Olson, Phys. Lett. A **77**, 143 (1980).
[79]R. E. Olson, J. Phys. B **15**, L163 (1982).
[80]R. E. Olson, M. Kimura, and H. Sato, Phys. Rev. A **30**, 1692 (1984).
[81]R. E. Olson and B. Liu, J. Chem. Phys. **73**, 2817 (1980).
[82]R. E. Olson and B. Liu, Phys. Rev. A **20**, 1366 (1979).
[83]R. E. Olson, E. J. Shipsey, and J. C. Browne, Phys. Rev. A **13**, 180 (1976).
[84]V. A. Oparin, R. N. Il'in, and E. S. Solovev, Zh. Eksp. Teor. Fiz. **52**, 369 (1967) [Sov. Phys. JETP **25**, 240 (1967)].
[85]H. Sato and M. Kimura, Phys. Lett. A **96**, 286 (1983).
[86]P. A. Schmelzbach, W. Gruebler, V. Konig, and P. Marmier, Helv. Phys. Acta **41**, 310 (1968).
[87]I. A. Sellin and L. Granoff, Phys. Lett. A **25**, 484 (1967).
[88]V. Sidis and C. Kubach, J. Phys. B **11**, 2687 (1978).
[89]G. Spiess, A. Valance, and P. Pradel, Phys. Rev. A **6**, 746 (1972).
[90]G. Spiess, A. Valance, and P. Pradel, Phys. Lett. A **31**, 434 (1970).
[91]S. L. Varghese, W. Waggoner, and C. L. Cocke, Phys. Rev. A **29**, 2453 (1984).

17 July 2023 14:50:05